DOT/FAA/AR-03/56

Office of Aviation Research
Washington, D.C. 20591

Fatigue and Stress Relaxation of Adhesives in Bonded Joints

October 2003

Final Report

U.S. Department of Transportation
Federal Aviation Administration

NOTICE

Technical Report Documentation Page

1. Report No.	2. Government Accession No.	3. Recipient's Catalog No.
DOT/FAA/AR-03/56		

4. Title and Subtitle	5. Report Date
FATIGUE AND STRESS RELAXATION OF ADHESIVES IN BONDED JOINTS	October 2003
	6. Performing Organization Code

7. Author(s)	8. Performing Organization Report No.
John Tomblin, Waruna Seneviratne, Paulo Escobar, and Yoon-Khian Yap	

9. Performing Organization Name and Address	10. Work Unit No. (TRAIS)
Department of Aerospace Engineering Wichita State University Wichita, KS 67260-0093	11. Contract or Grant No. 00-C-WSU-00-007

12. Sponsoring Agency Name and Address	13. Type of Report and Period Covered
U.S. Department of Transportation Federal Aviation Administration Office of Aviation Research Washington, DC 20591	Final Report
	14. Sponsoring Agency Code ACE-110

15. Supplementary Notes

The FAA William J. Hughes Technical Center COTR was Peter Shyprykevich.

16. Abstract

Increased confidence in composite materials have increased the use of adhesively bonded components in primary aircraft structures. Applications on primary structures require rigorous characterization of the material, unlike applications on secondary structures. Previously funded Federal Aviation Administration programs at the National Institute for Aviation Research at Wichita State University in Wichita, Kansas, have extensively researched thick bondline adhesive joint behavior, as well as adhesive joint behavior for a wide range of bondline thickness, with respect to several aircraft operating environmental conditions. The primary goal of this investigation was to characterize the long-term durability of adhesives. Two simultaneous investigations were performed to characterize fatigue and stress relaxation behavior. To gain more information about high-stress behavior (low-cycle fatigue), stress amplitudes resulting in adhesive failure at low levels of 1,000 to 100,000 cycles were used. Other subsequent tests were conducted at those levels, including temperature and frequency dependence of adhesives. In addition, stress relaxation behavior of various cases, such as during fuselage pressurization, was studied under three different environmental conditions and at three different stress levels. Both fatigue and stress relaxation tests provide vital design data for long-term durability of adhesive-bonded structures. Fatigue tests showed that moisture absorption shortened the fatigue life of adhesives from the lives at ambient room temperature or cold dry conditions. For most cases, stress relaxation tests indicated that the higher the stress level and test temperature, the higher the stress decay during relaxation. These results also revealed the danger of designing an adhesive structure to operate at temperatures near the glass transition temperature.

17. Key Words	18. Distribution Statement
Adhesive joints, Fatigue, Stress relaxation, ALCOA stress fixture	This document is available to the public through the National Technical Information Service (NTIS), Springfield, Virginia 22161.

19. Security Classif. (of this report)	20. Security Classif. (of this page)	21. No. of Pages	22. Price
Unclassified	Unclassified	94	

ACKNOWLEDGEMENT

The authors would like to acknowledge the technical guidance and support of Mr. Peter Shyprykevich and Dr. Larry Ilcewicz of the Federal Aviation Administration. The authors thank Cessna Aircraft Company of Wichita, Kansas, and Cirrus Design Corporation of Duluth, Minnesota, for supplying adhesive.

TABLE OF CONTENTS

LIST OF FIGURES

LIST OF TABLES

EXECUTIVE SUMMARY

Increased confidence in composite materials have increased the use of adhesively bonded components in primary aircraft structures. Applications on primary structures require rigorous characterization of the material, unlike applications on secondary structures. Previously funded Federal Aviation Administration programs at the National Institute for Aviation Research at Wichita State University in Wichita, Kansas, have extensively researched thick bondline adhesive joint behavior, as well as adhesive joint behavior for a wide range of bondline thickness, with respect to several aircraft operating environmental conditions. The primary goal of this investigation was to characterize the long-term durability of adhesives. Two simultaneous investigations were performed to characterize fatigue and stress relaxation behavior. To gain more information about high-stress behavior (low-cycle fatigue), stress amplitudes resulting in adhesive failure at low levels of 1,000 to 100,000 cycles were used. Other subsequent tests were conducted at those levels, including temperature and frequency dependence of adhesives. In addition, stress relaxation behavior of various cases, such as during fuselage pressurization, was studied under three different environmental conditions and at three different stress levels. Both fatigue and stress relaxation tests provide vital design data for long-term durability of adhesive-bonded structures. Fatigue tests showed that moisture absorption shortened the fatigue life of adhesive joints from lives at ambient room temperature or cold dry conditions. For most cases, stress relaxation tests indicated that the higher the stress level and test temperature, the higher the stress decay during relaxation. These results also revealed the danger of designing an adhesive structure to operate at temperatures near the glass transition temperature.

1. INTRODUCTION.

Increased confidence in composite materials have increased the use of adhesively bonded components in primary aircraft structures. Applications on primary structures require rigorous characterization of the material, unlike applications on secondary structures. Previously funded Federal Aviation Administration programs at the National Institute for Aviation Research at Wichita State University in Wichita, Kansas, have extensively researched thick bondline adhesive joint behavior, as well as adhesive joint behavior for a wide range of bondline thicknesses, with respect to several aircraft operating environmental conditions. The primary goal of this investigation was to characterize the long-term durability of adhesives. Two simultaneous procedures were used to characterize fatigue and stress relaxation behavior. In order to gain more information about high-stress behavior (low-cycle fatigue), stress amplitudes resulting in adhesive failure at low levels of 1,000 to 100,000 cycles were determined, and subsequent tests were conducted at those levels, including temperature and frequency dependence of adhesive joints. In addition, stress relaxation behavior of various cases, such as during fuselage pressurization, was also investigated under three different environmental conditions and at three different stress levels.

Typical commercial transport aircraft may be required to fly as many as 60,000 hours over a span of 30 years and 20,000 flights, plus approximately 100,000 miles in taxi operations. During this period of time, commercial aircraft structures will experience thousands of fatigue cycles at high and low magnitudes under many adverse climatic conditions. On the other hand, typical military aircraft designed for 6000 hours of service operations are subject to fatigue cycles at higher magnitudes due to extreme accelerations and maneuvers.

Because bonded joints are preferred over riveted, spot-welded, and fastened structures [1, 2, 3], the use of bonded structures has been growing in the aircraft industry over the past few years. Based on a lack of reliable methods for stress analysis and life prediction, particularly for low-cycle, high-stress levels under cold (-40°F), wet, and room temperature conditions (which are representative of service conditions where fatigue exists), this document aims to provide an understanding of adhesive behavior. To accomplish the previously mentioned goals, stress amplitudes producing failure at 10^3, 10^4, and 10^5 cycles were determined. In addition, frequencies of 2, 5, and 10 Hz were investigated to determine the frequency sensitivity of adhesives. The stress ratio, R (minimum stress/maximum stress), was kept at 0.1.

Aircraft cyclic loads are classified into three main groups depending upon frequency: (1) pressurization and depressurization, considered low-cycle fatigue, (2) gust loading, considered intermediate-to-high-cycle fatigue, and (3) acoustic and buffeting loading, representative of high-cycle fatigue. Fatigue testing conducted in this investigation focused on intermediate cycles but high-stress levels. Stress levels needed to cause failure at 1,000, 10,000, and 100,000 cycles were determined based on signal to noise ratio (S-N) curves generated through an initial fatigue study. These levels were mostly beyond the linear-limit but below the knee point of the shear stress-strain curves. Fatigue testing was performed according to the modified ASTM test method for fatigue properties of adhesives in shear by tension loading (ASTM D 3166-99). The standard specimen configuration consisted of thin adherend single lap joints, which have stress concentrations and generate unreliable results, as reported by Hart-Smith [4]. Therefore, the

specimen was modified according to the ASTM test method for thick adherend metal lapshear joints for determination of the stress-strain behavior of adhesives in shear by tension loading (ASTM D 5656), which uses 0.375-inch-thick aluminum adherends. Since the effect of fatigue on thick bondline joints has not been widely investigated, a modified ASTM D 3166-99 procedure for single lap shear specimens with 0.375-inch thickness phosphoric acid-anodized aluminum adherends. Thick adherends were used to minimize the peel effect of the adhesive test section, which facilitates the investigation of adhesive behavior rather than joint behavior during fatigue.

Marceau, et al. [5] performed fatigue tests on thick adherend (2024-T3) lap shear and double cantilever beam (DCB) specimens. They studied the effects of environmental conditions (room temperature, elevated temperature, and wet specimens conditioned at 140°F) at different stress levels and frequencies (0.8 cph, 10 cph, and 1800 cpm) using sinusoidal and trapezoidal waveforms at a fixed stress ratio of R = 0.06. Their results showed 100 percent cohesive failure for wet specimens, which also survived a lower number of cycles than specimens tested at room temperature. The lowest frequency produced the most severe and damaging case. In 1978, Romanko [6] tested FM-73M using thick adherend (0.25-inch-thick bare aluminum 7075-T651, alkaline-cleaned, and phosphoric acid-anodized) single lap shear joint specimens under different environmental conditions with a wide range of fatigue loads at low-cycle frequencies (10^{-4}, 10^{-2}, 3, and 30 Hz). The adhesive thickness was set at 45 mils (0.045 inch), and the group of specimens was conditioned at 150°F and 100% relative humidity (r.h.) for suitable periods of time. The sinusoidal waveform with a stress ratio of R = 0.1 was used for test temperatures ranging from -65° to 140°F. The shear strain was calculated using the KGR extensometer data. Results showed the influence of moisture on fatigue life. Additionally, optical and Scanning Electron Microscope analysis indicated two types of failure modes in the overlap area. The first was an adhesion failure in the high-stress region of the overlap (edges of the gage section), called the slow crack growth or adhesive-failed zone. The second was a cohesive failure in the region between the edges, called the fast crack growth or cohesive-failed zone. Both are shown in figure 1-1. These failure modes changed as a function of length, depending on environmental conditions and frequency. Furthermore, attempts to measure crack growth using the da/dN theory, as in metals, proved to be unsuccessful. Sancaktar [7 and 8] showed that the thick adherend single lap joints were better than thin adherend specimens for quantitative purposes.

Bethune [9] and Kinloch, et al. [10] studied the fatigue behavior of DCB specimens using linear elastic fracture mechanics and developed mechanistic models measuring the rate of crack growth per cycle (da/dN) as a function of the strain energy release rate (ΔG). The data obtained was used to predict the number of cycles to failure on single lap joints. The equation obtained was a function of the geometry, adherend properties, maximum applied load per width, and strain energy. Though frequency and environmental conditions were not taken into account, analytical results were comparable with test results.

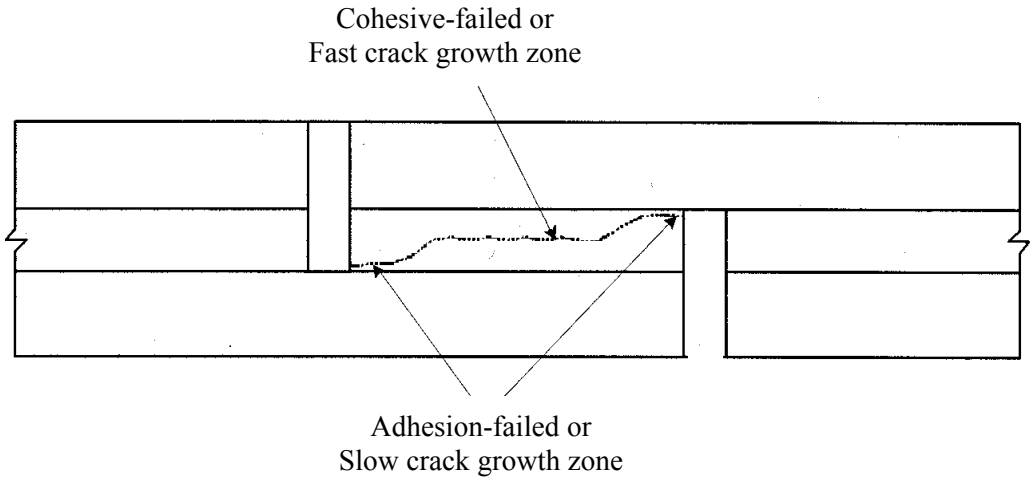

FIGURE 1-1. FAILURE MODES IN THE OVERLAP REGION

To determine the most suitable analysis method for dealing with the overdesign tendency in bonded structures, Broughton and Mera [11] reviewed different approaches (mechanistic, fracture mechanic, and stress analysis models plus finite element analysis packages). They found that a statistical approach using a two-parameter Weibull function could be used to predict the fatigue life of bonded joints subjected to different environmental conditions and frequencies. In addition, they showed that fracture mechanics models have a high potential for predicting the fatigue life of bonded single lap joints, even when the equations involved are relatively complex. They also emphasized the fact that from the design engineer point of view, crack initiation stress or energy is the most important piece of information within stress analysis.

Section 3.3 describes the stress relaxation in detail, including a mathematical representation of the theory. When a material is loaded rapidly and then held, the applied stress will decrease and asymptotically approaches a constant value in time. This loss of stress is called stress relaxation. In this time frame, the initial elastic strain is gradually replaced by creep strain until the asymptotic stress value is obtained. The stress relaxation is idealized by using spring and dashpot rheological models, which assume steady-state creep and linear viscoelastic material behavior. Depending on the combination of springs and dashpots in the rheological model, the stress relaxation material response may vary. The stress relaxation behavior was idealized by a three-parameter equation, which was obtained by curve fitting the experimental data.

2. MATERIALS AND SPECIMEN FABRICATION.

This section discusses the adhesive and adherend materials used in this investigation along with the test matrices for static, fatigue, and stress relaxation tests.

2.1 ADHESIVES.

This study investigated the fatigue and stress relaxation behaviors of one film adhesive and two paste adhesives. Two epoxy adhesive systems were selected based on the results of a previous investigation [12], which generated characteristic shear responses of 18 different structural adhesive systems. The following adhesives were used:

- HYSOL EA9696—Moisture-resistant modified epoxy film used in structural repair of composites, cure and co-cure of composite laminates, metals and honeycomb bonding, and some space applications designed to survive extreme temperature exposure.

- PTM&W ES6292—Two-part epoxy adhesive cured at elevated temperature, suitable for composite laminates as well as metallic substrates, and ideal to bond highly irregular surfaces.

- Loctite—Two-part epoxy adhesive cured at elevated temperature and pressure, designed for Cessna Aircraft in Wichita, Kansas.

The EA9696 and Loctite adhesives were supplied by Cessna Aircraft of Wichita, Kansas, and the ES6292 adhesive was supplied by Cirrus Design of Duluth, Minnesota.

2.2 ADHEREND.

Each adhesive test panel was fabricated by bonding two 10- by 10-inch 2024-T3 aluminum subpanels with a thickness of 0.375 inch. All subpanels were phosphoric acid-anodized, creating aluminum oxide layers with a fibrous-like shape. This method has demonstrated its superiority in previous studies by Brockmann [13], who concluded, based on the nature of bond mechanisms, that the adhesive mechanism is unstable when the Forest Products Laboratory (FPL) etching process is used compared to the chromic acid-anodizing process. Additionally, McMillan [14] showed the superiority of phosphoric acid anodizing, mainly because the thickness of the oxide layer is increased considerably compared to the FPL process. In addition to the thickness increment, this treatment makes the oxide layer stronger but not brittle, wettable by the adhesive, suitable for mechanical hooking, and environmentally stable and durable.

Phosphoric acid-anodized and bond-primed aluminum subpanels were supplied by Cessna Aircraft Company of Wichita, Kansas.

2.3 TEST MATRIX.

Test specimens were categorized into three groups:

1. Static
2. Fatigue
3. Stress Relaxation

In order to determine the stress levels for fatigue tests and the percentage of yield for stress relaxation testing, the characteristic shear response of each adhesive with relevant bondline thickness was generated according to the ASTM D 5656 test standard. Three replicates for each adhesive/bondline thickness for six different environmental conditions were tested (table 2-1).

TABLE 2-1. TEST MATRIX FOR STATIC TESTING

	Bondline Thickness (in)	-40°F	RTD	RTW	150°F	180°F	210°F
EA9696	0.020	3	3	3	3	3	3
Loctite	0.032	3	3	3	3	3	3
ES6292	0.060	3	3	3	3	3	3
ES6292	0.160	3	3	3	3	3	3

Fatigue tests were conducted under room temperature ambient (RTD), room temperature wet (RTW), and -65°F dry (CTD) conditions, and stress relaxation tests were conducted at 150°, 180°, and 210°F elevated temperature dry (ETD). Tables 2-2 and 2-3 show that a minimum of 324 fatigue specimens and 144 stress relaxation specimens, respectively, were tested for adhesive durability as there were three adhesives and an additional adhesive thickness for ES6292. As shown in table 2-2, cyclic stress levels were chosen to obtain failures at 1,000, 10,000, and 100,000 cycles. The stress levels, which correspond to the above-mentioned number of cycles, were determined using the initial S-N curves generated for each adhesive.

TABLE 2-2. TEST MATRIX FOR FATIGUE TESTING OF EACH ADHESIVE AND BONDLINE THICKNESS

Stress Level	Cycles to Failure	Frequency (Hz)	Number of Specimens		
			CTD	RTD	RTW
1	1,000	2	3	3	3
	1,000	5	3	3	3
	1,000	10	3	3	3
2	10,000	2	3	3	3
	10,000	5	3	3	3
	10,000	10	3	3	3
3	100,000	2	3	3	3
	100,000	5	3	3	3
	100,000	10	3	3	3

TABLE 2-3. TEST MATRIX FOR STRESS RELAXATION TESTING OF EACH ADHESIVE AND BONDLINE THICKNESS

Stress Level (% of Yield Strength in Shear)	Number of Coupons		
	150°F	180°F	210°F
0	3	3	3
10	3	3	3
15	3	3	3
25	3	3	3

Specimens corresponding to 0% yield strength in table 2-3 were conditioned under the prescribed temperatures for 400 hours (approximately 2 weeks) and then tested at the same temperatures according to ASTM D 5656 test standard to determine the apparent shear strength and shear modulus. Subsequently, these data were compared with static tests conducted under corresponding temperatures.

Yield strength was determined by the intersection of the tangent drawn to the bilinear constitutive behavior, as shown in figure 2-1. For specimens that did not indicate bilinear constitutive behavior, a horizontal line was drawn across the maximum stress, and its intersection point with the initial linear curves was used to determine the yield point.

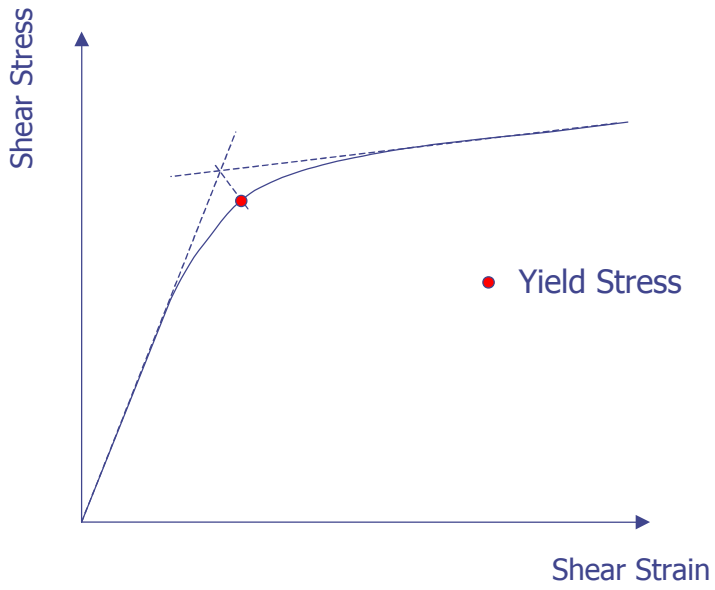

FIGURE 2-1. YIELD STRESS DETERMINATION

In addition, the glass transition temperature, Tg, of each adhesive was determined according to Suppliers of Advanced Composites Materials Association SRM 18-94 for dry specimens.

2.4 SPECIMEN NOMENCLATURE.

Test panels were cured according to specifications provided by the manufacturer. Then the adhesive lap shear specimens were machined according to the test standard recommendations of ASTM D 5656 using a Bridgeport® CNC machine. Tool paths were created using MasterCam Version 9. A detailed description of machining single lap shear adhesive specimens according to the dimensions given in ASTM D 5656 is included in reference 12.

For tracking purposes following machining, specimens were identified using the nomenclature shown in figure 2-2. This convention was used for static, fatigue, and stress relaxation specimens. The first and second letters correspond to adhesive type and bondline thickness, respectively. The third letter represents the type of loading condition, i.e., fatigue, stress relaxation, or static. The fourth and fifth characters represent stress level and frequency. The last three characters represent panel identification number, specimen number, and test condition, respectively.

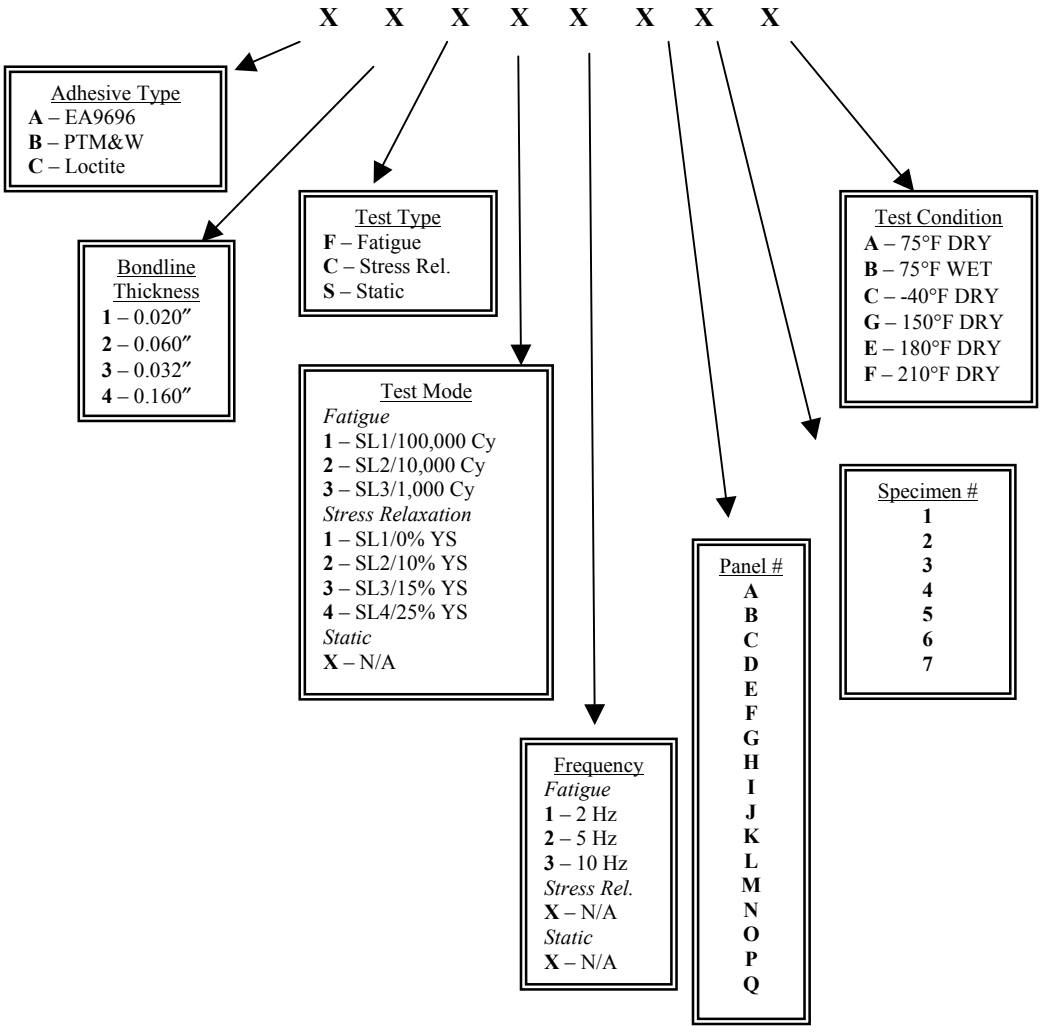

FIGURE 2-2. NOMENCLATURE FOR ADHESIVE TEST SPECIMENS

3. EXPERIMENTAL PROCEDURE.

Specimens were measured using digital calipers and micrometers that automatically record the dimensions in a data file. Two gage width readings, two gage length readings, and two gage thickness readings were recorded. The adhesive layer thickness was calculated by subtracting the two subpanel thicknesses, which were recorded before panel fabrication, from the final panel thickness after adhesive cure.

Wet test specimens were conditioned at 145°F and 85% r.h. for a period of 1000 hours (approximately 42 days) [15] in a humidity chamber in the National Institute Aeronautical Research Composites Laboratory at Wichita State University. Following conditioning, specimens were removed from the chamber, placed in polyethylene bags with wet cotton towels, and stored inside a cabinet to prevent exposure to light or heat until testing.

3.1 ADHESIVE CHARACTERIZATION.

Adhesives exhibit either brittle or ductile behavior. Brittle failure is abrupt, showing no significant elongation of the material. In other words, adhesives showing brittle failure are considered intolerant to stress concentrations. On the other hand, ductile materials can still be loaded after substantial yielding due to plasticity. The point at which the load applied on the specimen remains constant is typically associated with plastic deformation. Previous investigations have shown that adhesives exhibit brittle behavior under low temperatures and ductile behavior at higher temperatures.

To determine fatigue stress levels, static tests were performed on adhesive specimens, and characteristic shear responses were generated for each environmental condition. These tests were conducted according to recommendations in the ASTM D 5656 test standard for tension loading under the displacement control mode. Two self-aligning clevis fixtures were used at each end of the specimen, thus allowing the long axis of the specimen to coincide with the direction of the applied load. Two half-inch steel bushings were inserted into the loading holes of the specimen, and 0.375-inch steel dowel pins were used to attach the specimen to the clevis arrangement. Tests were performed on a 22-kip MTS servo-hydraulic load frame at a fixed rate of 0.05 inch per minute. Tests were conducted using a computer-controlled environmental chamber connected to a low-pressure liquid nitrogen tank, typically used for cryogenic temperature tests. Two thermocouples, one attached to the chamber wall and the other taped to the gage section of the specimen, monitored the temperature. Once both thermocouples reached the targeted temperature, the specimen was exposed to 3 minutes of soak time. During testing, the temperature was maintained within ±3°F of the targeted value.

Shear deformation was recorded with two modified four-pin, KGR-type extensometers (figure 3-1) to reduce the rotation and slippage of the extensometer attachment caused by peeling stresses [16]. This modified extensometer with an additional fourth pin was developed to characterize thick adherend lap shear adhesive specimens [12, 17, and 18]. Two of these modified extensometers were mounted using the attachment holes drilled on the port and starboard sides of the specimens. The KGR extensometer was originally developed by Krieger [19], who used a three-pin configuration. Measurements of adhesive layer movement and data

were recorded, and characteristic shear responses of the adhesives were plotted according to the ASTM D 5656 test method. Figure 3-2 shows a typical characteristic shear response for a structural adhesive. Characteristic shear responses of each adhesive for each environmental condition were used to obtain the linear limit, knee point, ultimate strength, yield stress, etc., which were useful in determining fatigue and stress relaxation test parameters.

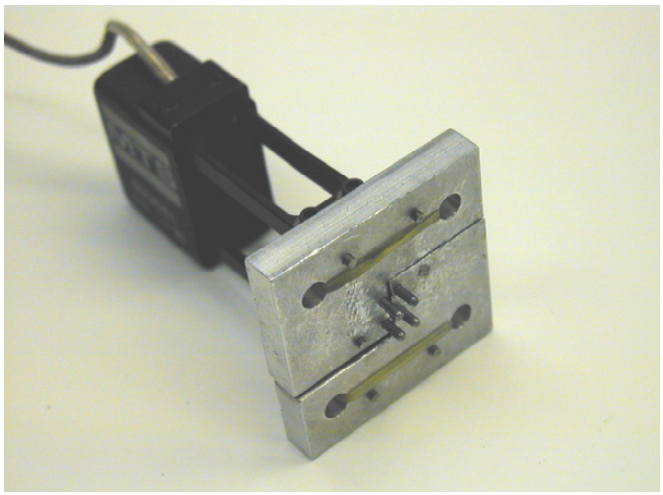

FIGURE 3-1. MODIFIED KGR-TYPE EXTENSOMETER

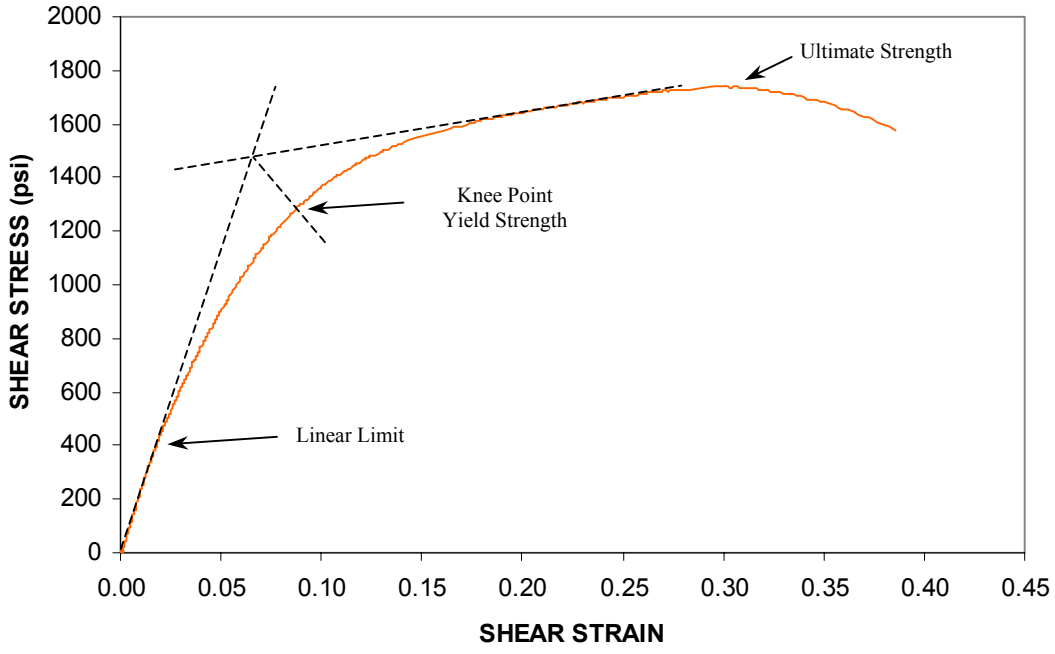

FIGURE 3-2. TYPICAL ADHESIVE STRESS-STRAIN CURVE USING KGR-TYPE EXTENSOMETER DATA

3.2 FATIGUE OF ADHESIVE JOINTS.

Specimens were mounted inside the test machine using a clevis fixture arrangement similar to the one used for static testing. Fatigue tests were performed on two MTS servo-hydraulic test machines under force control mode. Using MTS Basic TestWorks® software (figure 3-3), specimens were loaded in a sinusoidal waveform and tension-tension mode with a fixed stress ratio of R = 0.1 (minimum stress/maximum stress) for all conditions.

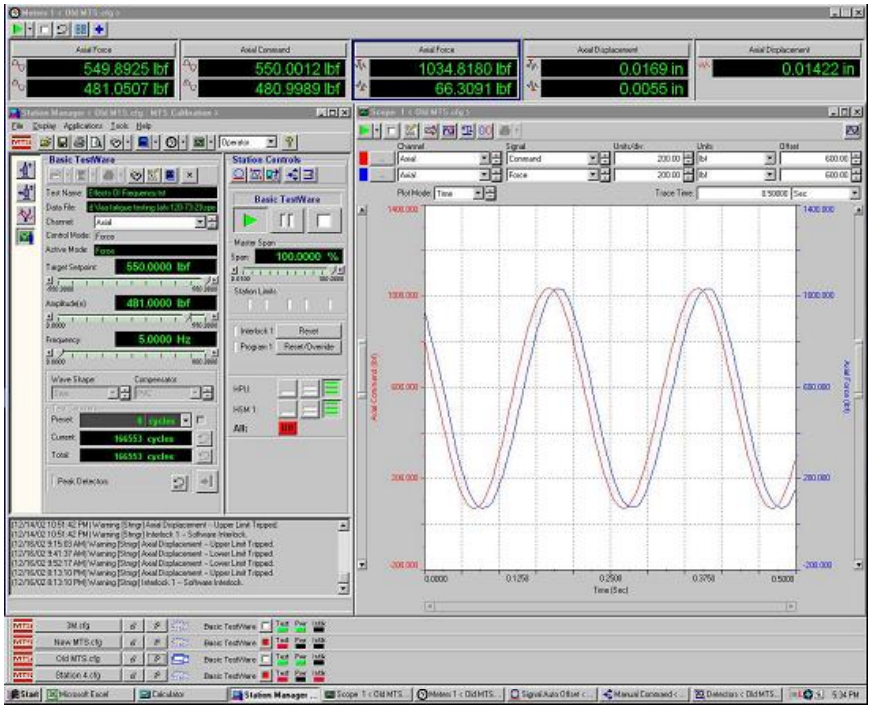

FIGURE 3-3. MTS BASIC TESTWORKS® WINDOW

3.2.1 S-N Curve Generation.

Since no previous fatigue data was available for the selected adhesives, initially only a few specimens were fatigued until failure to generate S-N curves under RTD conditions at 5 Hz. These curves were used to determine stress levels corresponding to the targeted number of fatigue cycles. The same S-N curves, with some adjustments, were used for all environmental conditions and frequencies.

3.2.2 Fatigue Test Setup.

Fatigue tests were performed according to recommendations in the ASTM D 3166 test method, with modification to the test specimen according to test standard ASTM D 5656 (thick adherend) in order to minimize peel stresses. In addition, the number of replicas recommended by test standard ASTM D 3166 was reduced to three instead of five. The present study was intended to characterize fatigue behavior of the adhesive rather than the joint. The thick adherend

minimized peel stresses as well as stress concentrations at the edges of the gage section, which affect the specimen's fatigue life. Based on the initial S-N curve data, stress levels corresponding to 1,000, 10,000, and 100,000 cycles were determined, and then the set point and amplitude were calculated with a stress ratio of 0.1. Test frequencies were set at 2, 5, or 10 Hz using MTS Basic TestWorks® software.

Cold temperature tests were conducted inside an environmental chamber (figure 3-4) attached to the MTS system, which maintained the cryogenic temperature by injecting liquid nitrogen through a solenoid valve connected to the controller. Each CTD test was started after a 3-minute soak time.

FIGURE 3-4. COLD TEMPERATURE TESTING (AFTER SPECIMEN FAILURE)

3.3 STRESS RELAXATION OF ADHESIVE JOINTS.

Stress relaxation tests were conducted using calibrated ALCOA stressing fixtures by monitoring the strain exerted on the rings during load application. Initial stress levels were determined as 10%, 15%, and 25% of the yield stress of the adhesive under test conditions. Specimens were fabricated according to the dimensions specified in test standard ASTM D 5656. Three test environments were selected for testing at 150°F, 180°F, and 210°F. Specimens were held at selected temperatures while monitoring the relaxation for 400 hours. Once testing was complete, the shear deformation of the material was photographed using a stereoscope. Specimens were then tested (static) according to ASTM D 5656 at corresponding test temperatures to obtain characteristic shear responses. In addition, some test specimens were conditioned at the above-mentioned temperatures for 400 hours and tested according to ASTM D 5656 to compare the characteristics of specimens tested for 3-minute conditioning at selected temperatures.

3.3.1 Theory.

When a material is loaded rapidly and then held, the applied stress will decrease and asymptotically approach a constant value in time. This loss in stress is called stress relaxation. The time it takes to reach the constant value, as well as the constant value itself, are dependant on viscoelastic characteristics of the material at a given temperature and magnitude of the applied stress. Stress relaxation is observed under constant strain rather than constant stress as in creep testing. During stress relaxation, some of the elastic strain that appears during initial rapid loading is slowly replaced by creep strain with the total of the two being constant, according to the constraint of the test [20]. For simplicity, most idealized models assume steady-state creep and linear viscoelastic material behavior, and therefore the relaxation behavior based on spring-dashpot rheological models.

In the Maxwell model (figure 3-5), the most simplistic stress relaxation model, the force on each spring-dashpot pair relaxes exponentially. This is expressed in terms of the modulus analogy, $G_i(t)$ —contribution of the *i*th pair to the modulus, given by equations 3-1 and 3-2, in which the time constants τ_i, the relaxation times, are defined as η_i/G_i. Even though the rheological model geometry corresponds to an extension rather than shear loading, the mathematical analogy is valid for both load cases.

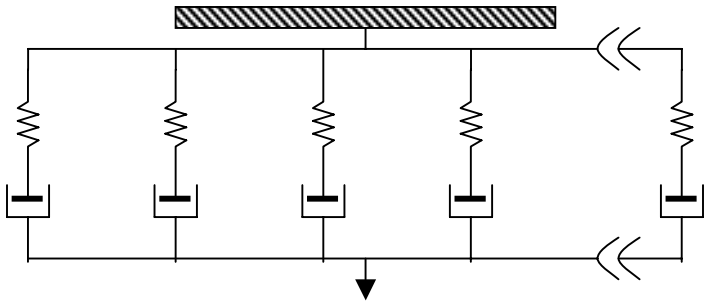

FIGURE 3-5. GENERALIZED MAXWELL MODEL [21]

$$\tau_i \equiv \frac{\eta_i}{G_i} \tag{3-1}$$

$$G(t) = \sigma(t)/\gamma = \sum_i G_i e^{-t/\tau_i} \tag{3-2}$$

where

τ_i = relaxation time for *i*th element (spring-dashpot configuration)
η_i = viscosity contribution of *i*th dashpot
$G_{(t)}$ = relaxation shear modulus
$\sigma_{(t)}$ = shear stress at time t
γ = shear strain
G_i = shear modulus contribution of *i*th spring element

For a solid, *G(t)* approaches a constant finite value *(G_e)*, resulting in an added constant term G_e in equation 3-3 using the rheological model shown in figure 3-6 [21]. The asymptotic value of equation 3-3 is an important design parameter, as it represents the maximum safe stress value below which creep failures are not expected to occur [22].

$$\sigma = G_e\varepsilon' + (G_1 - G_e)\varepsilon' e^{-(G_1+G_2)t/\eta_2} \tag{3-3}$$

where

$$G_e = \frac{G_1 G_2}{G_1 + G_2} \tag{3-4}$$

Dowling [20] explained stress relaxation by using the rheological model, which is similar to the Hata model shown in figure 3-6 that was later simplified to the three-parameter equation detailed in the next section.

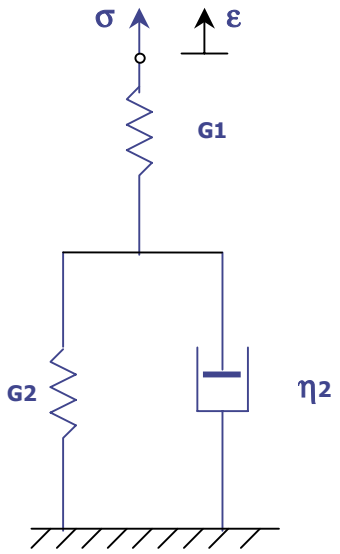

FIGURE 3-6. HATA MODEL FOR MECHANICAL RESPONSE OF ADHESIVE JOINTS

3.3.2 ALCOA Stressing Fixture.

The ALCOA stressing fixture dimensions were designed according to a finite element analysis that provide sufficient sensitivity but not exceed the linear elastic limit of the material for the applied load. Nine steel rings were machined and calibrated using four strain gages (full-bridge) mounted on each ring (figure 3-7). During calibration, a load cell was mounted and both strain and the applied load at each test environment were recorded. Representative curves are shown in figure 3-8. Using these curves, the measured strain percentage during relaxation testing can be converted to an applied stress. In addition, a solid aluminum specimen was tested at 210°F with an applied load of 200 lbf (worst-case scenario) to determine fixture compliance.

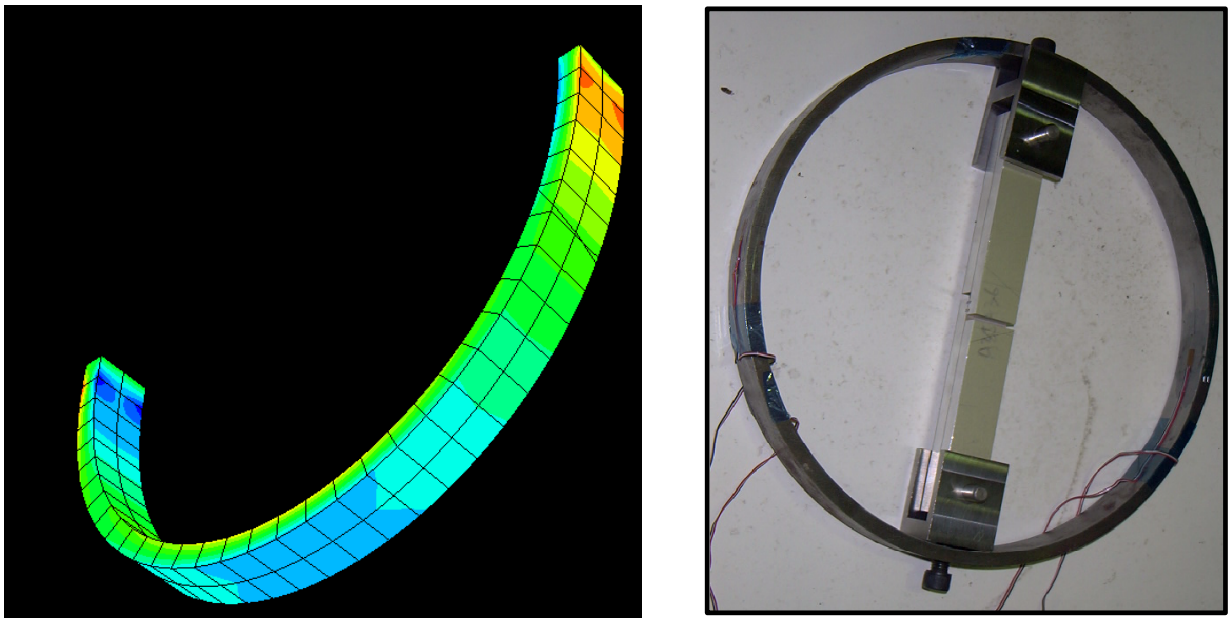

FIGURE 3-7. ALCOA STRESSING FIXTURE FOR STRESS RELAXATION TESTING

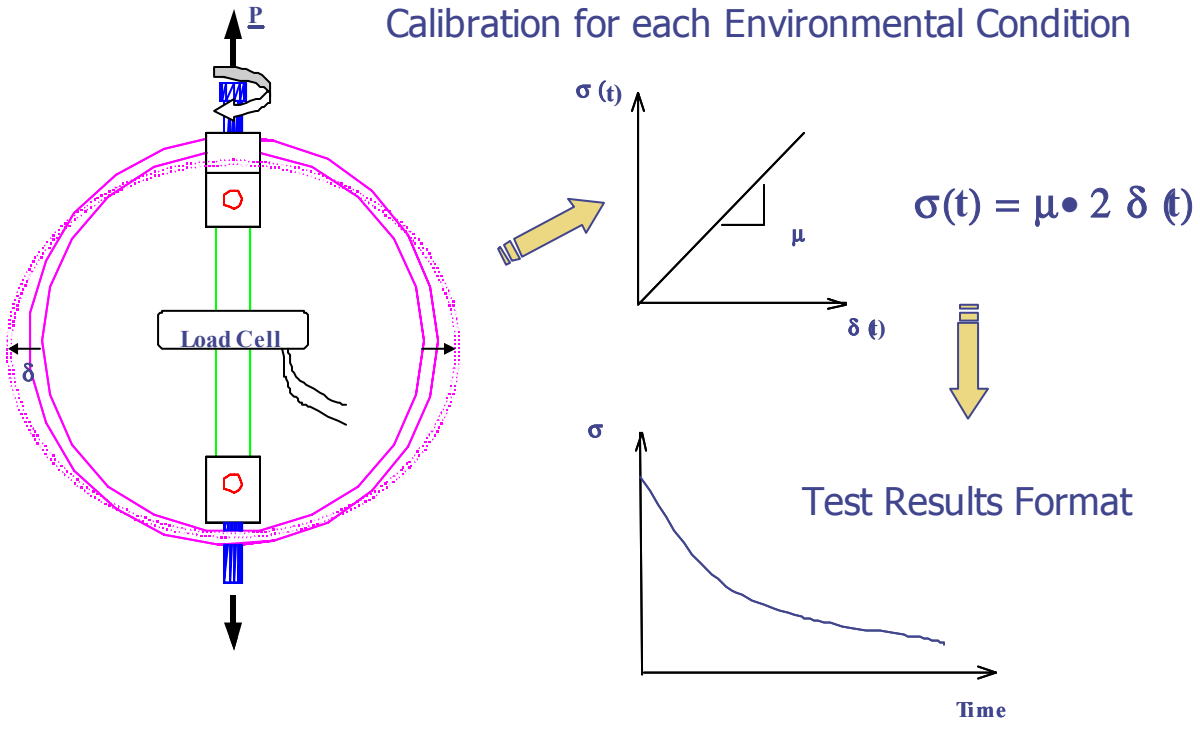

FIGURE 3-8. REPRESENTATIVE CURVE GENERATION FOR LAP JOINT SPECIMEN TESTING

3.3.3 Data Reduction.

The viscoelasticity of the adhesive material is often modeled by a combination of spring and dashpot models, as shown in figures 3-5 and 3-6. In such models, springs and dashpot(s) represent elasticity and viscosity, respectively, by assuming a linear viscoelastic behavior of the material [23].

Strain data acquired during relaxation testing were converted into stress relaxation plots using representative curves, as shown in figure 3-8. Then the test data were curve-fitted using TableCurve software with three-parameter viscoelastic equations in the following form:

$$\sigma \approx a + b \cdot \exp(-c \cdot t) \tag{3-5}$$

where, σ and t are shear stress and relaxation time, respectively, and a, b, and c are fitting parameters.

These curve-fitting parameters were developed using a rheological model, as shown in figure 3-6, by coupling the simple Kelvin-Voigt model [24] with an additional spring. Assuming linear viscoelastic behavior of the material, the relaxation under constant strain was modeled as follows:

$$\sigma = G_e \cdot \varepsilon' + (G_1 - G_e) \cdot \varepsilon' \cdot \exp[-(G_1 + G_2) \cdot t / \eta 2] \tag{3-6}$$

where

ε' = Total strain
η = Dashpot viscosity
G_1 = Shear modulus at test temperature according to ASTM D 5656 test method
G_e = Shear modulus at test temperature (ASTM D 5656) after relaxation test
G_2 = Calculated as in equation 3-4

Therefore, curve-fitting parameters can be expressed as follows:

$$a = G_e \cdot \varepsilon' \tag{3-7a}$$

$$b = (G_1 - G_e) \cdot \varepsilon' \tag{3-7b}$$

$$c = (G_1 + G_2) / \eta_2 \tag{3-7c}$$

Curve-fitted data assume the form shown in figure 3-9. The stress relaxation results for all three stress levels were plotted in the same graph under each environmental condition. In addition, the change in stress ($\Delta\sigma$ (= σ_0 - $\sigma(t)$) was tabulated for each condition.

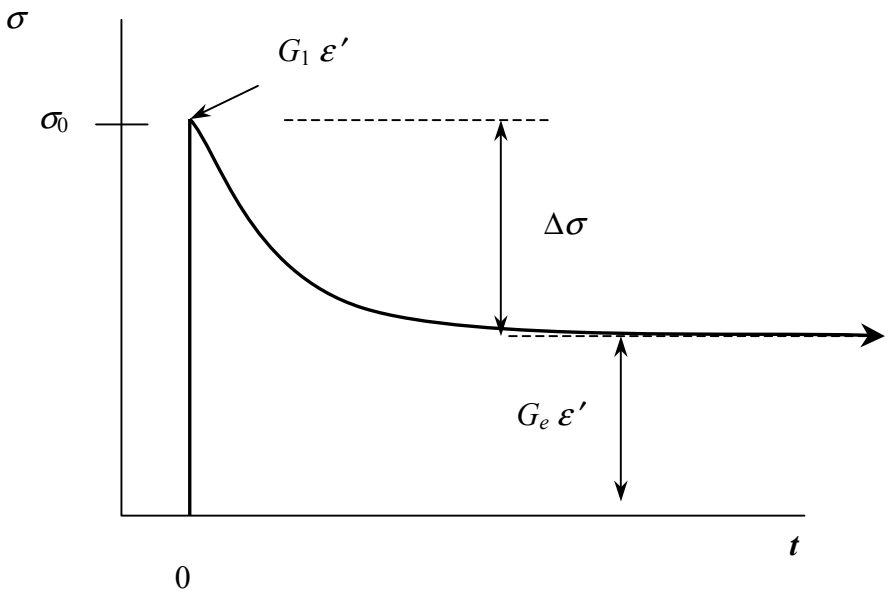

FIGURE 3-9. RELAXATION UNDER CONSTANT STRAIN FOR THE THREE-PARAMETER LINEAR VISCOELASTIC MODEL

3.4 FAILURE MODES.

To characterize an adhesive for various environmental conditions, the failure mode must be evaluated. The bonded joint failure mode depends on bondline thickness, frequency (for fatigue tests), environmental conditions, adherend material and thickness, surface preparation, etc. The failure mode of a bonded joint can be primarily categorized into three groups:

- Adherend failure or substrate failure is characterized by failure of the adherend rather than the adhesive. For metal and composite substrates, the adherend yielding (figure 3-10(a)) and interlaminar fracture (figure 3-10(b)), respectively, indicate joint failure rather than adhesive failure.

- Cohesive failure is characterized by bulk adhesive failure and is caused by either shear (figure 3-10(c)) or peel (figure 3-10(d)).

- Adhesion failure is characterized by a failure in the adhesive-adherend interface and is typically caused by inadequate surface preparation (chemical and/or mechanical) and water or moisture attack, where oxide layers created by phosphoric acid anodizing (for metal adherends) are easily separated from the adherend, causing catastrophic failure (figure 3-10(e)). Excessive peel stresses can also cause adhesive failure (figure 3-10(f)). This is a very undesirable failure mode.

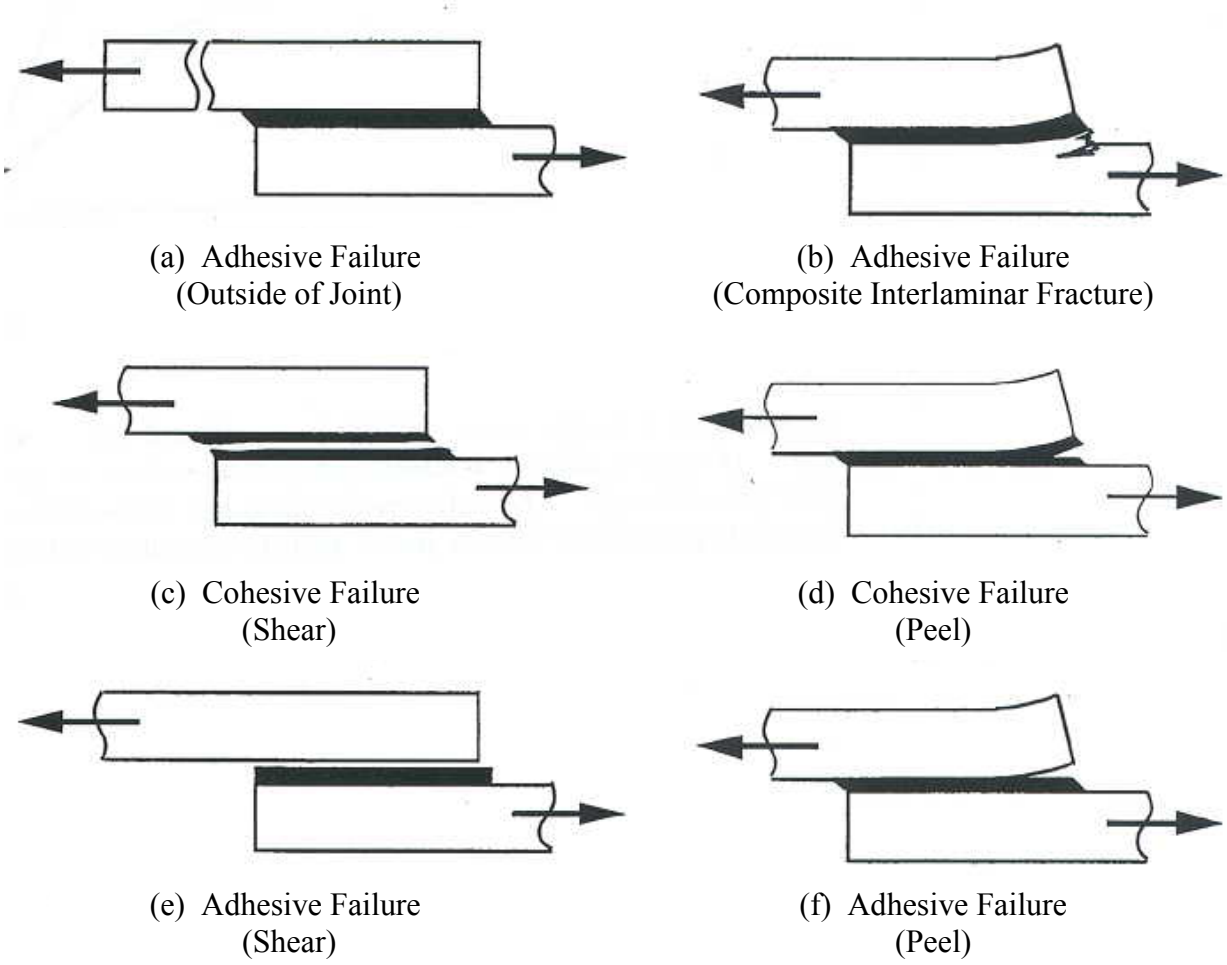

(a) Adhesive Failure (Outside of Joint)

(b) Adhesive Failure (Composite Interlaminar Fracture)

(c) Cohesive Failure (Shear)

(d) Cohesive Failure (Peel)

(e) Adhesive Failure (Shear)

(f) Adhesive Failure (Peel)

FIGURE 3-10. FAILURE MODES OF ADHESIVE JOINTS

4. RESULTS.

4.1 ADHESIVE CHARACTERIZATION.

The average values of apparent shear strength and initial modulus for all three adhesives under six environmental conditions are shown in table 4-1 and illustrated in figures 4-1 and 4-2. The characteristic shear responses and a comparison of apparent shear strengths and moduli for all adhesives can be found in appendix A. From the plots in appendix A, linear limit points and the ultimate stress for fatigue testing and yield stress for stress relaxation testing were determined.

Except for the CTD strength of ES6292 specimens, apparent shear strength and initial modulus results indicated the general trend that CTD > RTD > RTW > ETD. This is consistent with previous investigations [12]. As bondline thickness increased in these specimens, apparent shear strength decreased due to the unstable damage propagation in the adhesive [25]. These specimens exhibited brittle behavior and less plastic strain accumulations below the glass transition temperature compared to thin bondline data. Overall, ES6292 specimens indicated more brittle behavior compared to EA9696 and Loctite adhesives. EA9696 adhesive showed the highest strength values and the largest plastic strain accumulation for all six environmental conditions, indicating stable damage growth of these specimens.

The adhesives became stiffer (brittle) under CTD environmental conditions and weaker as temperature and moisture concentrations were increased. The plastic strain accumulation was directly proportional to the increment in temperature and moisture concentration. Moisture concentration did not have a considerable influence on apparent shear strength, compared to dry specimens at room temperature, but it had a significant influence on shear initial modulus. The apparent shear strength of ES6292 specimens was least affected by temperature and moisture concentration.

The most common failure modes observed under each environmental condition are shown in table 4-2. Failure analysis showed that the low-temperature condition tended to degrade the hydroxide layer formed by phosphoric acid anodizing and caused it to separate easily from the adherend surface. This layer was almost completely detached and stuck to the adhesive layer. One possible explanation for this might be the difference in the thermal expansion coefficient of the anodized layer and the adherend material. The RTW specimens mostly failed cohesively and were consistent with the theory that indicates moisture enters into the adhesive by diffusion through the adhesive, filling the free molecule spaces inside. Once these spaces are filled, water either pushes away the adhesive molecules or degrades the adhesive-adherend interface.

TABLE 4-1. AVERAGE APPARENT SHEAR STRENGTH AND INITIAL MODULUS

Adhesive	Avg. Bond Thick. (in)	Strength (ksi)						Initial Modulus (Msi)					
		-40°F	RTD	RTW	150°F	180°F	210°F	-40°F	RTD	RTW	150°F	180°F	210°F
Loctite	0.0338	4.946	2.924	2.504	1.518	1.752	1.010	0.0613	0.0513	0.0364	0.0254	0.0238	0.0046
EA 9696	0.0226	6.601	0.083	4.889	3.748	3.195	2.865	0.0827	0.0829	0.0610	0.0570	0.0493	0.0352
ES6292 0.06 inch	0.0710	2.986	3.187	3.110	2.122	1.975	1.113	0.1231	0.0878	0.0689	0.0697	0.0564	0.0371
ES6292 0.16 inch	0.1665	1.863	2.036	2.141	1.536	1.478	0.886	0.0923	0.0842	0.0726	0.0519	0.0518	0.0352

TABLE 4-2. FAILURE MODES OF STATIC SPECIMENS

Adhesion	-40°F	RTD	RTW	150°F	180°F	210°F
Loctite	Adhesion	Cohesive	Adhesion/Cohesive	Adhesion/Cohesive	Cohesive	Cohesive
EA 9696	Adhesion/Cohesive	Cohesive	Adhesion/Cohesive	Cohesive	Cohesive	Cohesive
ES6292 0.06 inch	Adhesion	Cohesive	Cohesive	Adhesion	Adhesion/Cohesive	Cohesive
ES6292 0.16 inch	Adhesion	Cohesive	Cohesive	Adhesion/Cohesive	Cohesive	Cohesive

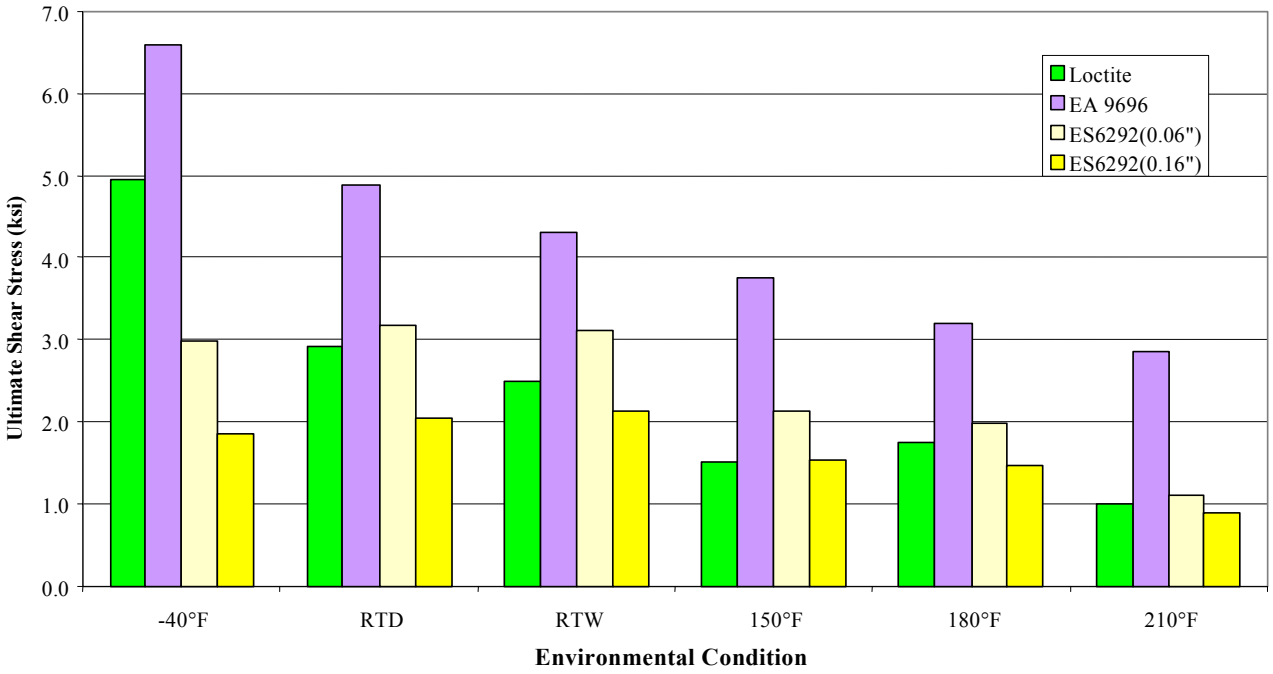

FIGURE 4-1. ULTIMATE SHEAR STRENGTH VS ENVIRONMENTAL CONDITION

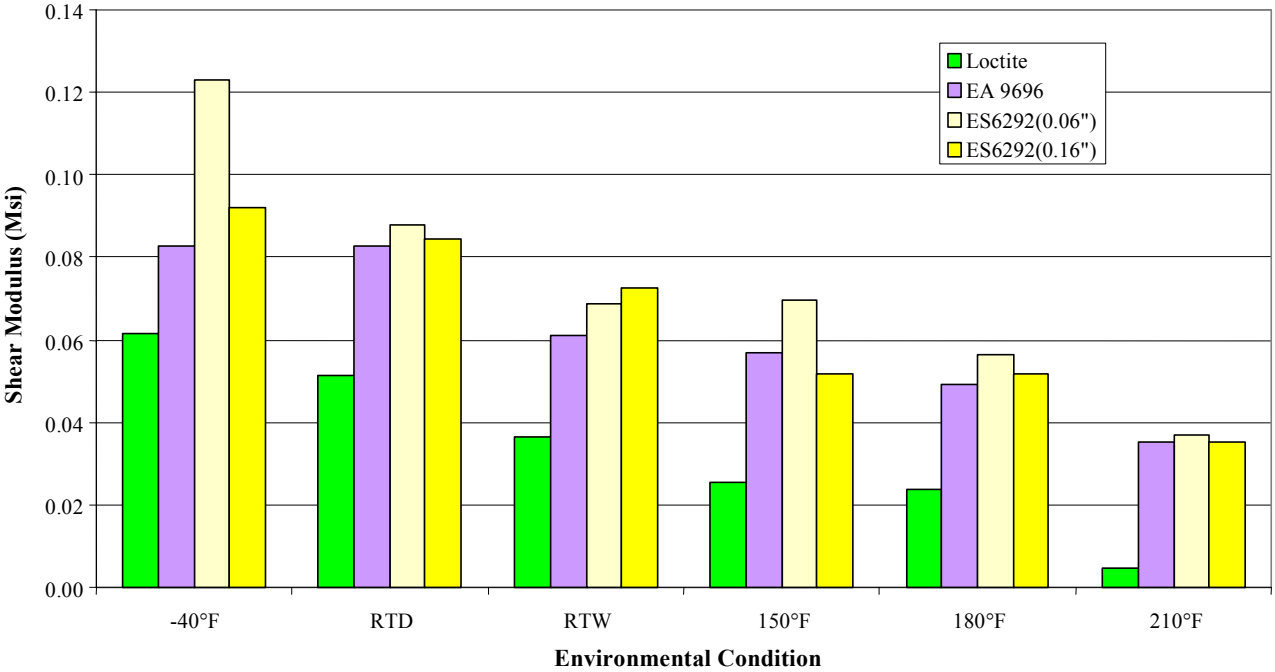

FIGURE 4-2. INITIAL SHEAR MODULUS VS ENVIRONMENTAL CONDITION

Stress levels for relaxation tests were determined at 10%, 15%, and 25% of yield stress, which was obtained using the bilinear constitutive behavior, as illustrated in figure 2-1. Figure 4-3 compares the yield stress of each adhesive for each environmental condition.

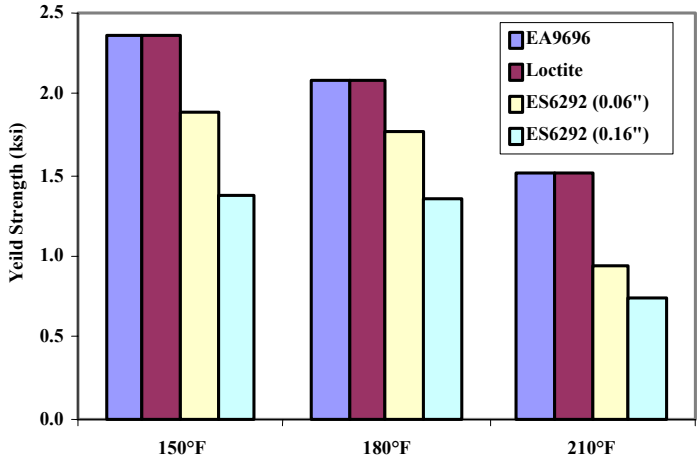

FIGURE 4-3. YIELD STRESS COMPARISON

4.2 FATIGUE TEST RESULTS.

For each adhesive stress, levels were chosen to expect failures at 1,000, 10,000, and 100,000 cycles by performing preliminary fatigue tests. The resulting S-N curves were then used to select the three stress levels. One such S-N curve generated from six specimens of Loctite adhesive shown in figure 4-4 is typical of data generated for the three adhesives. Once the stress levels were selected, they were superimposed on the static stress-strain curves to show in which zone, elastic or plastic, the stress levels fall. This is shown by plots in appendix B. This section discusses detailed fatigue results and failure modes for each adhesive.

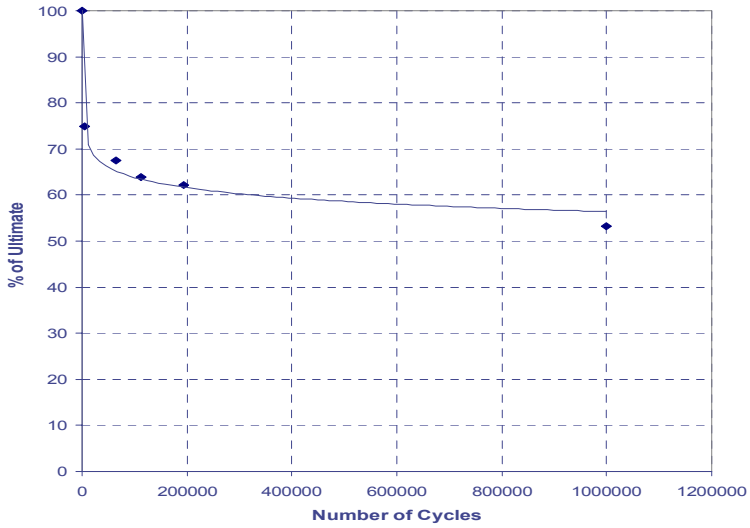

FIGURE 4-4. INITIAL S-N CURVE FOR LOCTITE ADHESIVE

4.2.1 Loctite.

The three stress levels selected from figure 4-4 were around 65%, 72%, and 78%, respectively, of ultimate stress under RTD conditions. Stress levels of Loctite fatigue specimens for all three environmental conditions, shown in figures B-1 through B-3, indicate that they were between the linear elastic limit and the knee point of the characteristic shear response.

Figures 4-5 through 4-7 show the effects of temperature and moisture concentration as well as the influence of frequency on the fatigue life of Loctite specimens for each stress level. Please note that the percentage of average ultimate shear stress for each adhesive, test environment, and bondline thickness was different; therefore, the magnitude of the applied stress levels was different for each case. Typically, the ultimate strength under CTD conditions is higher than under RTW conditions. Therefore, the fatigue stress levels selected for CTD conditions were higher than that of for RTW conditions.

Loctite test results indicated that moisture exposure weakened the fatigue life of adhesive joints more than the other two conditions. The second most damaging condition was CTD, but stress levels here were approximately 1000 psi higher than for RTD. Based on fatigue results for different frequencies, it was difficult to determine any significant influence of this parameter because the results were scattered throughout a wide range of failure cycles. As stress levels increased, the fatigue life of the adhesive was degraded as expected, except in a few cases, where the presence of voids precipitated early failures.

All fatigue stress levels that were tested were in the nonlinear zone of the stress-strain response, but unfortunately the levels were too close to each other to be able to define a reliable S-N curve, partly because the S-N curves are very flat. However, it should be noted that cyclic stresses below 40% of static ultimate load should assure long life under severe fatigue loads for this adhesive. It is also disturbing for RTW condition that an application of 200 cycles at about 50% ultimate strength can result in a fatigue failure.

The last three bars of figure 4-8 show the failure mode results for Loctite adhesive (i.e., for RTD, 93% of the specimens had adhesion failure and 7% had cohesive failure). For RTW, most of the failures were cohesive. In other words, moisture attacked the adhesive bulk and, in a few cases, migrated to the interface causing adhesion failure. The other two environmental conditions showed mostly adhesion failures, which usually result from inadequate surface preparation, weak adhesive forces acting across the adherend-adhesive interface, or high-peeling stresses. In this case, the brittle behavior of the adhesive under CTD conditions may have caused unstable damage due to thermal residual stresses during adhesive cure, which started at the adhesive-adherend interface. Figure 4-9 shows typical failure modes of Loctite under CTD, RTD, and RTW conditions.

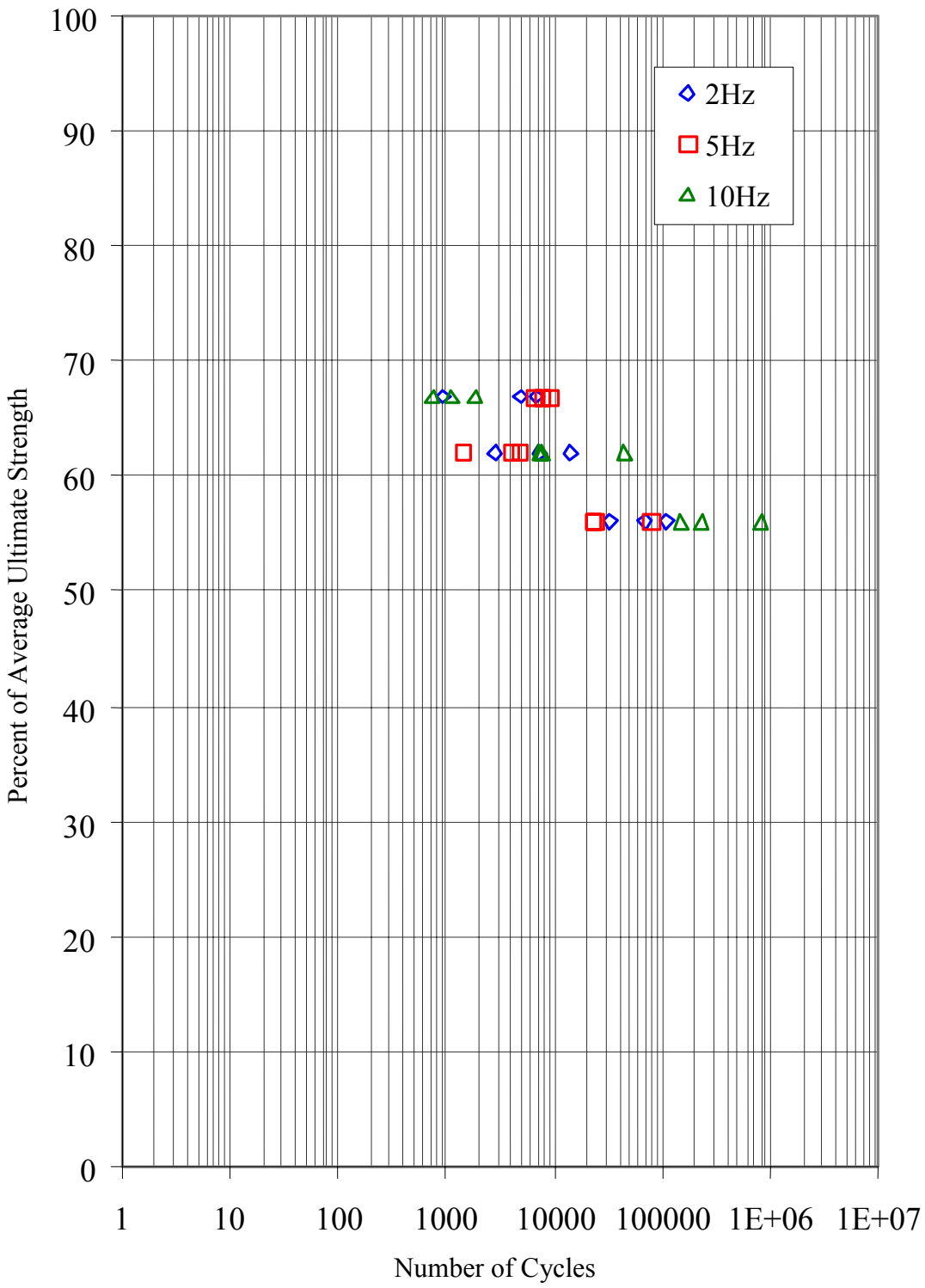

FIGURE 4-5. FREQUENCY INFLUENCE OF LOCTITE RESULTS UNDER CTD CONDITIONS

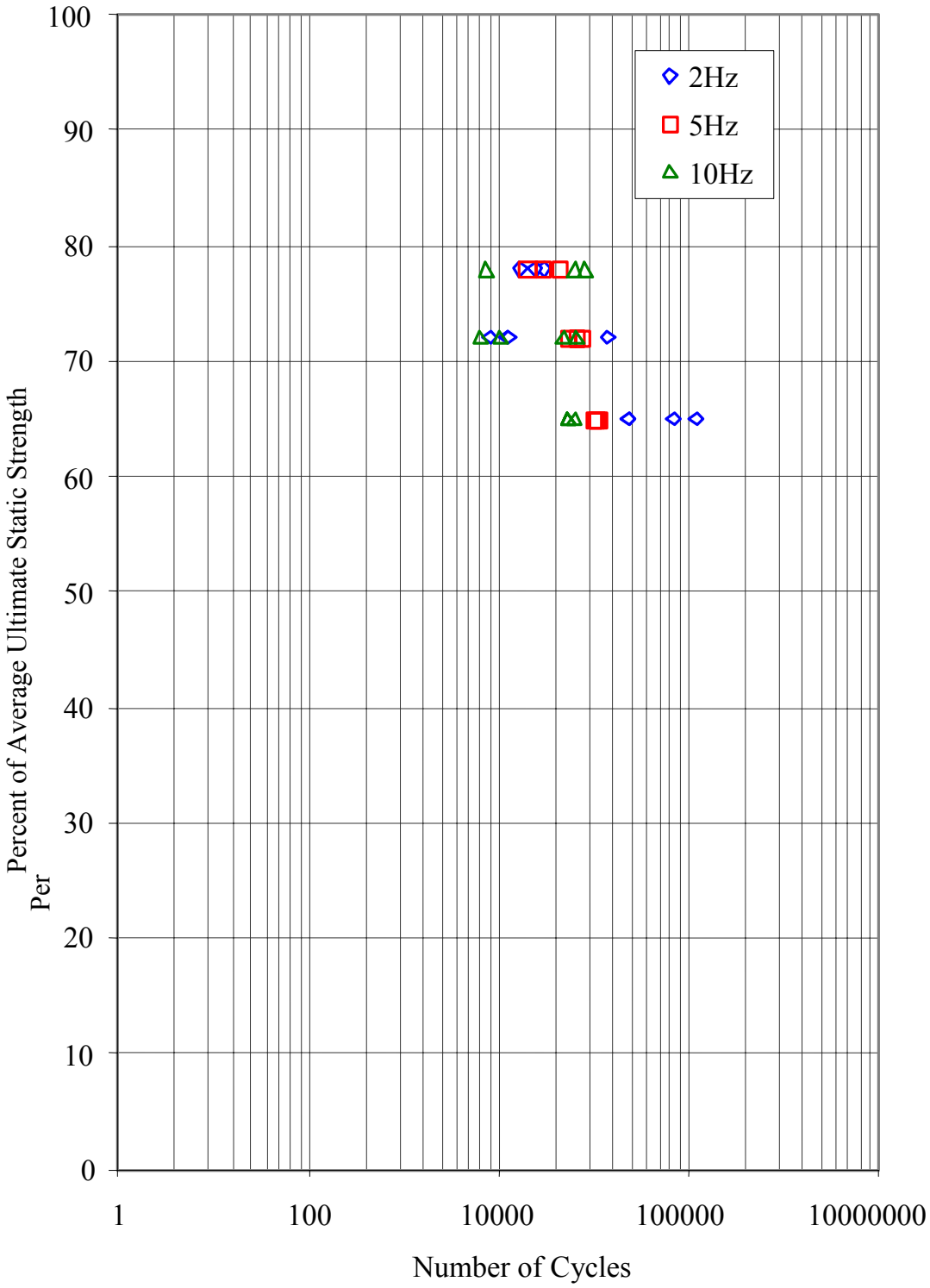

FIGURE 4-6. FREQUENCY INFLUENCE OF LOCTITE RESULTS UNDER RTD CONDITIONS

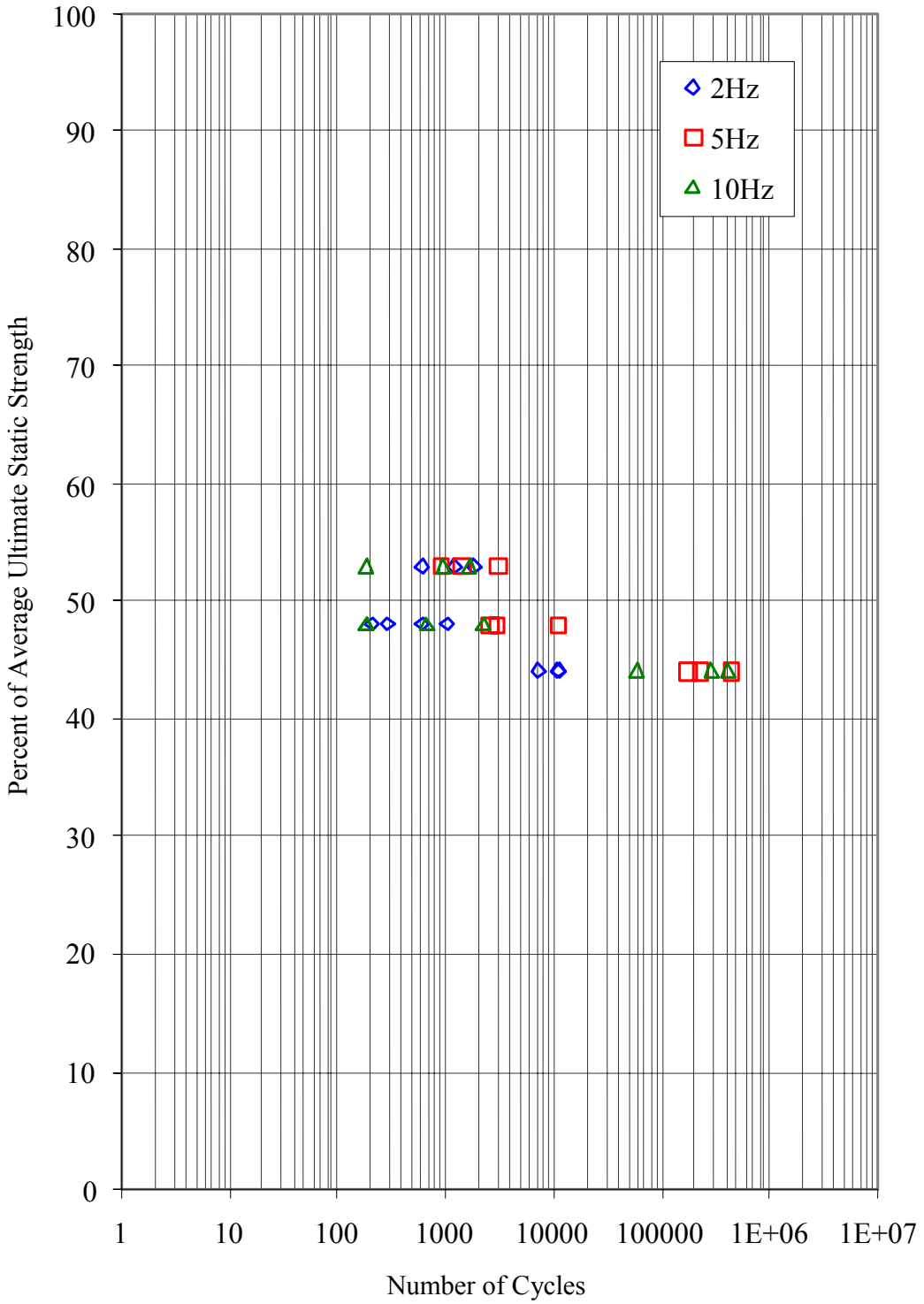

FIGURE 4-7. FREQUENCY INFLUENCE OF LOCTITE RESULTS UNDER RTW CONDITIONS

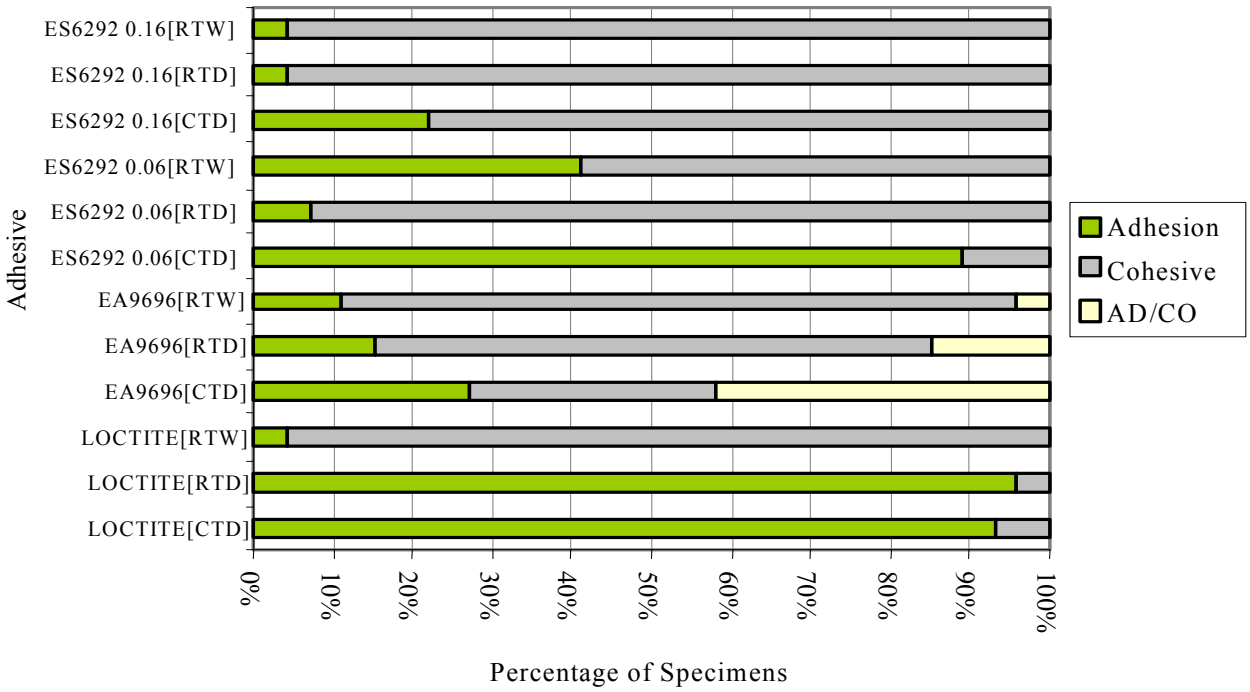

FIGURE 4-8. FAILURE MODES OF FATIGUE TEST SPECIMENS

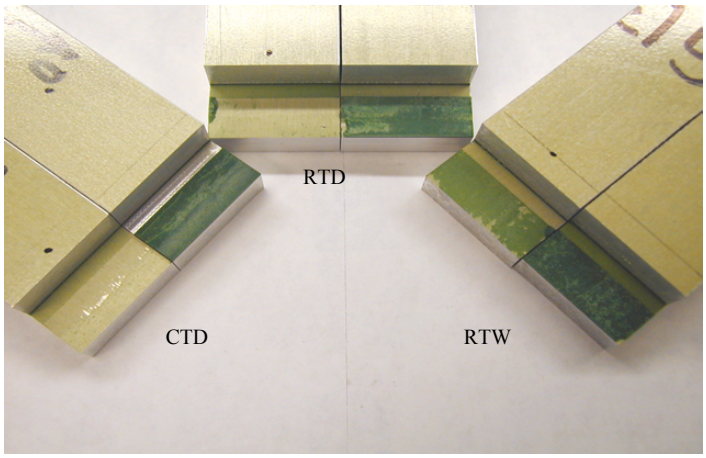

FIGURE 4-9. TYPICAL FAILURE MODES OF LOCTITE

4.2.2 EA9696.

Figures 4-10 through 4-12 show the effects of temperature and moisture concentration as well as the influence of frequency on the fatigue life of EA9696 adhesive specimens for each stress level. The stress levels at which the specimens were tested are shown in figures B-4 to B-6 in appendix B. Except for CTD results, data was scattered throughout a wide range of fatigue cycles and did not indicate any apparent influence of frequency. In most cases, RTW indicated the lowest fatigue life. CTD results indicated lowest and highest fatigue life at 2 and 10 Hz, respectively. However, for RTD, this was reversed.

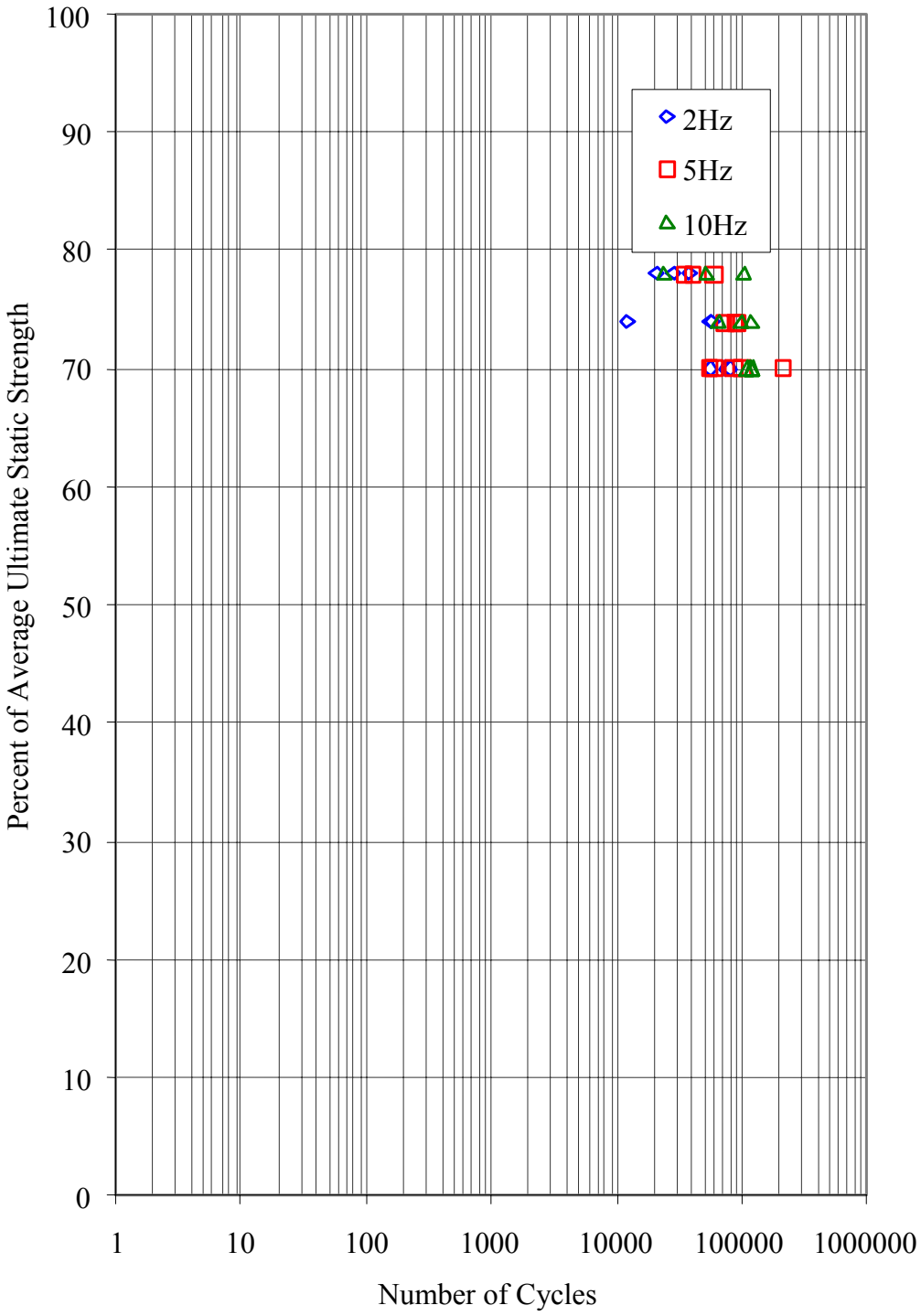

FIGURE 4-10. FREQUENCY INFLUENCE OF EA9696 RESULTS UNDER CTD CONDITIONS

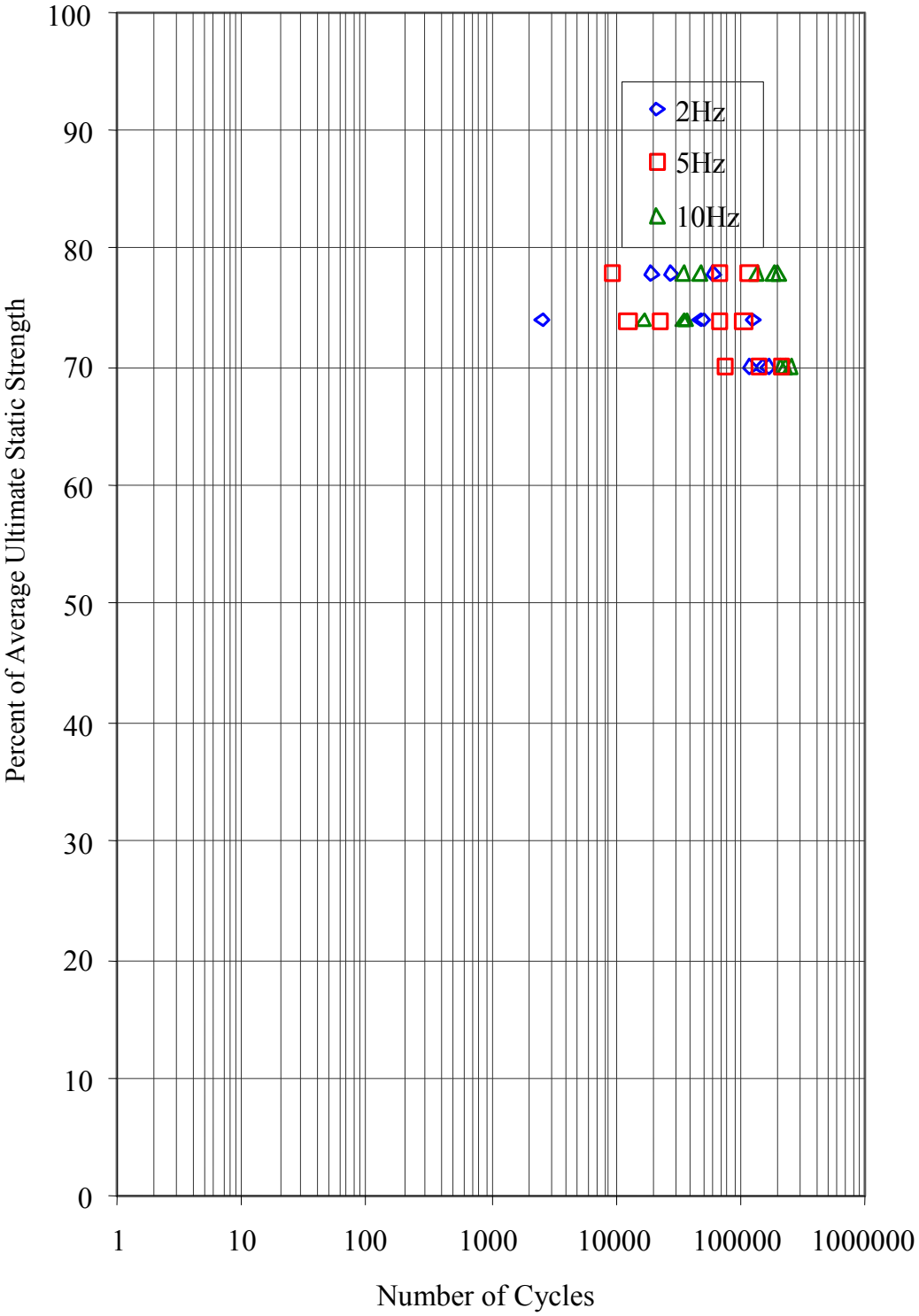

FIGURE 4-11. FREQUENCY INFLUENCE OF EA9696 RESULTS UNDER RTD CONDITIONS

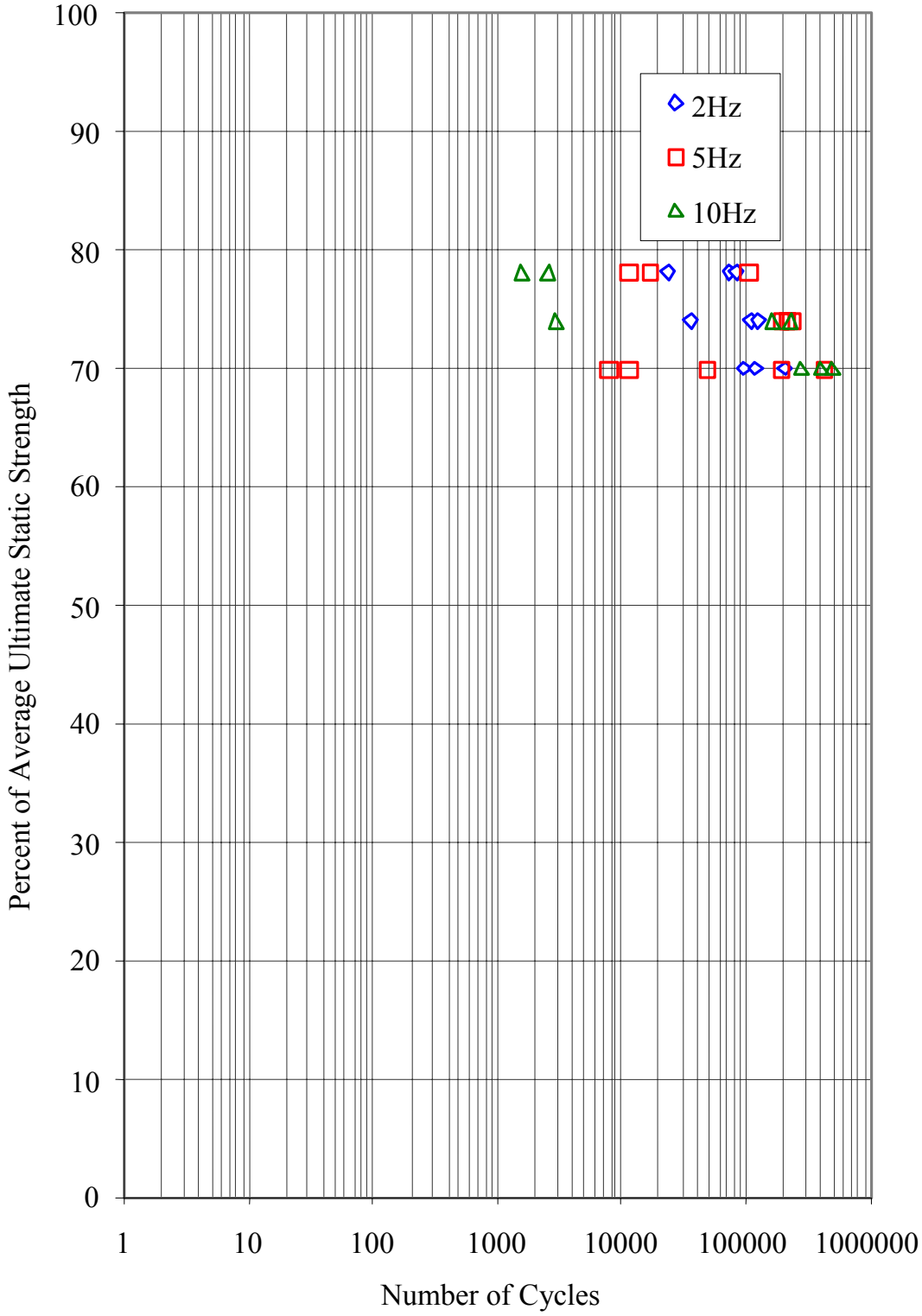

FIGURE 4-12. FREQUENCY INFLUENCE OF EA9696 RESULTS UNDER RTW CONDITIONS

Unlike Loctite specimens, EA9696 adhesive, in most cases, survived better under RTW conditions than under the other two conditions. However, RTW stress levels were approximately 2,000 psi lower than CTD stress levels and approximately 500 psi lower that RTD levels. In any case, in terms of average ultimate static strength, 70% was a threshold at all environments. The stress-strain curves for EA9696 (figures B-4 to B-6) have a sharp transition between elastic and plastic behavior and the three stress levels that were chosen exhibited similar fatigue levels.

For this adhesive, cohesive failure was common under RTW conditions, but there was a tendency to change towards adhesion and mixed failures as the temperature and moisture concentration decreased (figure 4-8). Figure 4-13 shows typical failure modes for EA9696 under all three environmental conditions. This figure also shows the growth of the cohesive failure area as temperature and moisture concentrations were increased. Failure of this particular adhesive closely follows the path shown in figure 1-1, where the middle section has a high-stress region, called the slow crack growth or fatigue-failed zone (figure 4-14). In addition, the edges of overlap have cohesive failures, called fast crack growth or statically failed zones.

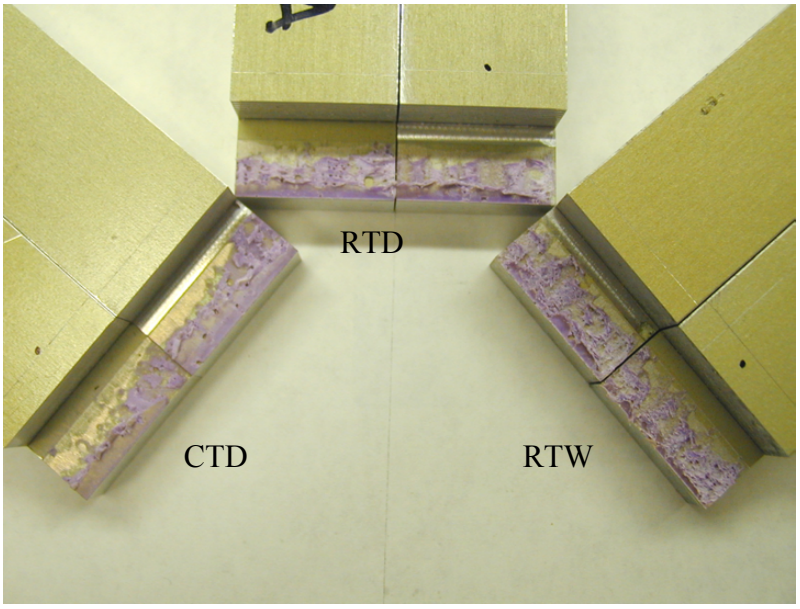

FIGURE 4-13. TYPICAL FAILURE MODES FOR EA9696

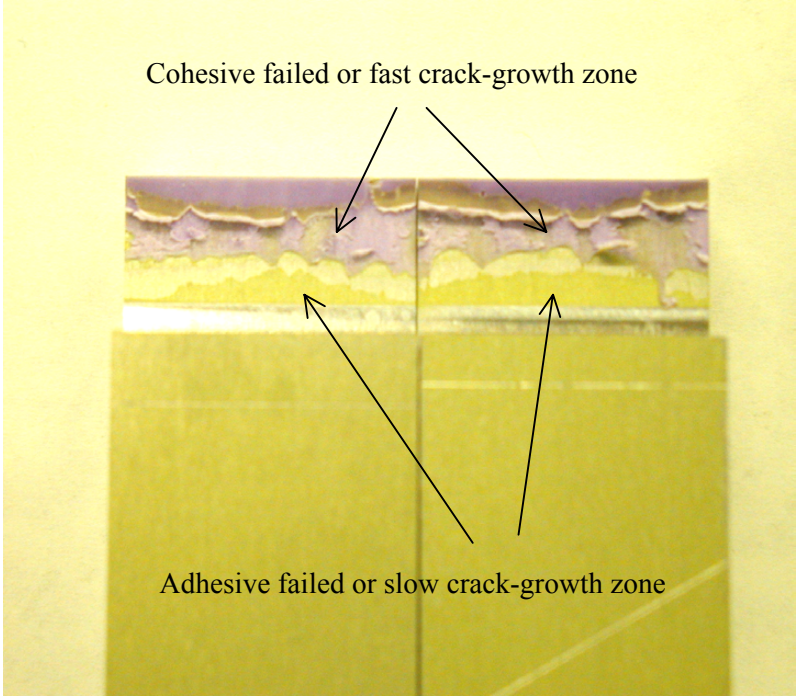

FIGURE 4-14. EA9696 SPECIMENS WITH CLEARLY DEFINED FATIGUE-FAILED AND STATICALLY FAILED REGIONS

4.2.3 ES6292.

Figures 4-15 through 4-20 show the effects of temperature and moisture concentration as well as the influence of frequency on the fatigue life of ES6292 specimens for each stress level and bondline thickness. The stress levels used are shown in figures B-7 to B-12 of appendix B. These figures indicate a much more brittle behavior for thicker bondline specimens.

At all environmental conditions and bondline thicknesses it appears that 40% of ultimate static strength for the particular condition is a threshold below which there appears to be infinite life. Regardless of bondline thickness, the RTW condition was the most critical for this adhesive. However, when comparing the fatigue data, CTD stress levels were significantly higher than RTW levels, yet seemed to survive better than under the other two conditions involving thin bondlines. For thick bondlines, RTD specimens indicated more survivability compared to the other two conditions. As bondline thickness increased, RTW specimens indicated lower fatigue life than those specimens with thin bondlines. In general, as the bondline thickness increased, adhesive plastic strain accumulation decreased and unstable damage growth was observed during static testing. This resulted in lower shear strength values for thick bondlines; therefore, the stress levels for these specimens were lower in magnitude than thin bondline specimens. In addition, the adhesive volume exposed to moisture was greater for thick bondlines than for thin bondlines, causing the adhesive to fail at a low number of cycles.

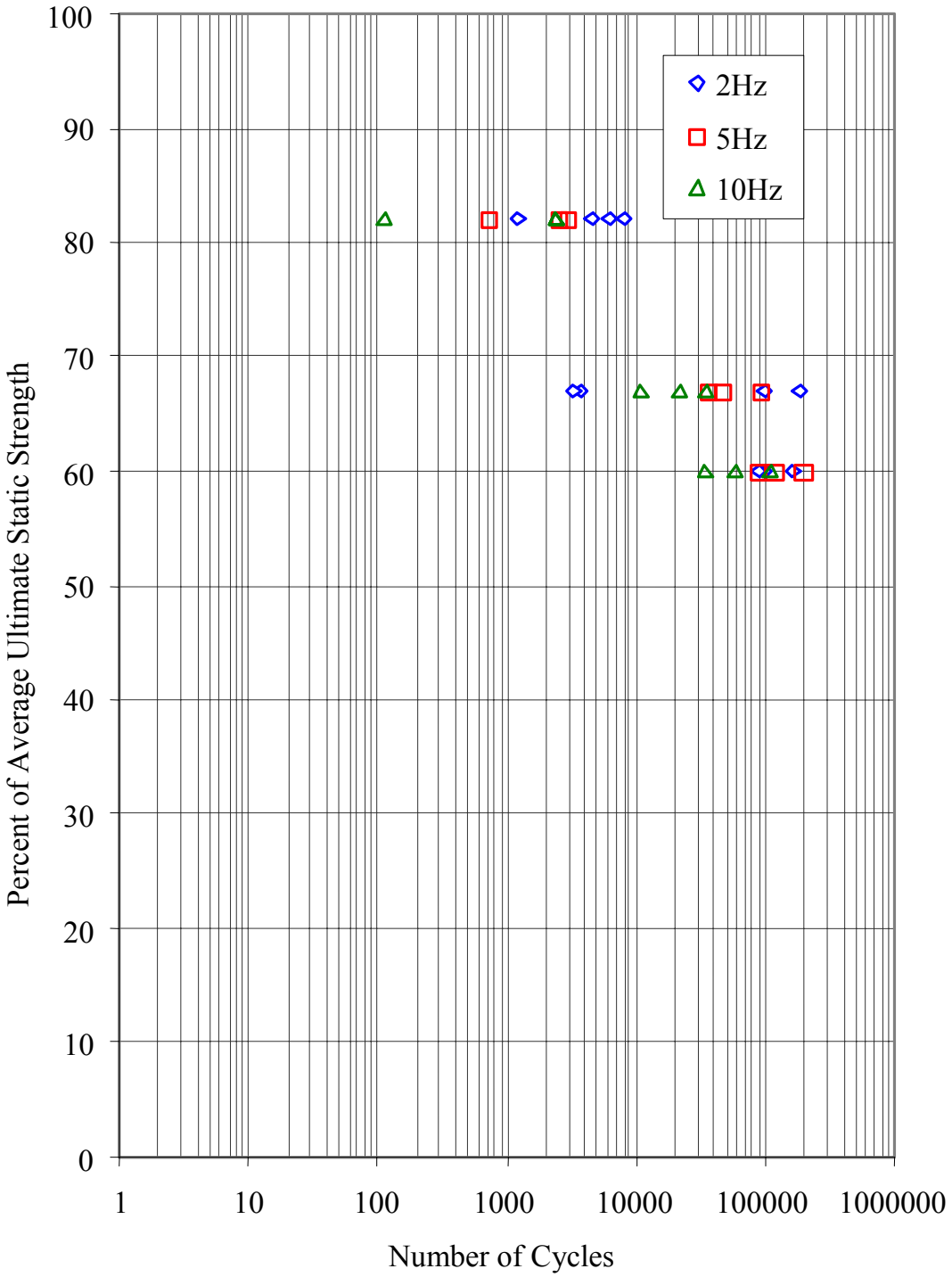

FIGURE 4-15. FREQUENCY INFLUENCE OF ES6292 (0.06 inch) RESULTS UNDER CTD CONDITIONS

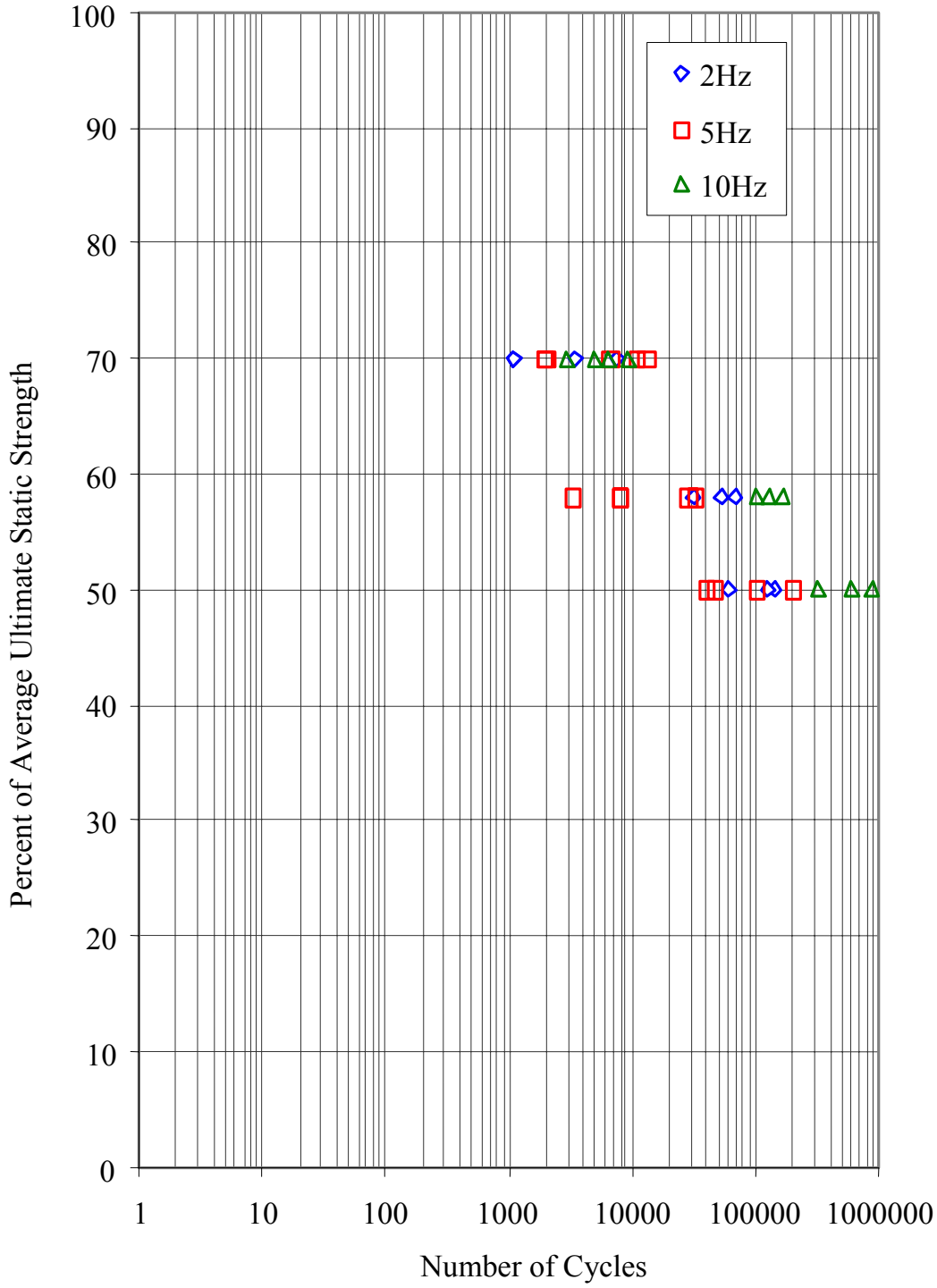

FIGURE 4-16. FREQUENCY INFLUENCE OF ES6292 (0.06 inch) RESULTS UNDER RTD CONDITIONS

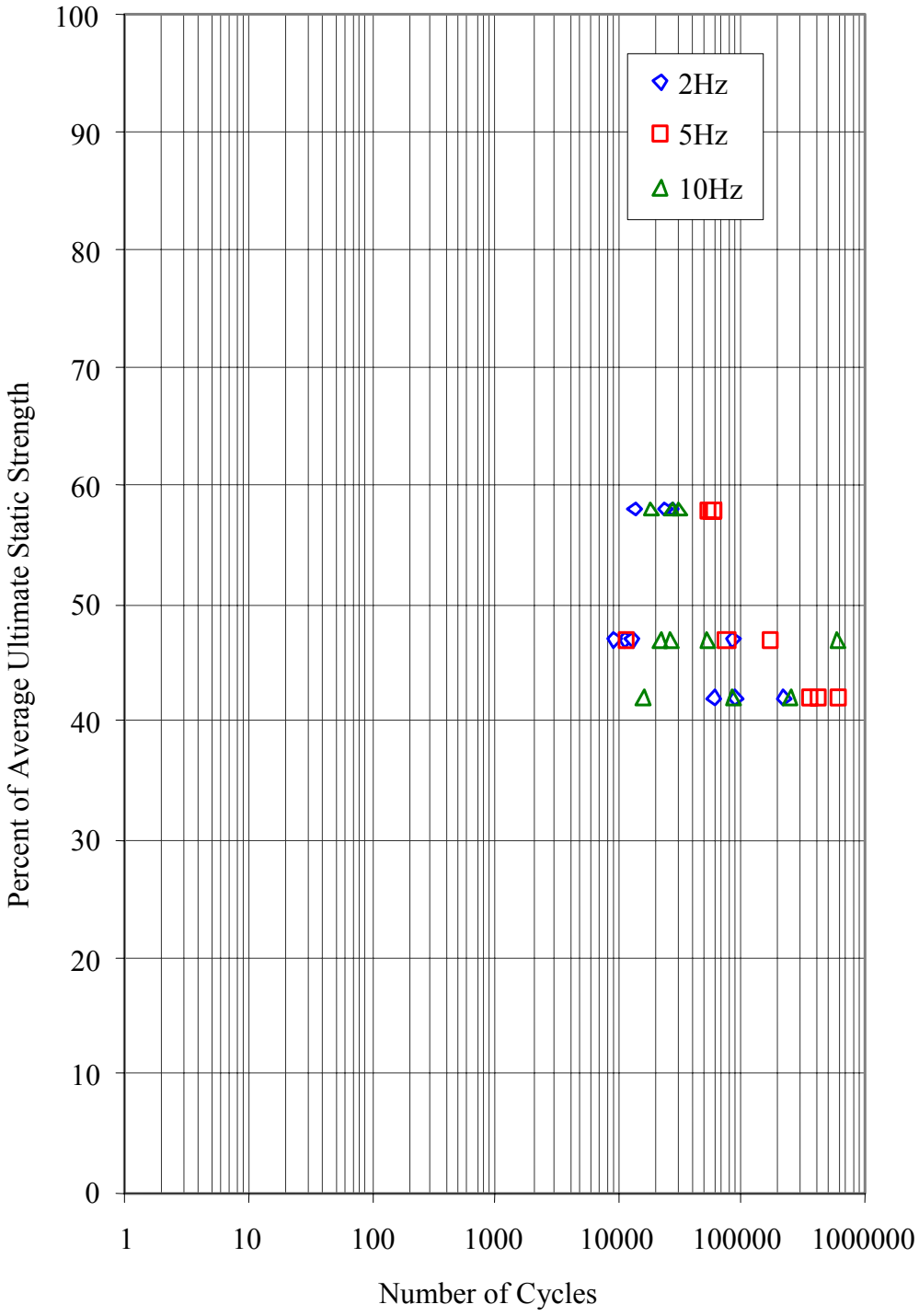

FIGURE 4-17. FREQUENCY INFLUENCE OF ES6292 (0.06 inch) RESULTS UNDER RTW CONDITIONS

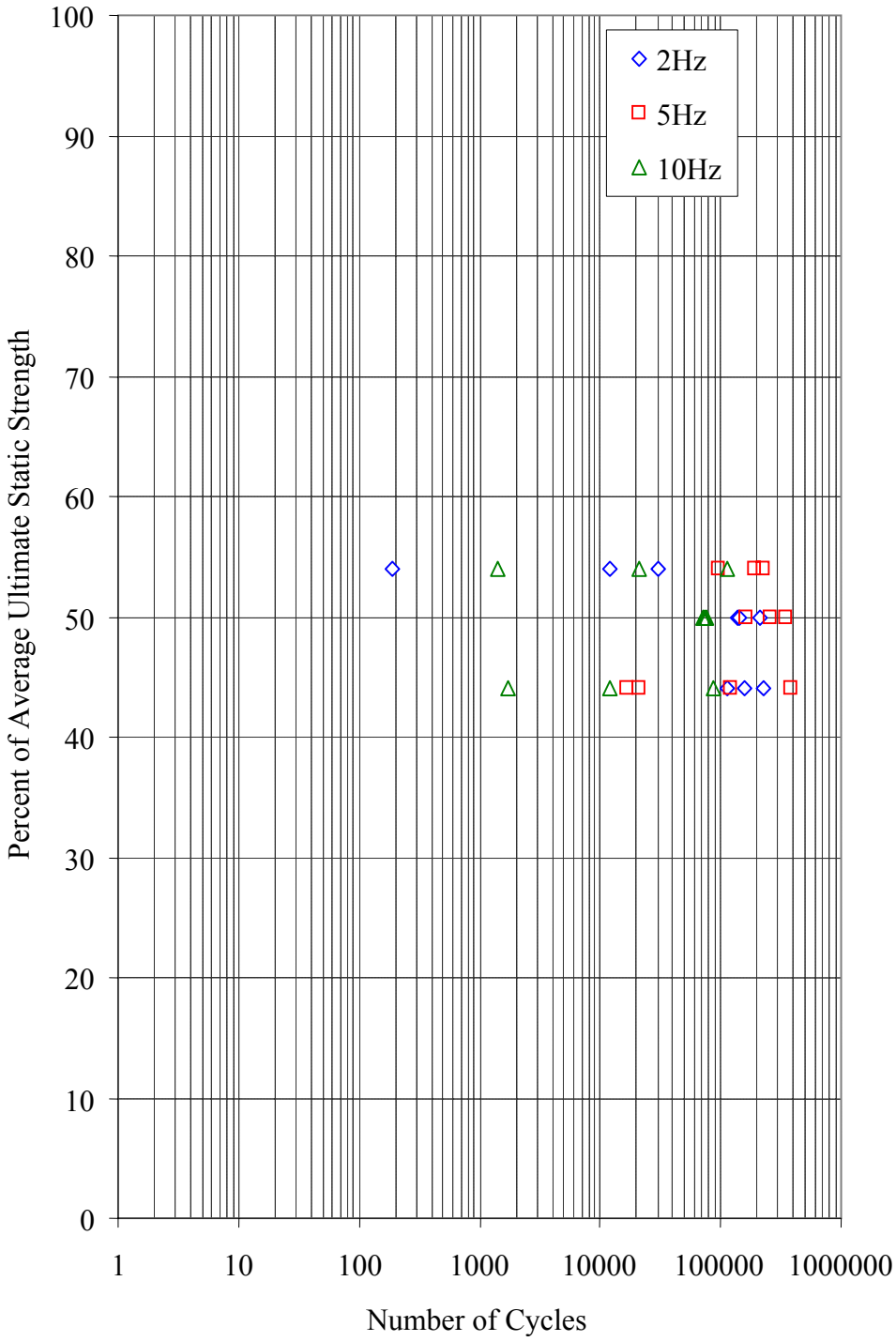

FIGURE 4-18. FREQUENCY INFLUENCE OF ES6292 (0.16 inch) RESULTS UNDER CTD CONDITIONS

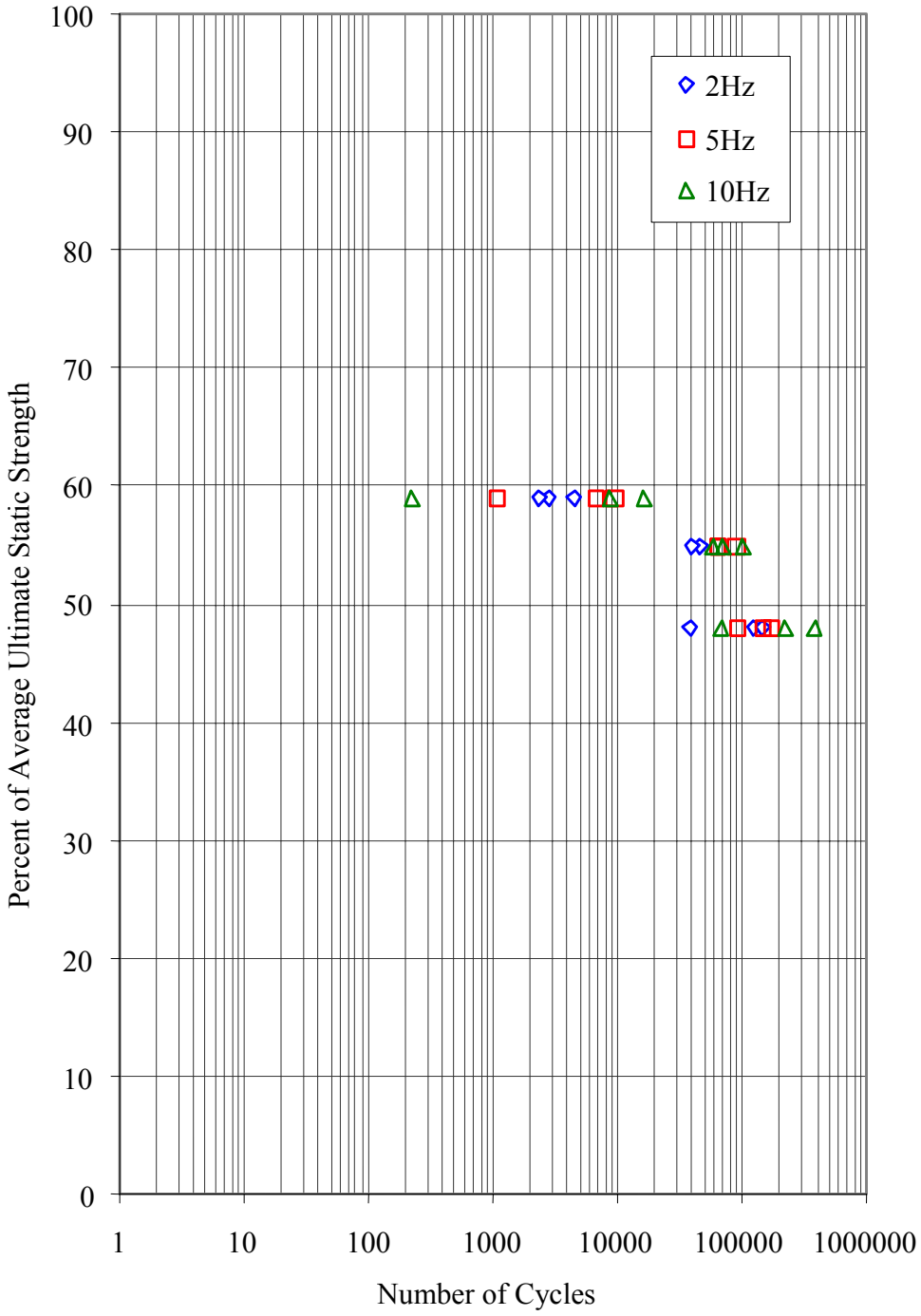

FIGURE 4-19. FREQUENCY INFLUENCE OF ES6292 (0.16 inch) RESULTS UNDER RTD CONDITIONS

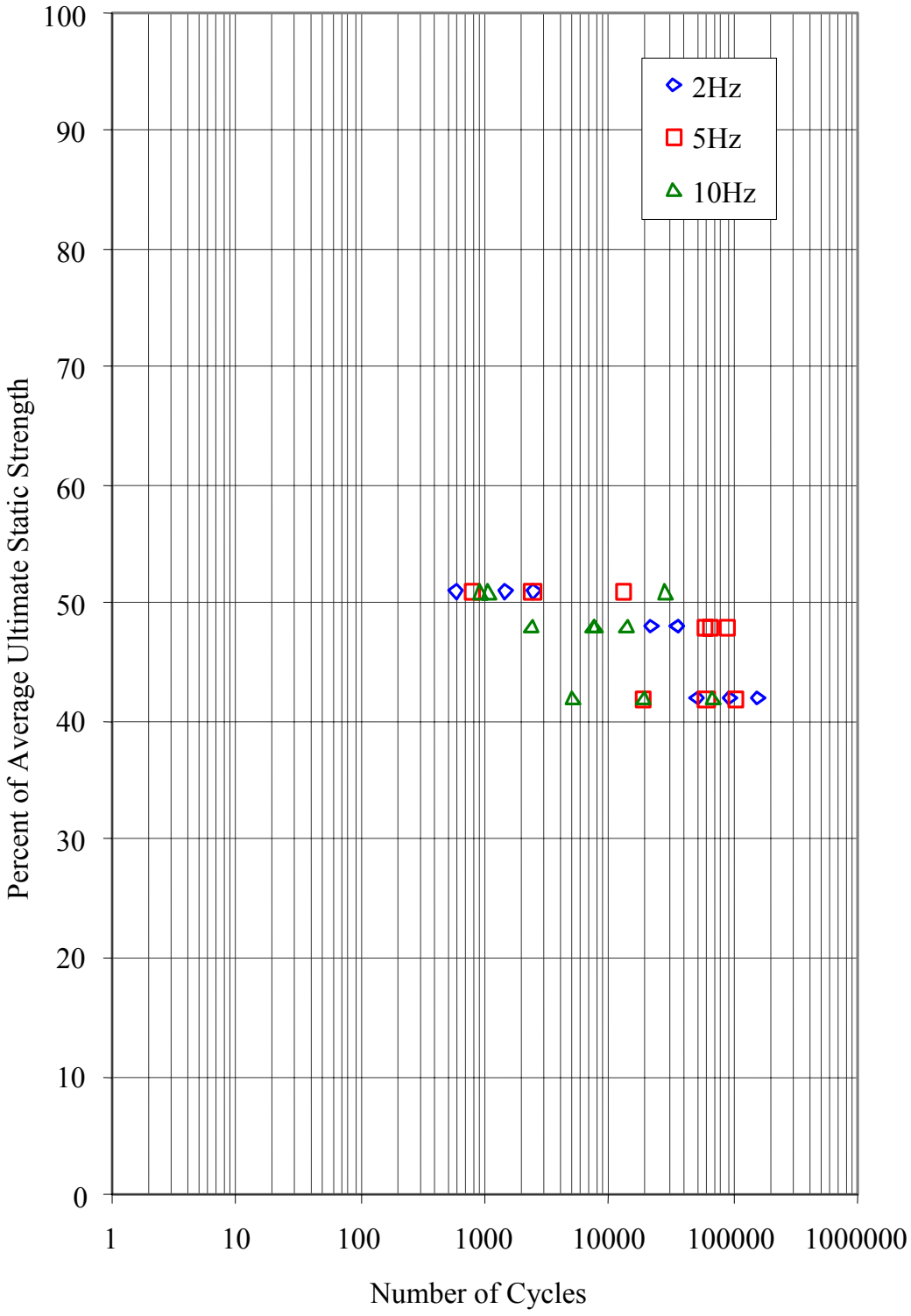

FIGURE 4-20. FREQUENCY INFLUENCE OF ES6292 (0.16 inch) RESULTS UNDER RTW CONDITIONS

Figure 4-8 shows that cohesive failure of ES6292 specimens was typical for most cases. A few adhesion failures, particular for 0.06″ at CTD, were observed. As the bondline thickness increased, more cohesive failure was observed. The unstable damage growth of thick bondlines usually resulted in microcracks at multiple locations of the adhesive bulk and then resulted in cohesive failure. Figures 4-21 and 4-22 illustrate some of the failure modes of ES6292 adhesive for thin and thick bondlines, respectively. The bond primer layer of some of the CTD specimens detached from the adherend and caused failure at the adhesive-adherend interface. Most of the specimens indicated 45° shear failure in the loading direction and some failure in both the loading direction and transverse direction. In addition, figure 4-23 shows the change in color for RTW specimens due to moisture absorption. Following exposure to moisture, these specimens indicated a dark yellow color.

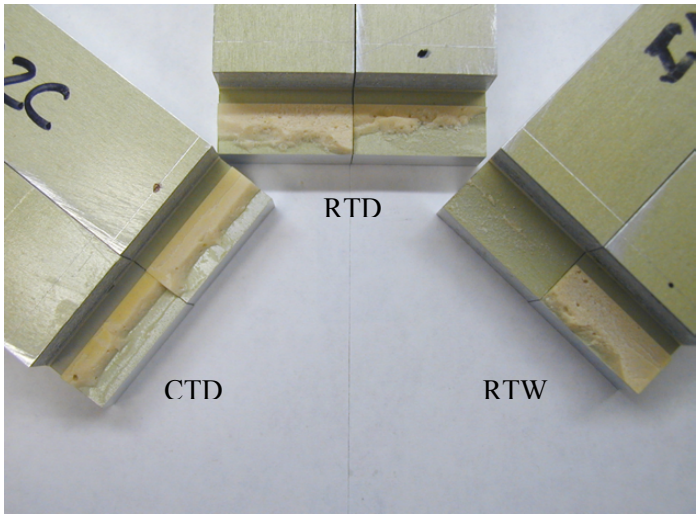

FIGURE 4-21. TYPICAL FAILURE MODES FOR ES6292 (BONDLINE = 0.06″)

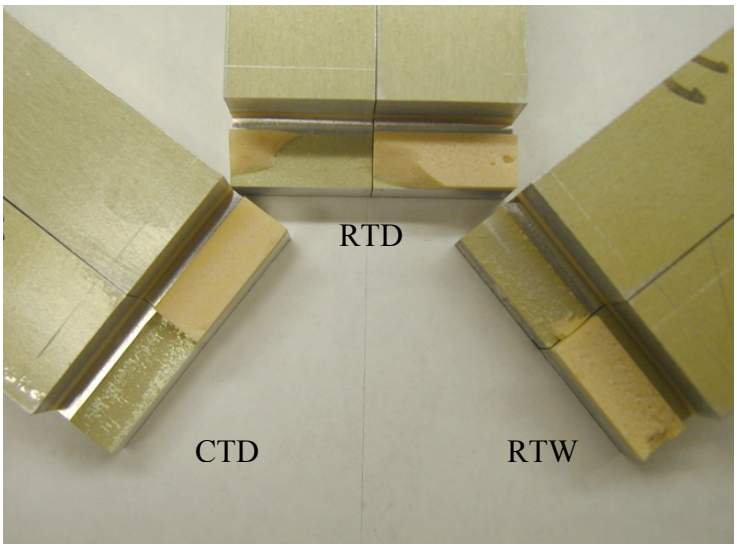

FIGURE 4-22. TYPICAL FAILURE MODES FOR ES6292 (BONDLINE = 0.16″)

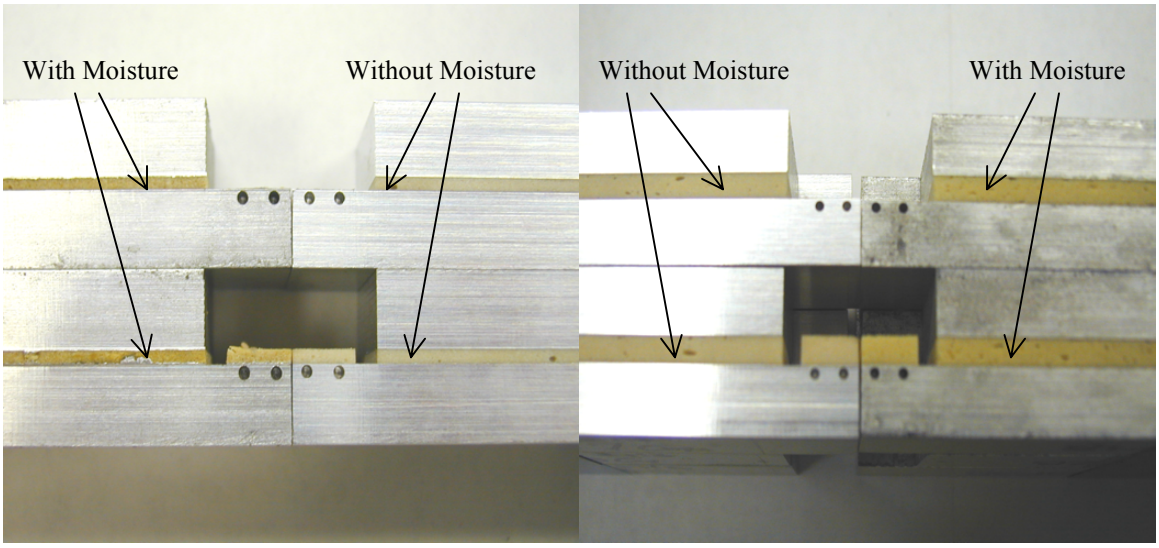

FIGURE 4-23. CHANGE IN COLOR OF ES6292 SPECIMENS AFTER MOISTURE EXPOSURE

4.3 STRESS RELAXATION.

4.3.1 Ring Calibration.

Test fixture calibration indicated no significant change due to temperature, as shown in figure 4-24. However, the calibration curve corresponding to a particular temperature was used for data reduction.

The solid aluminum specimen loaded at 210°F (worst-case scenario) indicated no stress relaxation. This test ensured that stress relaxation of the lap joint was exclusively due to relaxation of the adhesive layer present in the gage section. The calibration curve for each ring under each environmental condition indicated linear elastic behavior and, therefore, no ring deformation. The calibration curves were linearly curve-fitted and used to interpret the applied stress on the lap joint specimens during relaxation tests. The stress relaxation data were then curve-fitted, using TableCurve software to obtain the three fitting parameters defined by equation 3-7 for each adhesive under each environmental condition. The stress relaxation curves shown in this chapter are based on the three fitting parameters, except for EA9696 curve at 210°F.

Appendix C, figures C-1 to C-12, shows the stress relaxation data in the form of change in stress ($\Delta\sigma$) with respect to time. The plots in the body of the report will show the amount of decrease in shear stress as a function of time.

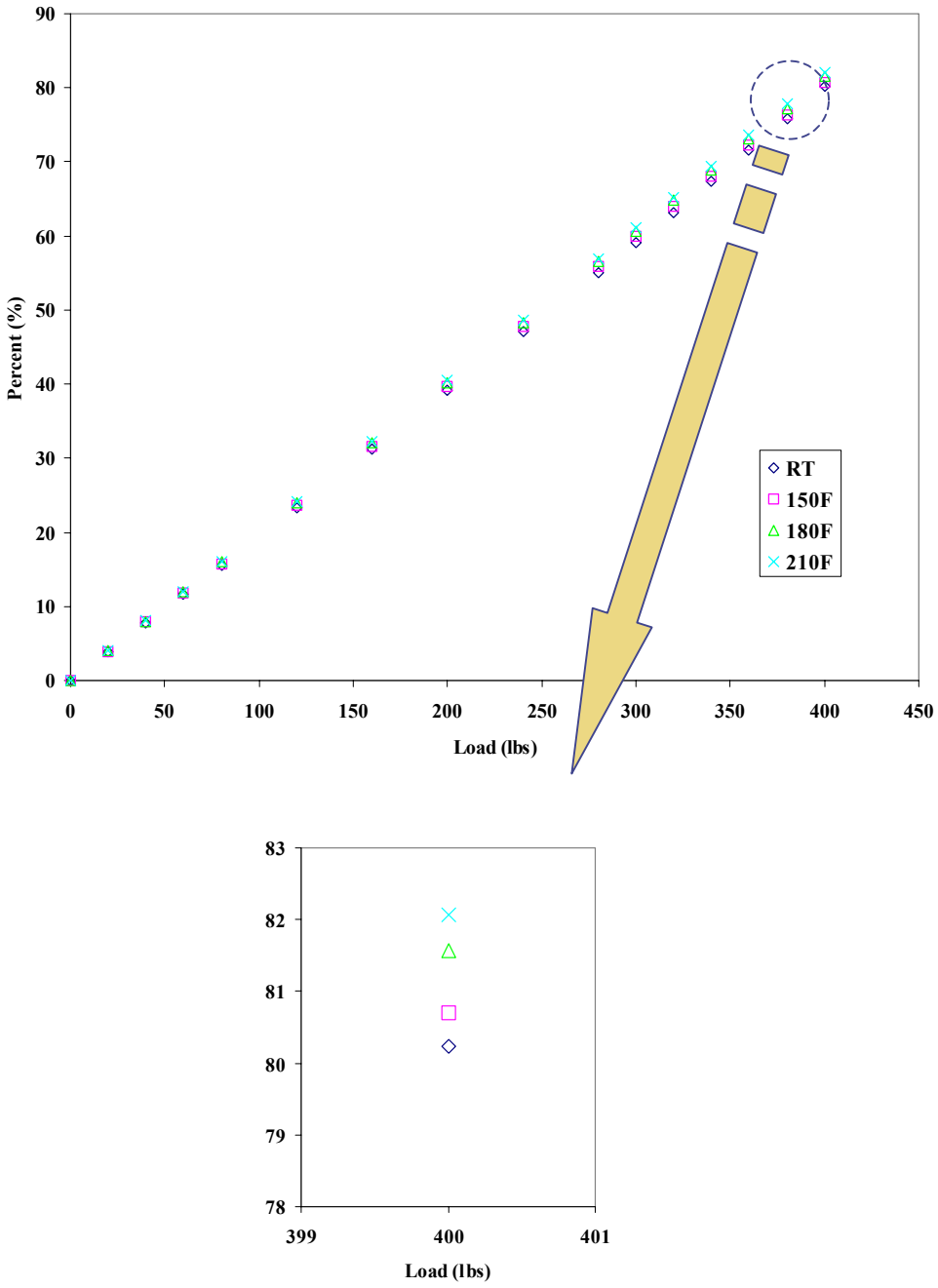

FIGURE 4-24. ALCOA STRESS FIXTURE CALIBRATION AT TEST TEMPERATURES

4.3.2 Loctite Adhesive.

Figures 4-25 through 4-27 summarize the results obtained for the stress relaxation tests performed on Loctite adhesive at 150°, 180°, and 210°F. Each plot shows the stress relaxation for all three stress levels at 10%, 15%, and 25% of yield stress. These results reflect the average value obtained from three replicates.

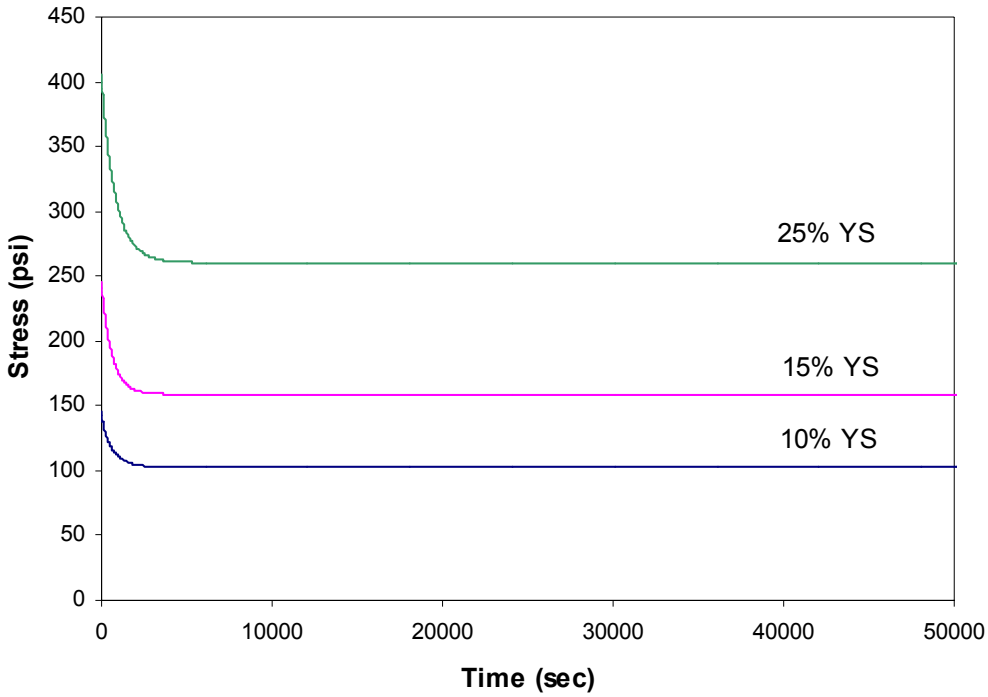

FIGURE 4-25. STRESS RELAXATION ($\Delta\sigma$) FOR LOCTITE AT 150°F

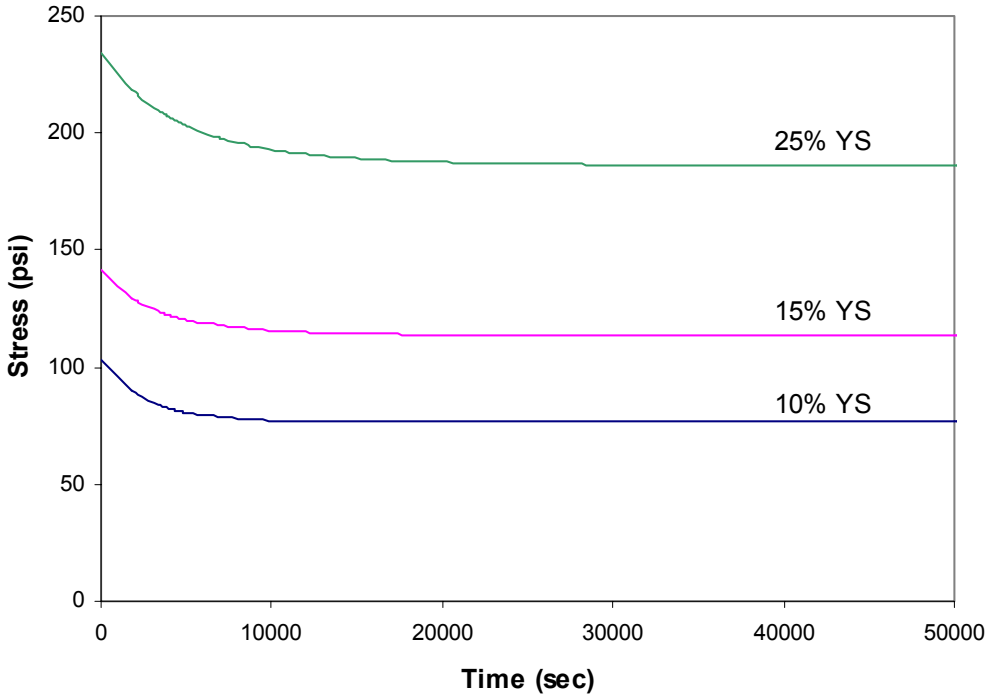

FIGURE 4-26. STRESS RELAXATION ($\Delta\sigma$) FOR LOCTITE AT 180°F

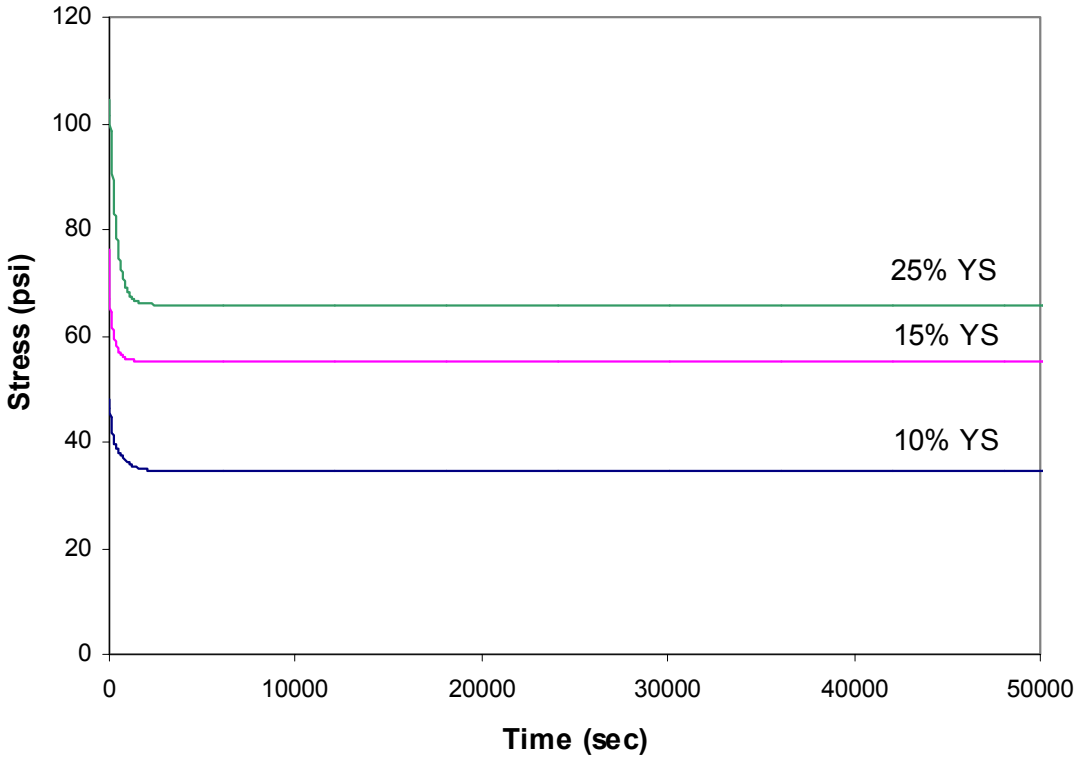

FIGURE 4-27. STRESS RELAXATION (Δσ) FOR LOCTITE AT 210°F

As the temperature and initial applied stress were increased, the relaxation of stress increased. For the 10% of yield stress case, the drop was from 29.5% (Δσ = 42.82 psi) at 150°F to 25.7% (Δσ = 26.47 psi) at 180°F and 28.5% (Δσ = 13.7 psi) at 210°F. The 15% case showed a decrease from 35.2% (Δσ = 86.35 psi) to 19.8% (Δσ = 28.04 psi) and then 28.8% (Δσ = 21.9 psi) as the temperature was increased. Lastly, the 25% case also followed the same trend as the 10% and 15% cases, dropping to 35.2% (Δσ = 144.55 psi), 20.6% (Δσ = 48.16 psi), and 37.1% (Δσ = 38.8 psi) as the temperature was increased. Overall, the percentage drop decreased and then increased at 210°F. The significantly higher relaxation at 210°F was due to the fact that the tests were conducted above the glass transition temperature of 169°F (table 4-3).

TABLE 4-3. DRY GLASS TRANSITION TEMPERATURE

	°C	°F
Loctite	76.260	169.268
EA9696	98.648	209.566
ES6292	89.594	193.269

4.3.3 EA9696 Adhesive.

Figures 4-28 through 4-30 summarize the results obtained for the stress relaxation tests performed on EA9696 adhesive at 150° and 180°F. These results show the average values obtained from three replicates.

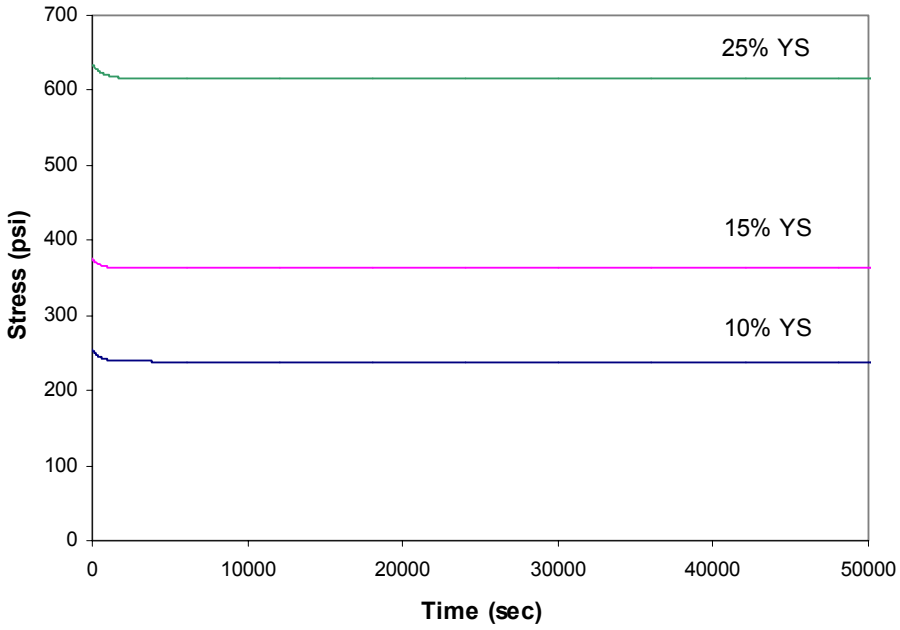

FIGURE 4-28. STRESS RELAXATION ($\Delta\sigma$) FOR EA9696 AT 150°F

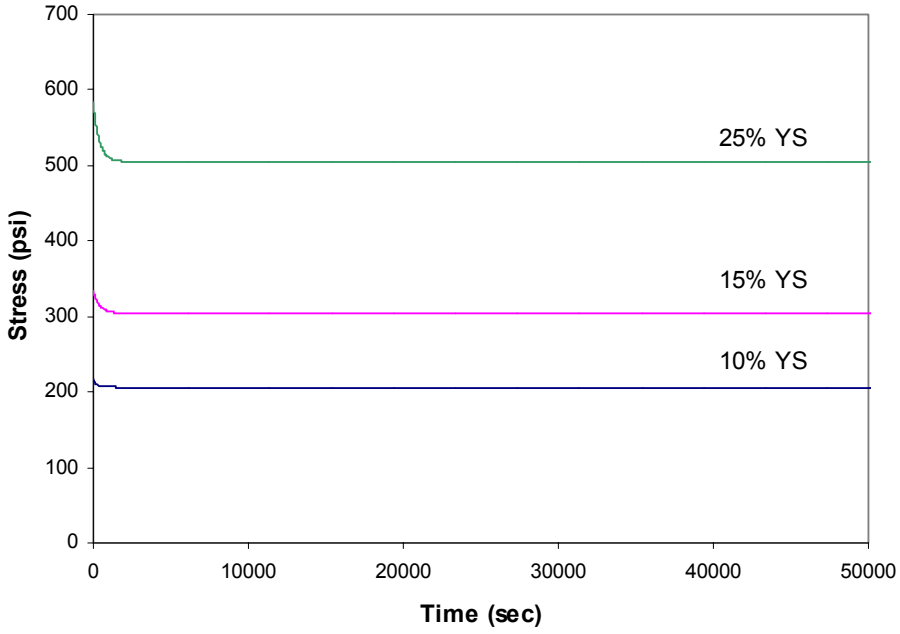

FIGURE 4-29. STRESS RELAXATION ($\Delta\sigma$) FOR EA9696 AT 180°F

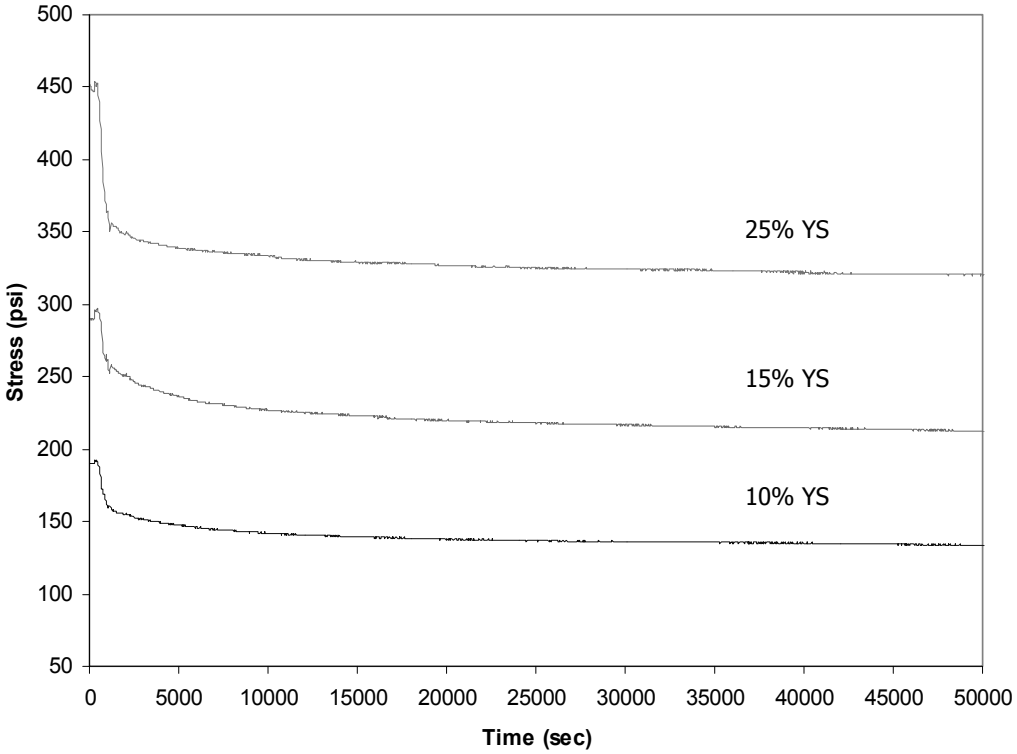

FIGURE 4-30. STRESS RELAXATION ($\Delta\sigma$) FOR EA9696 AT 210∞F (RAW DATA)

Stress drop percentages increased as adhesives were exposed to heat. For the 25% case, the drop increased from 2.86% ($\Delta\sigma$ = 18.16 psi) at 150∞F to 13.52% ($\Delta\sigma$ = 79.01 psi) at 180∞F. The same trend was observed for the 15% case, which increased from 3.27% ($\Delta\sigma$ = 12.27 psi) to 8.84% ($\Delta\sigma$ = 29.50 psi). However, the 10% case did not follow this trend, with percentages being about 1%, 5.91% ($\Delta\sigma$ = 15 psi), and 4.95% ($\Delta\sigma$ = 10.76 psi) as the temperature increased from 150∞to 210∞F.

Due to the high glass transition temperature, EA9696 specimens did not show as much relaxation as Loctite specimens. However, the stress relaxation plots at 210∞F (shown in figure 4-30) deviated from the ideal plot. Figure 4-30 is truncated at 50,000 seconds, but decrease in strength continued. The stress drop was significant enough to assume that it would be dangerous to build any structure to operate under these conditions. Since the relaxation curve did not asymptotically approach a stress value, as shown in the ideal plot (figure 3-9), these data were not curve-fitted to obtain three parameters.

4.3.4 PTM&W ES6292 Adhesive.

Figures 4-31 through 4-36 summarize the results obtained from the stress relaxation tests performed on ES6292 specimens at 150°F, 180∞F, and 210∞F. The stress-change curves for 0.06-inch-thick bondline specimens of this adhesive showed the same trend observed for the 10% and 15% cases of EA9696 specimens. For the 10% case, the initial applied stress dropped

6.5% ($\Delta\sigma$ = 13.72 psi), 12.2% ($\Delta\sigma$ = 26.47 psi), and 23.9% ($\Delta\sigma$ = 23.60 psi) as the temperature increased from 150°F to 210°F. For the 15% case, the stress dropped 5.4% ($\Delta\sigma$ = 18.01 psi), 13.1% ($\Delta\sigma$ = 36.45 psi), and 30.3% ($\Delta\sigma$ = 51.61 psi). For the 25% case at 210°F, stress decreased to 4% ($\Delta\sigma$ = 21.1 psi) of the initial applied stress and were considered failed (only the mechanical locking of adhesive surfaces was holding the load). However, for thick bondline specimens at 210°F, the relaxation was not as severe as for the thin bondline case. The yield strength of 0.06-inch bondline specimens was higher than that of 0.16-inch bondline specimen. Therefore, the applied stress on the thin bondline specimens was higher that that of the thick bondline specimens. In addition, compared to thin bondline specimens, the thick bondline specimens had more material for shear deformation due to relaxation and still carried the load. These two reasons were the cause of the thin bondline specimens at 210°F to undergo severe relaxation and that lead to failure.

For the 10% case with thicker bondlines (0.16 inch), the stress dropped 6.15% ($\Delta\sigma$ = 9.26 psi), 51.3% ($\Delta\sigma$ = 57.76 psi), and 42.3% ($\Delta\sigma$ = 38.39 psi) of the initial applied stress. For the 15% case, the stress dropped 5.8% ($\Delta\sigma$ = 13.80 psi), 62.5% (137.68 psi), and 51.9% ($\Delta\sigma$ = 77.06 psi) as the temperature increased. Finally, for the 25% case, the stress dropped 5.9% ($\Delta\sigma$ = 22.82 psi), 66.1% ($\Delta\sigma$ = 215.26 psi), and 62.4% ($\Delta\sigma$ = 145 psi).

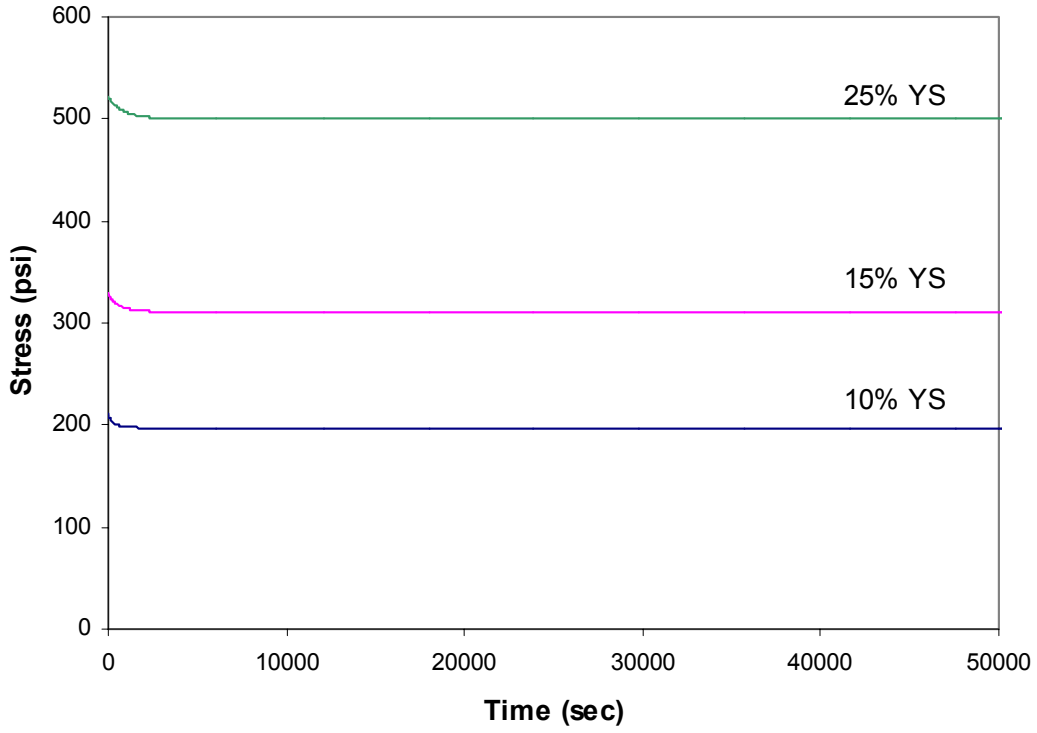

FIGURE 4-31. STRESS RELAXATION ($\Delta\sigma$) FOR ES6292 (0.06 inch) AT 150°F

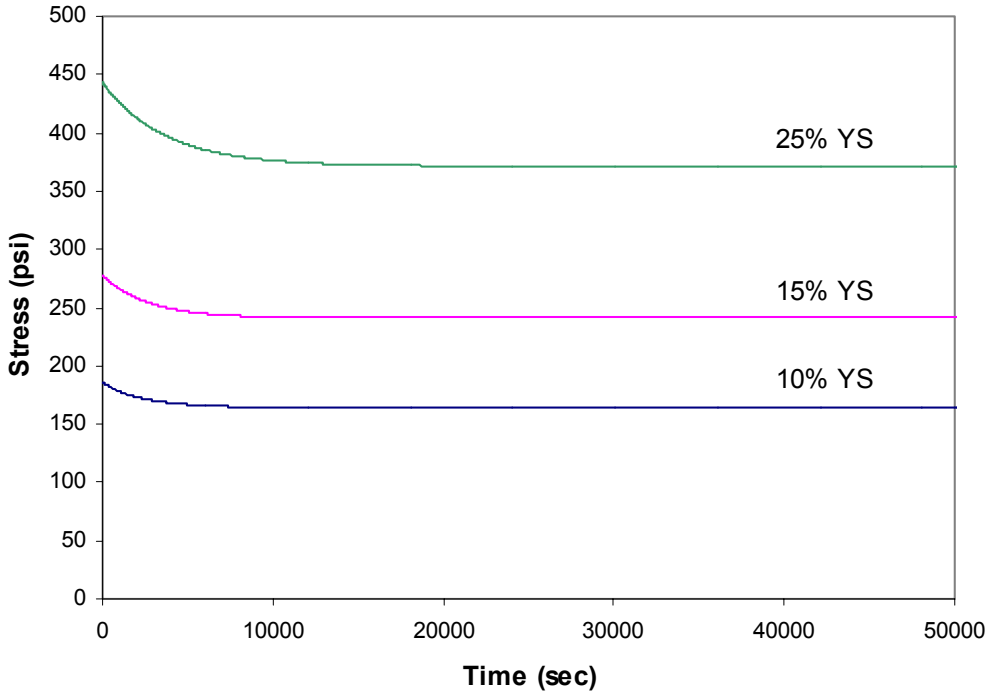

FIGURE 4-32. STRESS RELAXATION (Δσ) FOR ES6292 (0.06 inch) AT 180°F

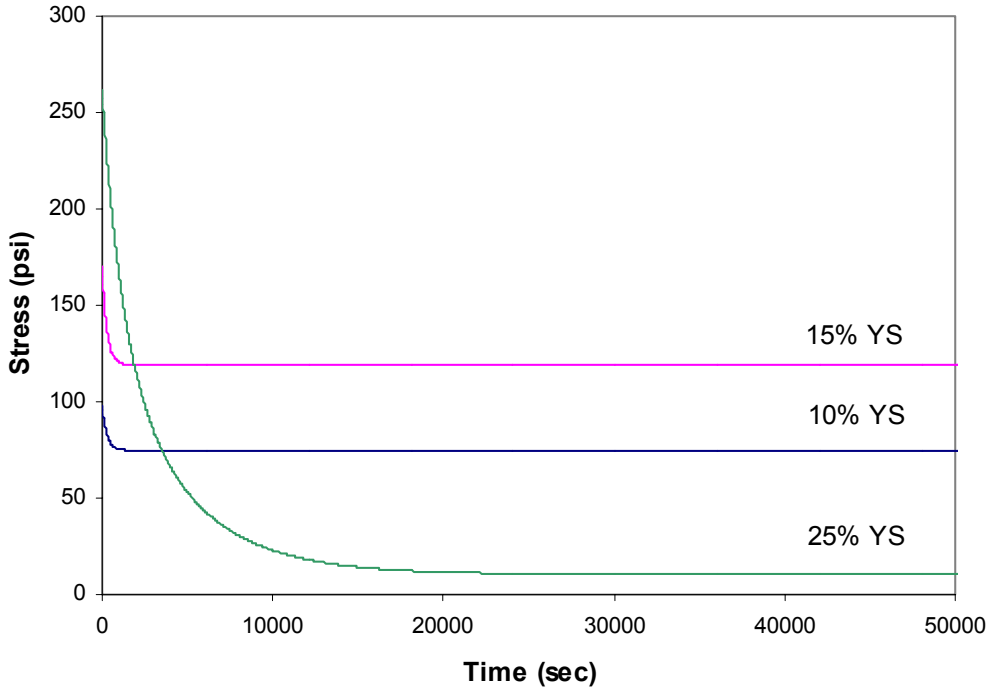

FIGURE 4-33. STRESS RELAXATION (Δσ) FOR ES6292 (0.06 inch) AT 210°F

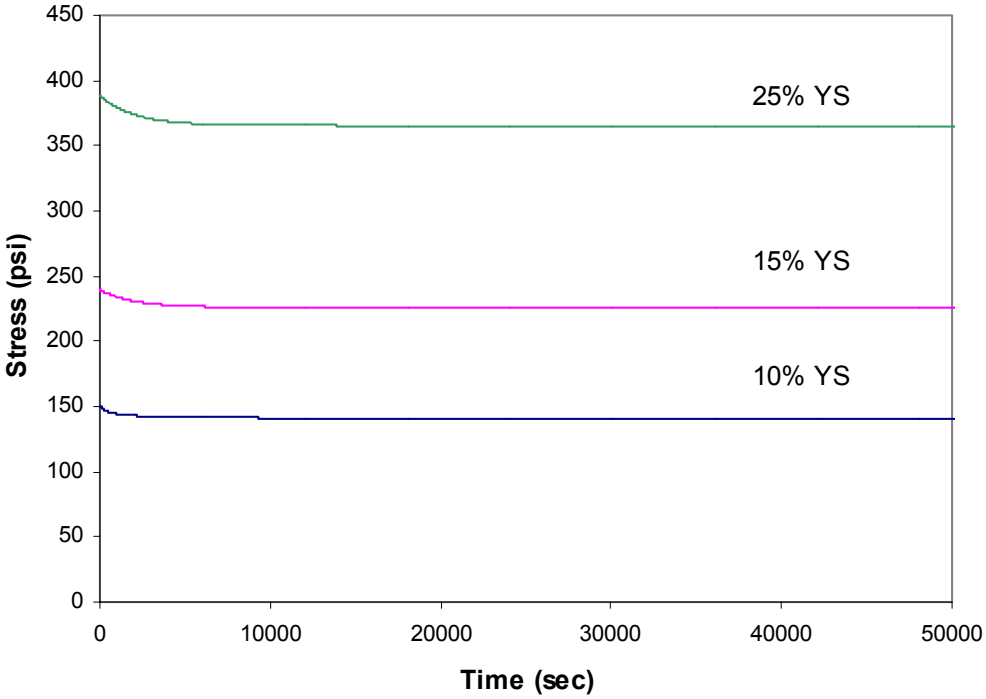

FIGURE 4-34. STRESS RELAXATION (Δσ) FOR ES6292 (0.16 inch) AT 150°F

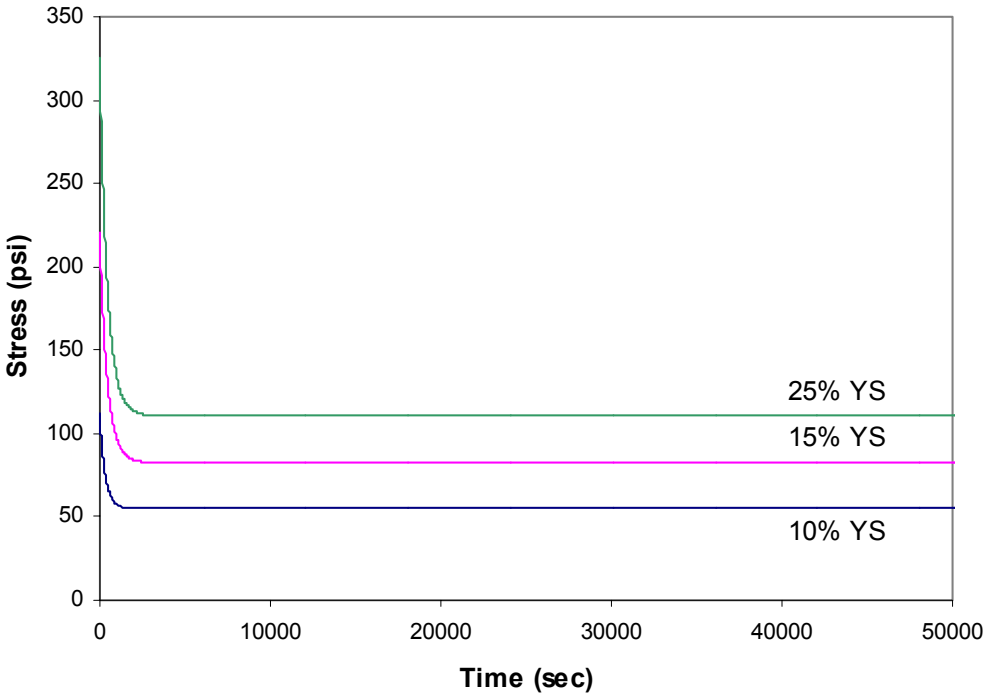

FIGURE 4-35. STRESS RELAXATION (Δσ) FOR ES6292 (0.16 inch) AT 180°F

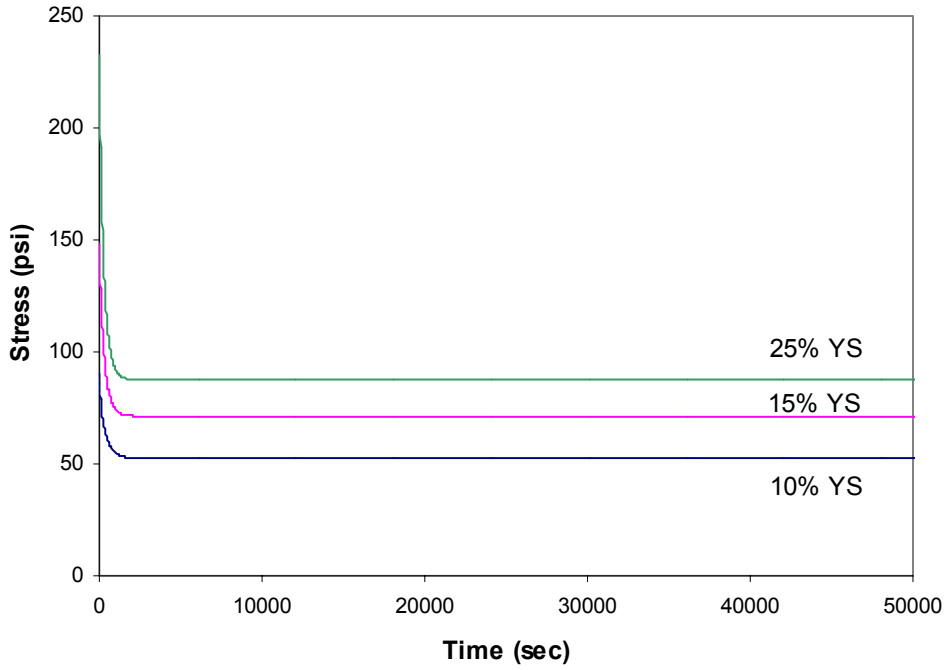

FIGURE 4-36. STRESS RELAXATION ($\Delta\sigma$) FOR ES6292 (0.16 inch) AT 210°F

The relaxation data for all three adhesives are summarized in table 4-4, and the fitting parameters obtained from the stress relaxation curves are listed in table 4-5.

4.3.5 Temperature-Immersed (Soaked) Specimens.

To study the adhesive stress-strain characteristics after exposure to elevated temperatures such as the stress relaxation test conditions (long-term exposure to elevated temperatures), a set of specimens from each adhesive was soaked at 150°, 180°, and 210°F in a temperature-controlled environmental chamber for 400 hours without applying any load. These specimens, and an additional set of specimens without 400-hour soak, were then tested according to ASTM D 5656 test procedure under the above-mentioned test temperatures. Since the elevated temperature tests were conducted with a 3-minute soak time, specimens without 400-hour soak time were identified as 3-min. soak specimens. The results for 400-hour soak and 3-min. soak specimens tested according to the ASTM D 5656 standard are tabulated in table 4-6 and illustrated in figures A-9 and A-10. These results reflect the average values obtained from two or three replicates.

Shear stress and initial shear modulus increased as the adhesives were conditioned for 400 hours. At 150°F, apparent shear strength and initial shear modulus for EA9696 specimens increased about 18.4% and 17.5%, respectively. There was an increase in the apparent shear strength (24.1%) and shear modulus (12.2%) for ES6292 (0.16 inch). At the same temperature, apparent shear strength for Loctite, ES6292 (0.06 inch), and ES6292 (0.16 inch) adhesives increased about 47.7%, 24.2%, and 28.1%, respectively. The initial shear modulus for Loctite, ES6292 (0.06 inch), and ES6292 (0.16 inch) adhesives increased 68%, 21.4%, and 38.5%, respectively.

TABLE 4-4. SUMMARY OF STRESS RELAXATION TEST RESULTS

Adhesives	Average Thick. (in)	Temp (°F)	Time (hrs)	Average Initial Stress (psi)	Average Final Stress (psi)	Change in Stress, $\Delta\sigma$ (psi)	Relaxation (%)
EA9696	0.02	150	164.3	253.68 (10% YS)	238.68	15.00	5.91
				375.25 (15% YS)	362.98	12.27	3.27
				633.49 (25% YS)	615.33	18.16	2.87
Loctite	0.32		217.55	145.19 (10% YS)	102.38	42.82	29.49
				245.36 (15% YS)	159.01	86.35	35.19
				404.90 (25% YS)	260.36	144.55	35.70
ES6292 (0.06″)	0.06		164.3	210.94 (10% YS)	197.21	13.72	6.51
				328.96 (15% YS)	310.95	18.01	5.47
				520.99 (25% YS)	499.91	21.08	4.05
ES6292 (0.16″)	0.16		212.4	150.51 (10% YS)	141.25	9.26	6.15
				239.57 (15% YS)	225.77	13.80	5.76
				388.33 (25% YS)	365.50	22.82	5.88
EA9696	0.02	180	157.8	217.25 (10% YS)	206.50	10.76	4.95
				333.38 (15% YS)	303.89	29.50	8.85
				584.17 (25% YS)	505.16	79.01	13.52
Loctite	0.32		238.9	103.09 (10% YS)	76.62	26.47	25.68
				141.66 (15% YS)	113.62	28.04	19.79
				234.34 (25% YS)	186.17	48.16	20.55
ES6292 (0.06″)	0.06		164.3	186.37 (10% YS)	163.56	22.81	12.24
				277.67 (15% YS)	241.22	36.45	13.13
				443.38 (25% YS)	371.37	72.01	16.24
ES6292 (0.16″)	0.16		233.5	112.68 (10% YS)	54.92	57.76	51.26
				220.20 (15% YS)	82.51	137.68	62.53
				325.88 (25% YS)	110.61	215.26	66.06
EA9696	0.02	210	164.3	N/A	N/A	N/A	N/A
				N/A	N/A	N/A	N/A
				N/A	N/A	N/A	N/A
Loctite	0.32		170.5	48.08 (10% YS)	34.37	13.71	28.52
				76.07 (15% YS)	54.19	21.88	28.77
				104.63 (25% YS)	65.83	38.80	37.08
ES6292 (0.06″)	0.06		161.9	98.39 (10% YS)	74.79	23.60	23.99
				170.43 (15% YS)	118.81	51.61	30.29
				261.76 (25% YS)	10.51	251.26	95.99
ES6292 (0.16″)	0.16		233.5	90.75 (10% YS)	52.36	38.39	42.30
				148.42 (15% YS)	71.35	77.06	51.92
				232.50 (25% YS)	87.50	145.00	62.37

TABLE 4-5. COEFFICIENTS FOR THE THREE-PARAMETER LINEAR VISCOELASTIC MODEL

Adhesives	Temperature (°F)	Stress Level	Coefficients		
			a	b	c
Loctite (0.032″)	150	10%	102.377	39.722	1.524E-03
		15%	159.013	86.181	1.646E-03
		25%	260.357	143.663	1.223E-03
	180	10%	76.617	26.389	3.812E-04
		15%	113.629	27.063	2.855E-04
		25%	186.184	46.320	1.991E-04
	210	10%	34.366	11.446	2.120E-03
		15%	55.257	15.926	5.434E-03
		25%	65.835	38.747	2.817E-03
EA9696 (0.02″)	150	10%	238.679	14.993	1.839E-03
		15%	362.978	12.168	1.992E-03
		25%	615.329	18.084	1.359E-03
	180	10%	206.498	11.327	4.450E-03
		15%	303.887	29.162	2.240E-03
		25%	505.165	78.986	2.587E-03
	210	10%	N/A	N/A	N/A
		15%	N/A	N/A	N/A
		25%	N/A	N/A	N/A
ES6292 (0.06″)	150	10%	197.214	12.158	2.756E-03
		15%	310.951	17.455	1.553E-03
		25%	499.914	20.656	1.090E-03
	180	10%	163.563	21.595	3.808E-04
		15%	241.221	36.430	3.800E-04
		25%	371.373	71.619	2.708E-04
	210	10%	74.793	23.562	3.675E-03
		15%	118.814	51.168	3.459E-03
		25%	10.582	226.034	3.439E-04
ES6292 (0.16″)	150	10%	141.252	7.603	7.389E-04
		15%	225.767	13.520	4.787E-04
		25%	365.502	22.822	4.941E-04
	180	10%	54.918	35.336	2.836E-03
		15%	82.512	137.581	2.231E-03
		25%	110.613	214.824	2.188E-03
	210	10%	52.361	32.789	2.248E-03
		15%	71.354	76.735	3.276E-03
		25%	87.501	143.212	3.539E-03

Note: Formula based on average of three replicas.

TABLE 4-6. COMPARISON OF TEST RESULTS FOR TEMPERATURE-IMMERSED (SOAKED) SPECIMENS

Adhesive	Test Temperature (°F)	Soaked at Test Temperature for 400 hrs		Soaked at Test Temperature for 3 min	
		Shear Stress (ksi)	Initial Shear Modulus (Msi)	Shear Stress (ksi)	Initial Shear Modulus (Msi)
EA9696	150	4.437	0.067	3.748	0.057
Loctite		2.242	0.042	1.518	0.025
ES6292 (0.06″)		2.636	0.085	2.122	0.070
ES6292 (0.16″)		1.968	0.072	1.536	0.052
EA9696	180	3.092	0.039	3.196	0.049
Loctite		1.933	0.031	1.752	0.024
ES6292 (0.06″)		2.102	0.057	1.975	0.056
ES6292 (0.16″)		1.833	0.058	1.478	0.052
EA9696	210	3.119	0.041	2.865	0.035
Loctite		1.376	0.013	1.010	0.005
ES6292 (0.06″)		1.364	0.026	1.113	0.037
ES6292 (0.16″)		1.503	0.048	0.886	0.035

At 180°F, the apparent shear stress and initial shear modulus for all adhesives, except for EA9696, increased. The apparent shear strength and initial shear modulus of EA9696 dropped about 3.3% and 21.9%, respectively. There was a significant increase in the apparent shear strength (24.1%) and initial shear modulus (12.2%) for ES6292 (0.16 inch). The apparent initial shear strength and initial shear modulus of Loctite also increased 10.3% and 31%, respectively, and for ES6292 (0.06 inch) 6.4% and 0.4%, respectively.

At 210°F, the shear modulus of ES6292 (0.06 inch) adhesive decreased 28.7%, but the apparent shear strength increased 22.5%. Loctite had the highest increase in initial shear modulus, which was 191.4%, and ES6292 (0.16 inch) had the highest increase in apparent shear strength, or 69.6%. The increments increase in apparent shear strength and initial shear modulus were due to the postcure and additional cross-linking of the adhesives beyond and closer to the glass transition temperature.

4.4 STEREOSCOPIC ANALYSIS.

A microscopic analysis of fatigue specimens was conducted using a high-resolution stereoscope with magnification levels ranging from 50x to 300x. Specimens were made out of sections of fatigue-failed specimens following the same methodology for preparing metallographic samples. In addition, stress relaxation specimens were examined for the shear deformation during relaxation.

4.4.1 Analysis of Metallographic Samples.

Some of the samples used for the analysis are shown in figure 4-37, where two small sections of fatigue-failed specimens were cured inside a resin mold. Then they were polished to get an appropriate surface for the analysis. Figure 4-38 shows where voids formed along the adherend-adhesive interface of the Loctite adhesive specimen that resulted in stress concentrations around the voids and a weakening of the bonds. When the specimens were exposed to moisture, water that reached the bubbles attacked the interface and also migrated through the adhesive bulk, deteriorating the joint. Figure 4-39 shows considerably fewer voids in this film adhesive layer, compared to the paste adhesives, which provided more consistent results and better resistance to heat and humidity conditions. The white horizontal lines are likely to be the bonds between the two film adhesive layers. Figures 4-40 and 4-41 show the porosity of the ES6292 adhesive, which may have caused weak bonds that resulted in premature failure as indicated by characteristic curves, especially for thick bondlines.

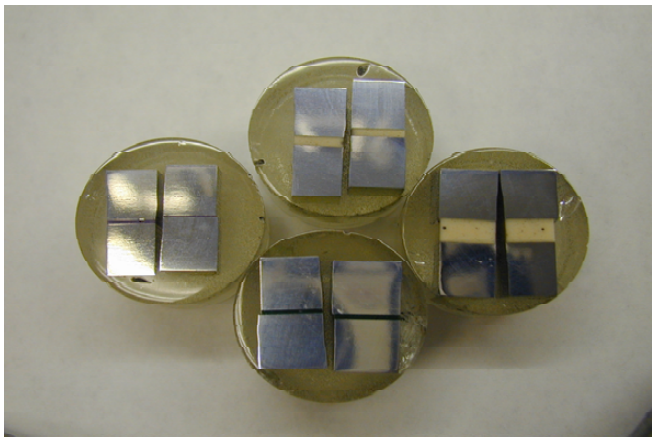

FIGURE 4-37. SMALL SAMPLES OF ADHEREND-ADHESIVE SYSTEM INSIDE RESIN MOLD

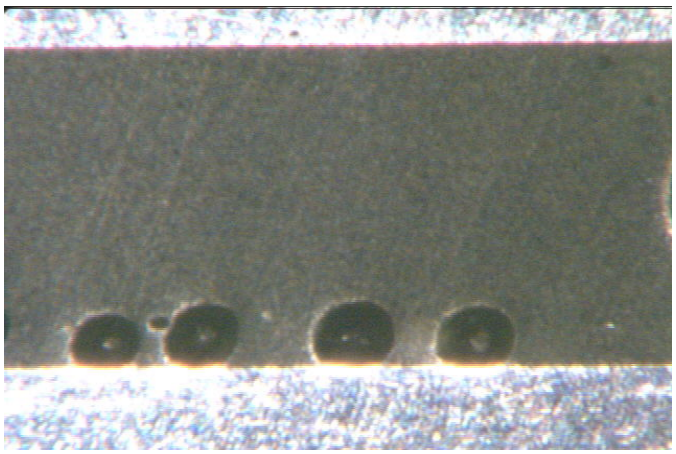

FIGURE 4-38. LOCTITE ADHESIVE WITH VOIDS (0.0013 TO 0.0069 inch DIAMETER) (200X ZOOM)

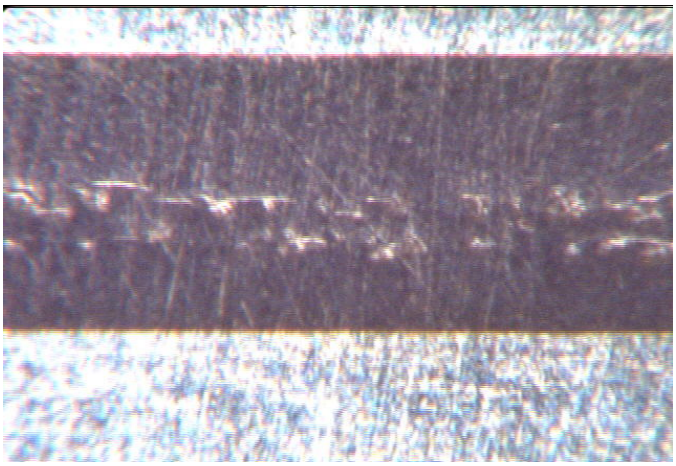

FIGURE 4-39. EA9696 ADHESIVE (260X ZOOM)

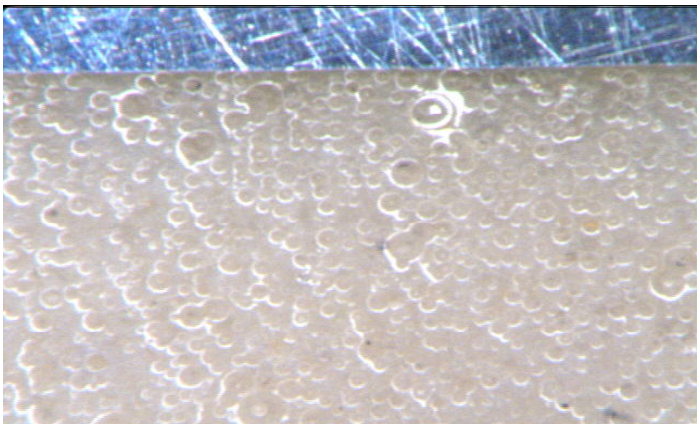

FIGURE 4-40. POROSITY OF ES6292 ADHESIVE (160X ZOOM)

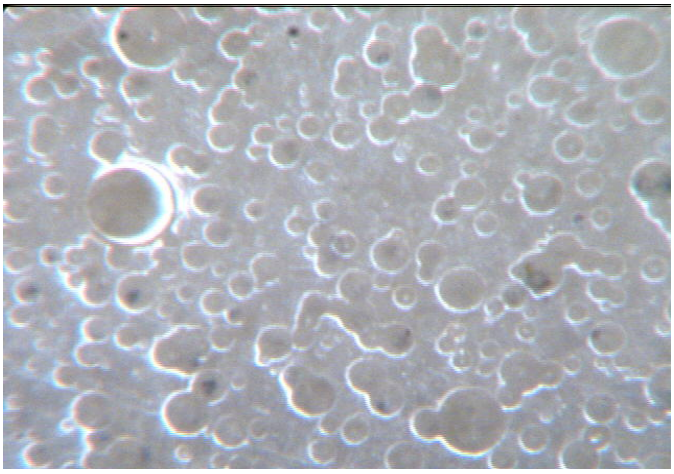

FIGURE 4-41. POROSITY OF ES6292 ADHESIVE (FROM APPROXIMATELY 0.0001 TO 0.0020 inch DIAMETER) (260X ZOOM)

4.4.2 Surface Analysis of Failed Fatigue Specimens.

Figure 4-42(a) shows the adhesion failure of Loctite adhesive under CTD conditions. Figure 4-42(b) indicates the crack initiation of Loctite specimens under this condition due to the stress concentration around the voids. Figures 4-43 and 4-44 show the adhesion failure of the RTD specimen and the cohesive failure of the RTW specimen, respectively. The RTD specimen had multiple cracks but relatively small cracks compared to the CTD specimen. The RTW specimen showed a moisture-attacked adhesive surface, especially around the voids. In addition, multiple cracks, which were smaller than the cracks observed on the CTD specimen surface, initiated from voids, were apparent.

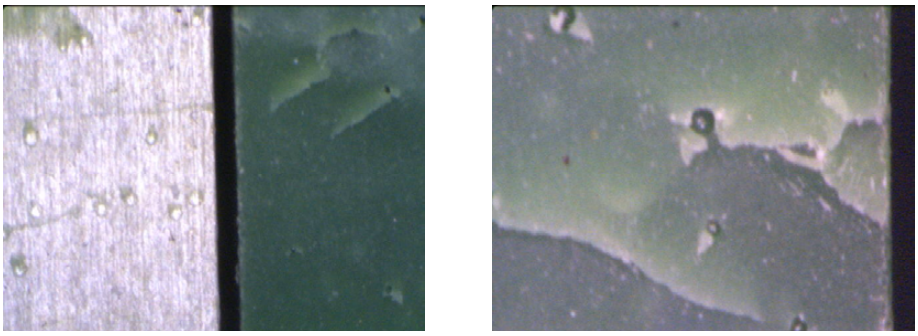

(a) (b)

FIGURE 4-42. LOCTITE ADHESIVE UNDER CTD CONDITIONS

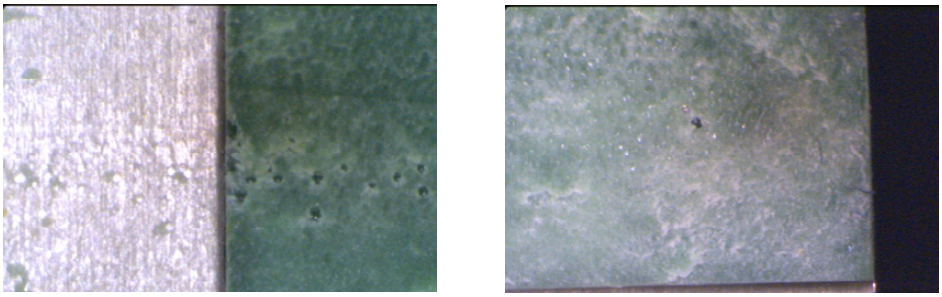

(a) (b)

FIGURE 4-43. LOCTITE ADHESIVE RTD

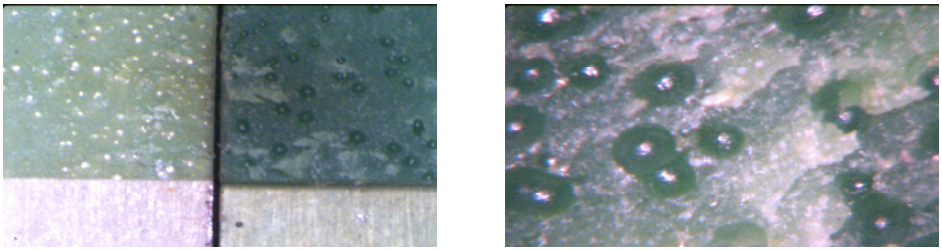

(a) (b)

FIGURE 4-44. LOCTITE ADHESIVE RTW

Figures 4-45 and 4-46 show the failure of EA9696 adhesive specimens under CTD and RTD conditions, respectively. These two specimens indicated the fast- and slow-growth paths illustrated in figure 1-1. The fast crack growth zone of the CTD specimen was shorter than that of the RTD specimen contrasting what one would expect from a brittle material, i.e., a lesser amount of stable crack growth zone or slow crack growth zone and more fast crack growth zone. Figure 4-46(b) shows multiple crack initiations. Figure 4-47 shows the formation of fibrils, which were more apparent in RTW specimens.

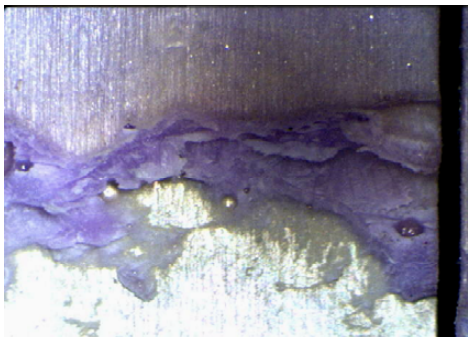

FIGURE 4-45. EA9696 ADHESIVE CTD

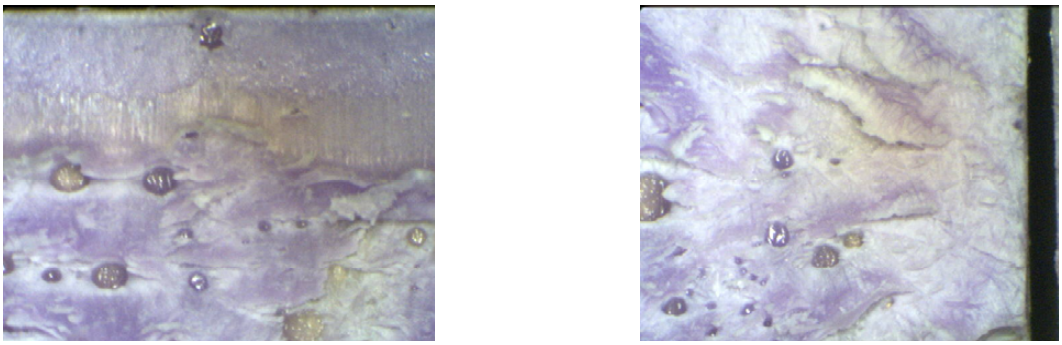

(a) (b)

FIGURE 4-46. EA9696 ADHESIVE RTD

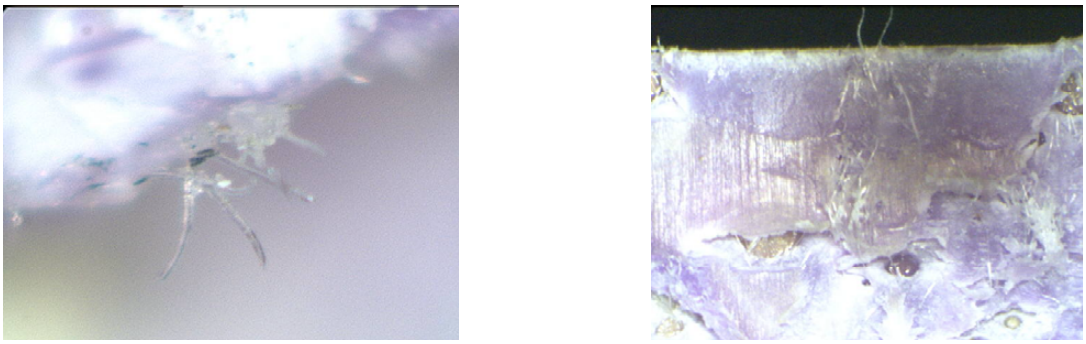

(a) (b)

FIGURE 4-47. EA9696 RTD AND RTW (FIBRILS)

Figure 4-48 shows the removal of the anodized layer of the adherend that could mistakenly be identified as an adhesion failure. The coefficient of thermal expansion difference in the adherend and the anodized layer may have caused the failure of the anodized layer rather than the adhesive-adherend interface.

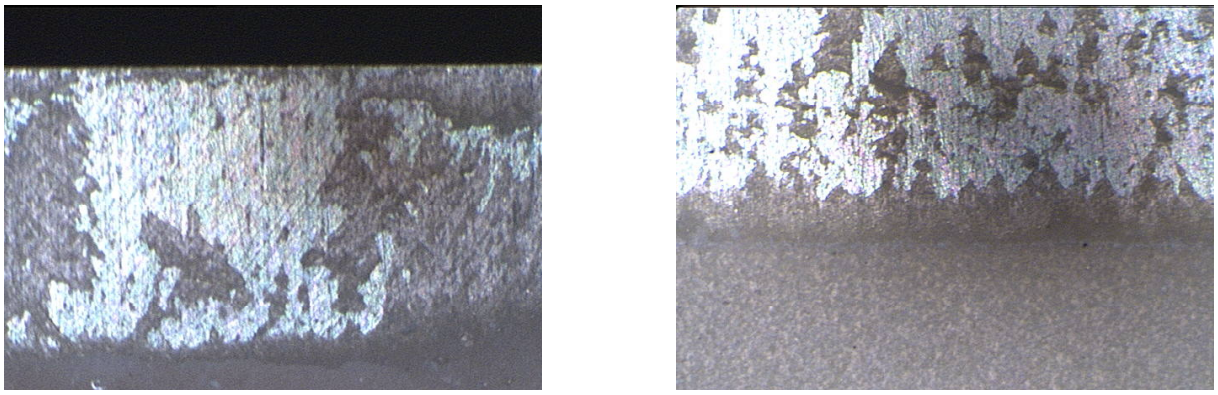

(a) (b)

FIGURE 4-48. ES6292 ADHESIVE CTD

4.4.3 Shear Deformation of the Stress Relaxation Specimens.

The shear deformation of the stress relaxation specimens was examined using the stereoscope. The images captured represent one of the edges of the gage section, as shown in figure 4-49. The image analysis software was used to measure the shear deformation.

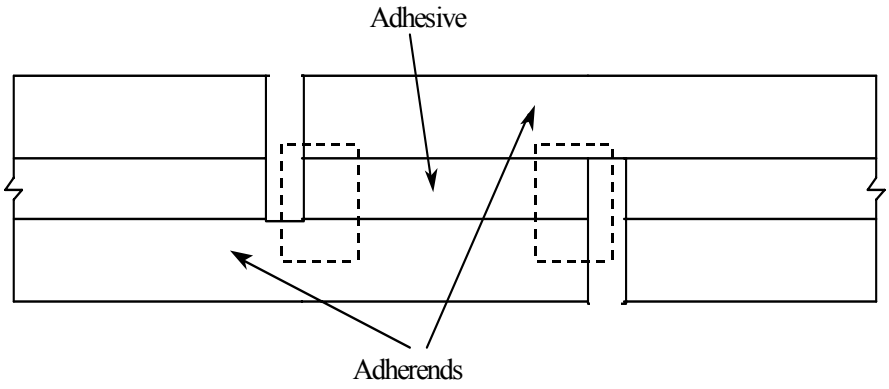

FIGURE 4-49. ADHESIVE SPECIMEN SECTIONS UNDER INVESTIGATION

Image analysis for the Loctite adhesive indicated substantial shear deformation even below the glass transition temperature of 169.3°F (figure 4-50). Surprisingly, shear deformation decreased as the temperature increased, as shown in figures 4-51 and 4-52. As expected, the majority of the results indicated an increase in shear deformation as the stress levels increased.

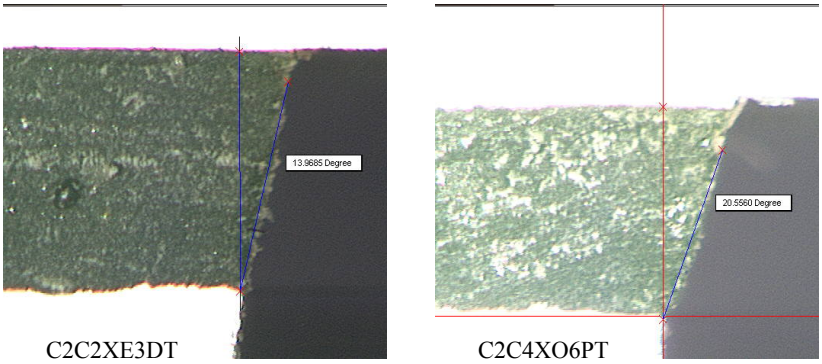

(a) 10% Yield Stress (b) 25% Yield Stress

FIGURE 4-50. SHEAR DEFORMATION OF LOCTITE 150°F SPECIMENS

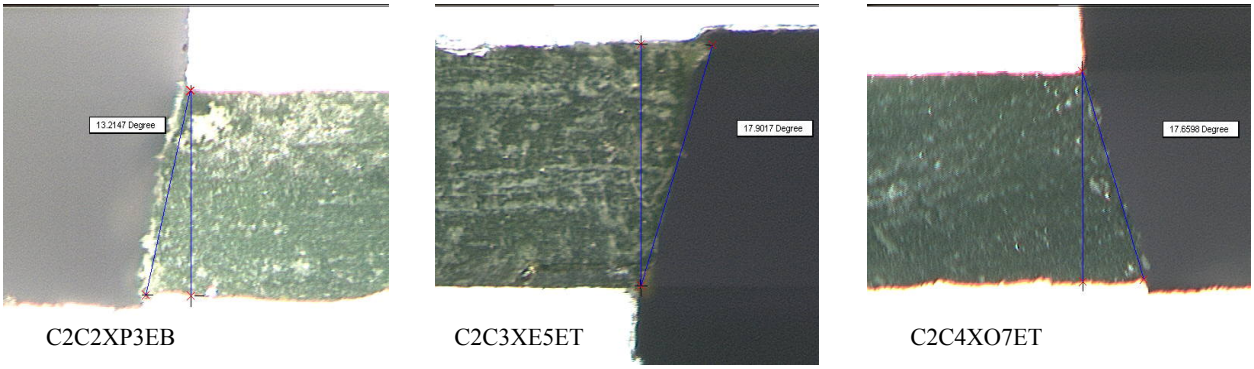

(a) 10% Yield Stress (b) 15% Yield Stress (c) 25% Yield Stress

FIGURE 4-51. SHEAR DEFORMATION OF LOCTITE 180°F SPECIMENS

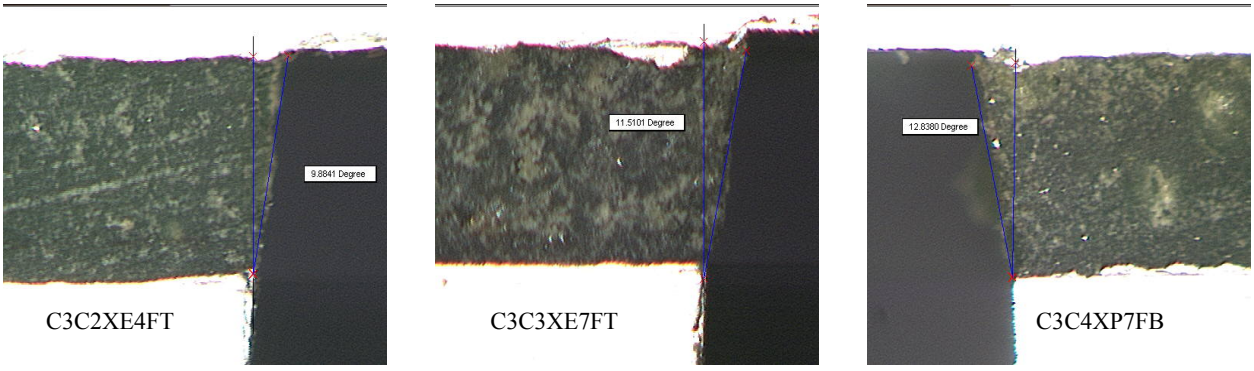

(a) 10% Yield Stress (b) 15% Yield Stress (c) 25% Yield Stress

FIGURE 4-52. SHEAR DEFORMATION OF LOCTITE 210°F SPECIMENS

Of the three adhesives under investigation, EA9696 adhesive had the highest dry glass transition temperature of 209.6°F and a relatively high modulus. However, the shear deformation data indicated unexpected shear deformation, as shown in figures 4-53 and 4-54. At 180°F, these specimens showed a shear deformation as high as 19 degrees for an applied stress level of 25% of the yield stress. This observation reveals the problem of designing a bonded structure to operate in close proximity to the glass transition temperature.

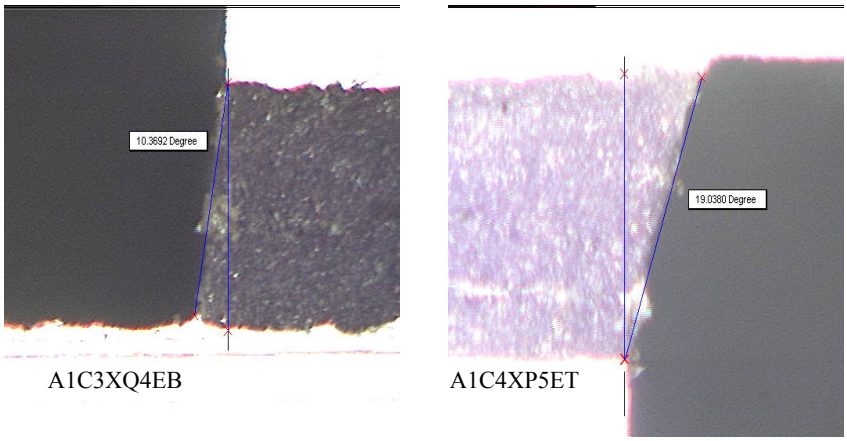

(a) 15% Yield Stress (b) 25% Yield Stress

FIGURE 4-53. SHEAR DEFORMATION OF EA9696 180°F SPECIMENS

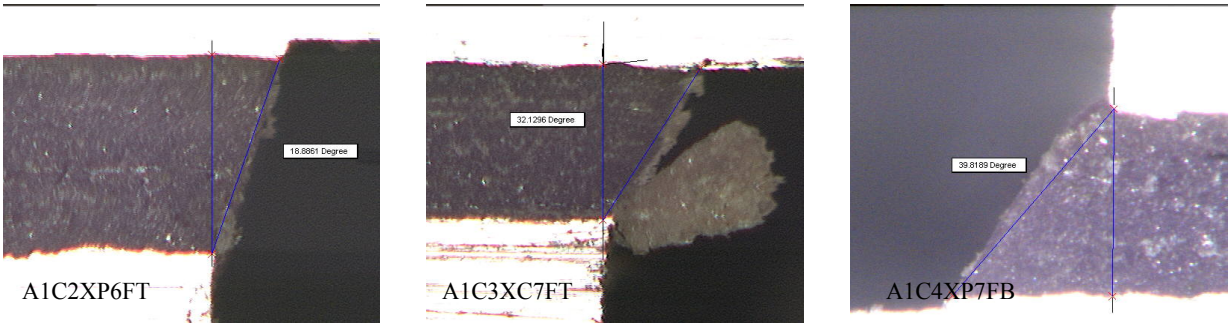

(a) 10% Yield Stress (b) 15% Yield Stress (c) 25% Yield Stress

FIGURE 4-54. SHEAR DEFORMATION OF EA9696 210°F SPECIMENS

Compared to the shear deformation results obtained for Loctite and EA9696, ES6292 adhesives results indicated considerably low values (figures 4-55 through 4-57). Even above the dry glass transition temperature, the shear deformation of 25% yield stress level was less than six degrees for 0.16-inch-thick specimens. The ES6292 adhesive is a more brittle material with a small plastic zone.

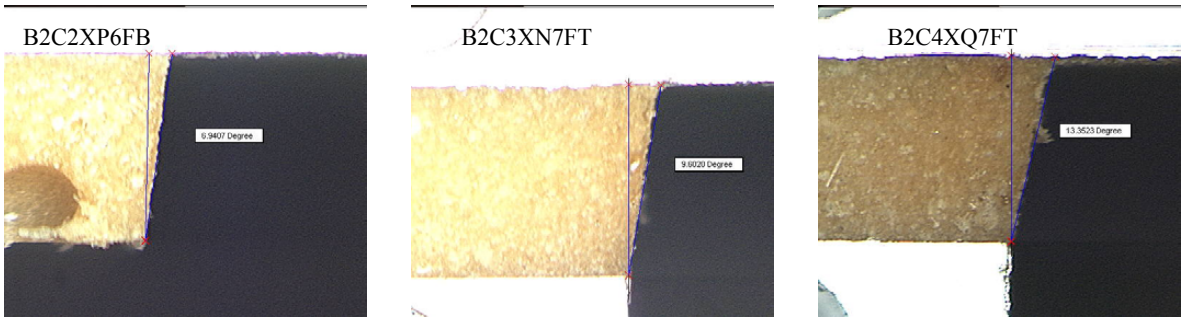

(a) 10% Yield Stress (b) 15% Yield Stress (c) 25% Yield Stress

FIGURE 4-55. SHEAR DEFORMATION OF ES6292 (BONDLINE THICKNESS = 0.06 inch) 210°F SPECIMENS

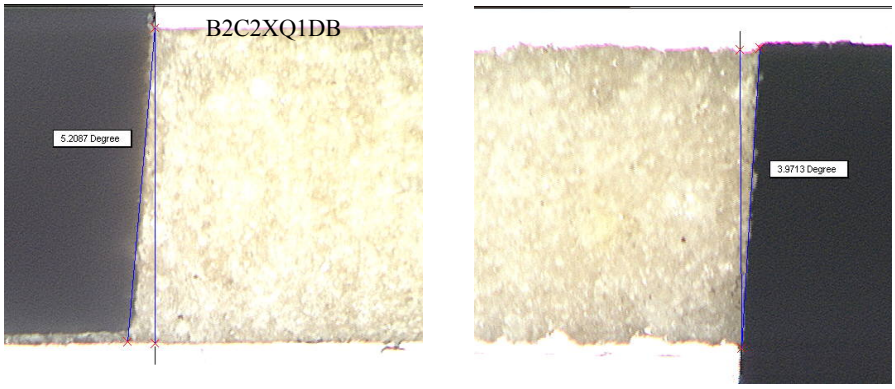

(a) 10% Yield Stress (b) 25% Yield Stress

FIGURE 4-56. SHEAR DEFORMATION OF ES6292 (BONDLINE THICKNESS = 0.16 inch) 150°F SPECIMENS

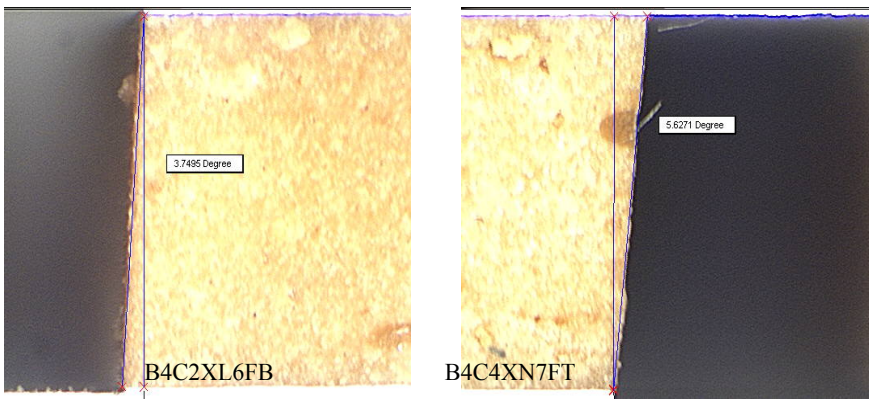

(a) 10% Yield Stress (b) 25% Yield Stress

FIGURE 4-57. SHEAR DEFORMATION OF ES6292 (BONDLINE THICKNESS = 0.16 inch) 210°F SPECIMENS

5. CONCLUSIONS.

Fatigue test results showed that RTW was the most damaging scenario among the test conditions investigated. Moisture attacked the adhesive bulk in some cases and the adhesive-adherend interface in others. However, based on failure mode results, most of the time moisture entered by diffusion through the adhesive, and in the remaining cases moisture entered either by diffusion through the adhesive-adherend interface or by migration to the interface once it was inside. As soon as moisture entered the adhesive, the degradation process began. The widely accepted concept provided by Sancakter, et al. [22] is confirmed here, whereby water molecules only entered and remained in those free spaces between adhesive molecules, and once these spaces were filled, a loss of strength resulted, attacking the interface and causing crack formation.

The influence of frequency on fatigue life was found in some of the scenarios, where low frequencies had the most damaging effect and high frequencies increased specimen longevity. These results were primarily due to the short time creep or behavior produced at low frequencies. At high frequencies, load was applied and removed so quickly that there was insufficient time for creep to occur or damage to accumulate. However, since not all specimens followed the trend of $10 > 5 > 2$ Hz (from the greatest to the lowest number of cycles), it is believed that frequency is simultaneously influenced by additional factors, such as specimen geometry, adhesive thickness, and environmental conditions. The influence of these factors could not be determined precisely, due to the few number of specimens and high variability of results. During fatigue testing, the temperature of the gage section was monitored and no increment was observed. Therefore, heat generation, especially at high frequencies, was minimal and did not affect the fatigue life of the adhesive joint.

Based on the type and intensity of loads that structures are intended to carry, the adhesive layer thickness must be carefully chosen during the design process. It was observed that thicker adhesive layers have considerable drops in ultimate shear strength, compared with thinner layers, as well as drastic drops in stress levels. Therefore, thin adhesive layers are recommended. As shown in appendix B, stress levels of specimens were either in the elastic-plastic range or in the plastic range. This indicates an additional source of variability due to regular damage accumulation produced by nonlinear strains.

Furthermore, the endurance limit for adhesives with a ductile behavior at room temperature ambient (RTD) was found between 40% or 50% of the ultimate, while for adhesives with a brittle behavior at RTD, this value was between 30% or 40% of the ultimate. Loctite and EA9696 adhesives had stress levels well above the linear limit points, while the ES6292 had stress levels near or sometimes well below the linear limit point. This was mainly due to its brittle mechanical behavior.

The stress relaxation characteristics of an adhesive highly depend on test temperature. Adhesive joints had a tendency to fail at high temperatures due to large shear deformations, as shown for ES6292 (0.06 inch) at 210°F; stress in the adhesive joint decayed about 95.99%, which caused the joint failure. The same observation was true for the EA9696 adhesive at the same

temperature, which caused the joint to deviate from the expected behavior. These results showed the consequences of designing an adhesive structure to operate near glass transition temperature. Stress relaxation behavior is also dependent on the bondline thickness of adhesive joints. It was observed that more stress relaxation occurred in thicker bondlines than thinner bondlines. Furthermore, results indicated that stress relaxation is also related to applied initial stress. Shear deformation results obtained through stereoscopic analysis further confirmed the severity of stress relaxation under elevated temperature conditions, especially closer to the glass transition temperature of the dry adhesive. The shear deformation of the ES6292 adhesive was considerably lower than the other two adhesives.

Temperature-immersed (soaked) specimens indicated an increase in the apparent shear strength and modulus for most of the adhesives after conditioning for 400 hours. This was probably caused by postcure and additional cross-linking beyond the glass transition temperature.

6. REFERENCES.

1. Cagle, C., *Handbook of Adhesive Bonding,* McGraw-Hill Book Company, New York, 1968, pp. 19-35.

2. Kinloch, A.J., "Adhesion and Adhesives," *Science and Technology*, Chapman and Hall, London, 1990, pp. 2-15.

3. Adams, R.D., Comyn, J., and Wake, W.C., *Structural Adhesive Joints in Engineering*, Chapman and Hall, London, 1997, p.8.

4. Hart-Smith, L.J., "Developments in Adhesives 2," Kinloch, A.J., ed., *Applied Science Publications,* London, 1981.

5. Marceau, J.A., McMillan, J.C., and Scardino, W.M., "Cyclic Stress Testing of Adhesive Bonds," *Proceedings of the 22nd National SAMPE Symposium,* San Diego, California, 1977.

6. Romanko, J., "Behavior of Adhesively Bonded Joints Under Cyclic Loading," Materials Research Laboratories, General Dynamics, Fort Worth Division, Fort Worth, Texas, 1976.

7. Sancaktar, E., "Static and Dynamic Fatigue Testing," *Engineering Materials Handbook, Adhesives and Sealants,* ASM International, Vol. 3, United States of America, 1990, pp. 349-371.

8. Sancaktar, E., "Fatigue and Fracture Mechanics," *Engineering Materials Handbook, Adhesives and Sealants,* ASM International, Vol. 3, United States of America, 1990, pp. 501-520.

9. Bethune, A.W., "Durability of Bonded Aluminum Structure," Boeing Commercial Airplane Company, *SAMPE Journal*, 1975, pp. 5-10.

10. Kinloch, A.J. and Osiyemi, S.O., "Predicting the Fatigue Life of Adhesively-Bonded Joints," *Journal of Adhesion,* Vol. 43, 1993, pp. 79-90.

11. Broughton, W.R. and Mera, R.D., "Review of Life Prediction Methodology and Adhesive Joint Design and Analysis Software," National Physical Laboratory, London, June 1997.

12. Tomblin, J., Seneviratne, W., Escobar, P., and Yap, Y., "Shear Stress-Strain Data for Structural Adhesives," FAA Report DOT/FAA/AR-02/97, November 2002.

13. Brockmann, W., "The Nature of Adhesion and the Influence of Surface Treatments on the Behavior of Bonded Joints," AGARD Lecture Series, No.102, France, 1979, pp. 6.1-17.

14. McMillan, J.C., "Surface Preparation—The Key to Bondment Durability," AGARD Lecture Series, No.102, France, 1979, pp. 7.1-25.

15. Bonded Joints, MIL-HDBK-17-1E, Working Draft, pp. 7.44-62.

16. Goland, M. and Reissner, E., "The Stresses in Cemented Joints," *Journal of Applied Mechanics 11,* 1944, pp. 17-27.

17. Tomblin, J., Yang, C., and Harter, P., "Investigation of Thick Bondline Adhesive Joints," FAA Report DOT/FAA/AR-01/33, June 2001.

18. Tomblin, J., Harter, P., Seneviratne W., and Yang, C., "Characterization of Bondline Thickness Effects in Adhesive Joints," *ASTM Journal of Testing and Evaluation*, JCTRER, Vol. 24, No 2, April 2002, pp. 332-344.

19. Krieger, R.B. Jr., "Stiffness Characteristics of Structural Adhesives for Stress Analysis in Hostile Environment," American Cyanamid Company, Maryland, 1975.

20. Dowling, Norman E., *Mechanical Behavior of Materials: Engineering Methods for Deformation, Fracture, and Fatigue*, 2nd ed., Prentice-Hill, New Jersey, 1998.

21. Ferry, John D., *Viscoelastic Properties of Polymers*, 3rd ed., John Wiley & Sons, Inc., New York, 1980.

22. Sancakter, Erol and Schenck, Steven C., "Material Characterization of Structural Adhesives in the Lap Shear: Mode 2 Temperature-Dependent Delayed Failure," *Industrial & Engineering Chemistry Product Research and Development,* Vol. 24, No. 2, June 1985, pp. 257-62.

23. Althof, W., "Creep, Recovery and Relaxation of Shear-Loaded Adhesive Bondlines," *Journal of Reinforced Plastics & Composites,* Vol. 1, January 1982, pp. 29-28.

24. Lewis, A. F. and Natarajan, G., *Permanence and Endurance of Structural Adhesive Joints, Treatise on Adhesion and Adhesives*, R. L. Patrick, ed. ,Vol. 5, Marcel Dekker, New York, 1981, pp. 313-81.

25. Tomblin, J., Seneviratne, W., Kim, H., and Lee, J., "Box Beam Lap Shear Torsion Testing for Evaluating Structural Performance of Adhesive Bonded Joints," *Joining of Composites Structures, ASTM STP 1455,* American Society for Testing and Materials, West Conshohocken, PA, 2003.

APPENDIX A—ADHESIVE CHARACTERIZATION

This appendix contains the data obtained for adhesive characterization. Figures A-1 through A-4 show the characteristic shear responses obtained under seven different environmental conditions. These curves represent the average shear strain calculated using two modified-KGR extensometers. Figures A-5 through A-8 show the ultimate shear strength and shear modulus obtained from the characteristic shear response curves. Wet, or room temperature wet, test specimens were conditioned at 145°F and 85% r.h. for a period of 1,000 hours (approximately 42 days) in a humidity chamber.

Figures A-9 and A-10 show the apparent shear strength results obtained after soaking specimens for 400 hours. These results were also compared with specimens that were tested with a typical soak time of 3 minutes.

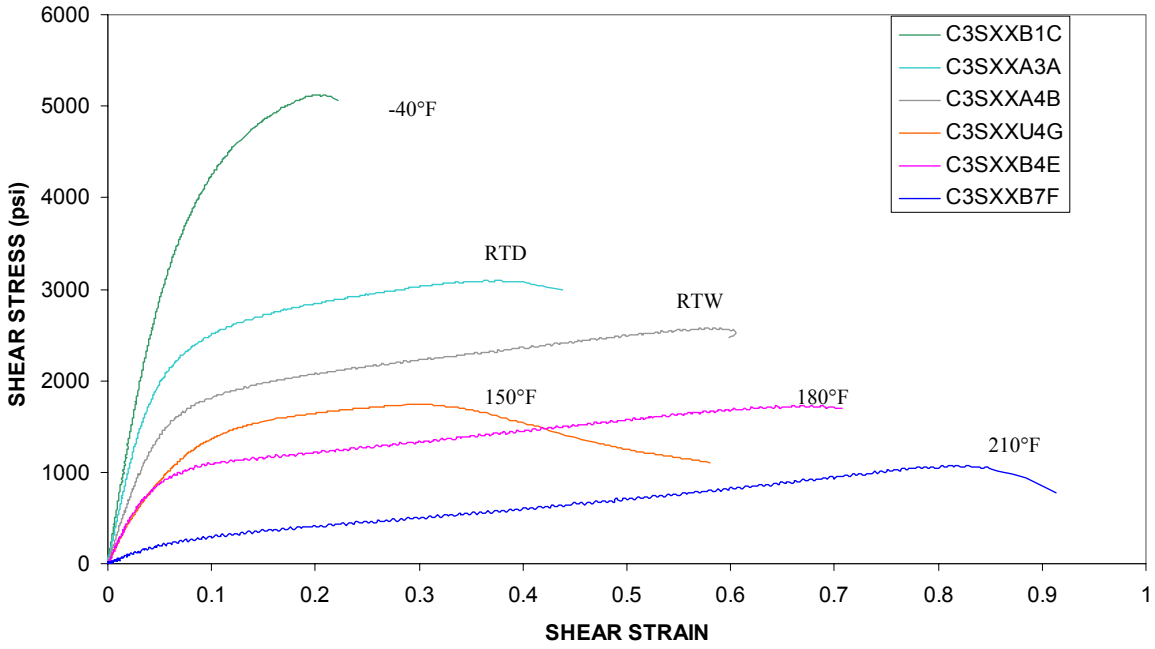

FIGURE A-1. CHARACTERISTIC SHEAR RESPONSE OF LOCTITE ADHESIVE

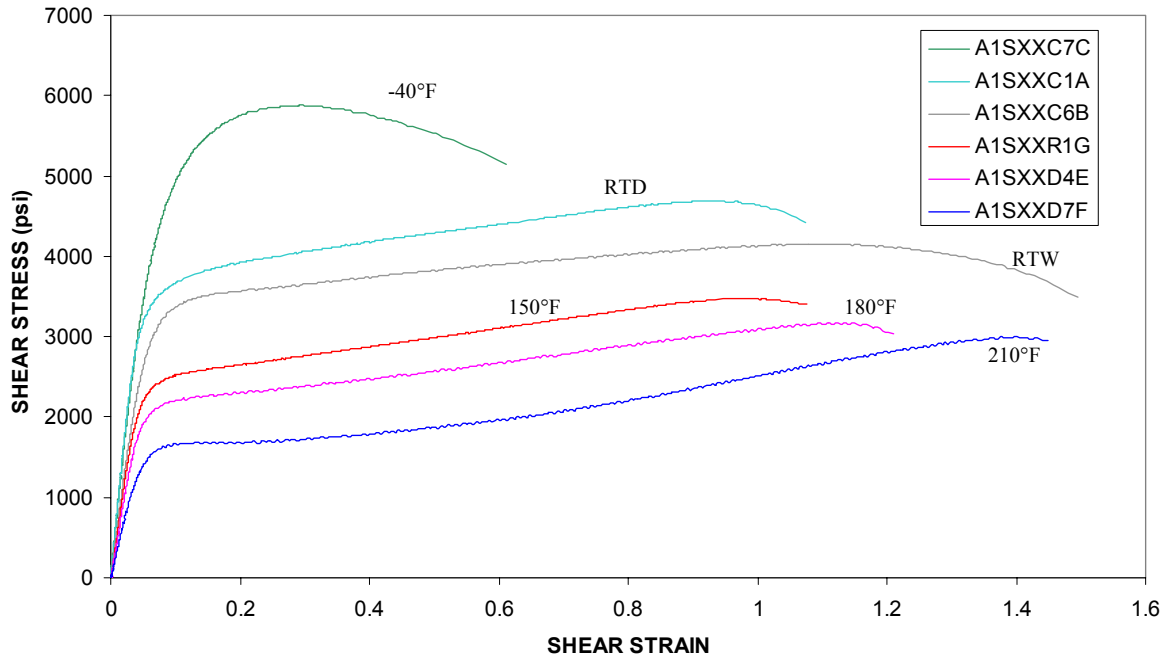

FIGURE A-2. CHARACTERISTIC SHEAR RESPONSE OF EA9696 ADHESIVE

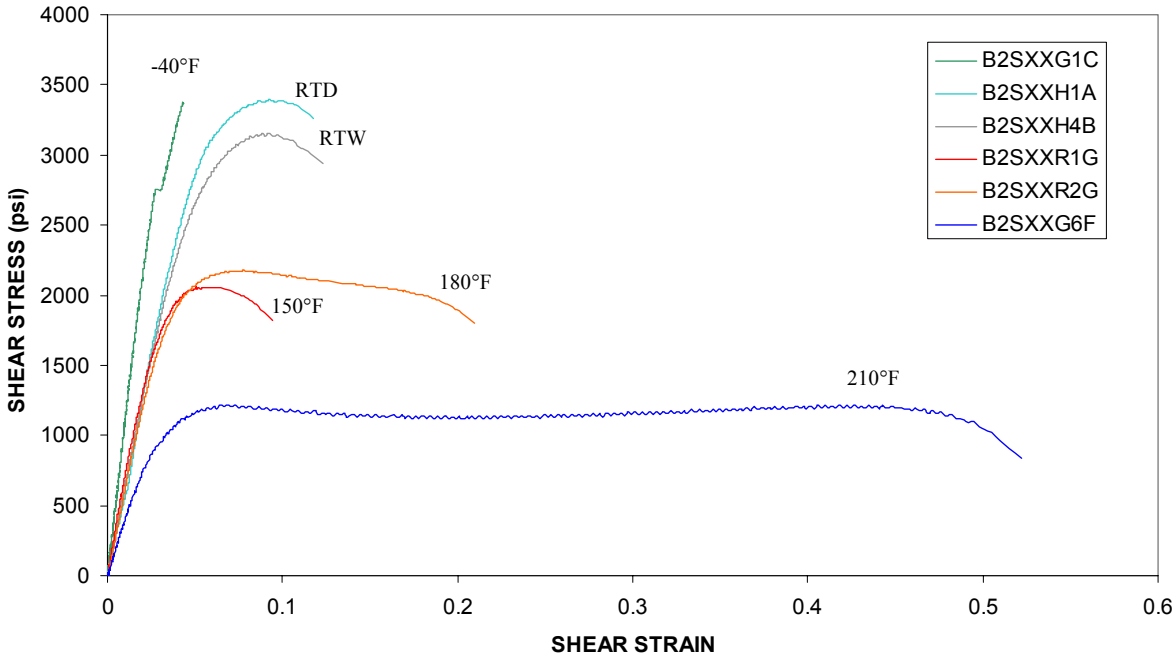

FIGURE A-3. CHARACTERISTIC SHEAR RESPONSE OF ES6292 0.06 inch

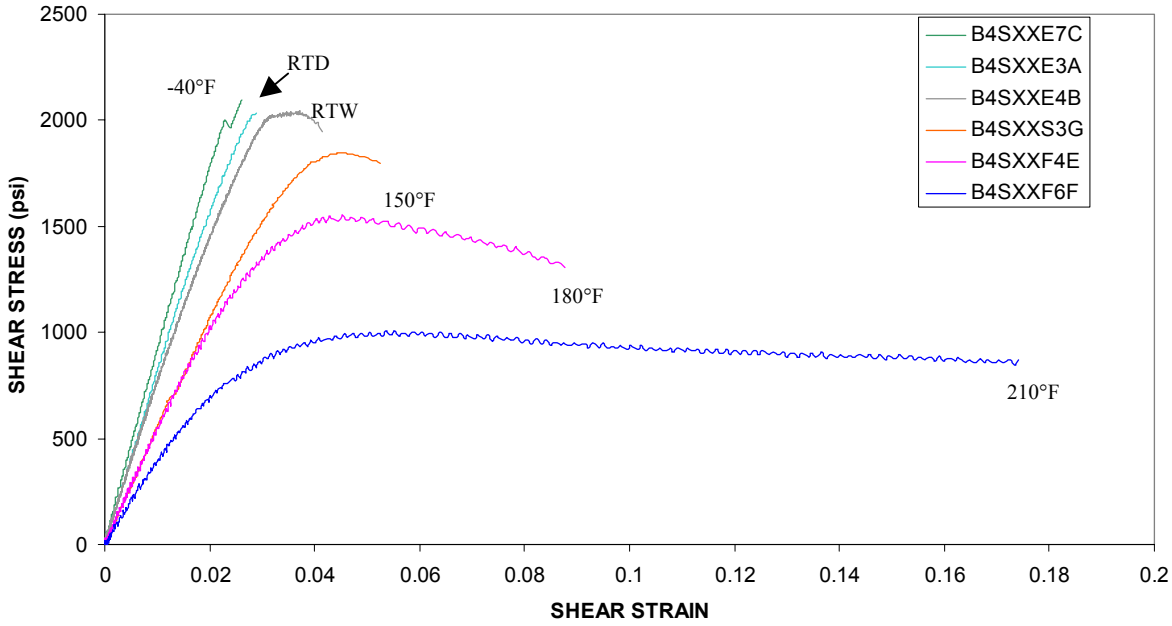

FIGURE A-4. CHARACTERISTIC SHEAR RESPONSE OF ES6292 0.16 inch

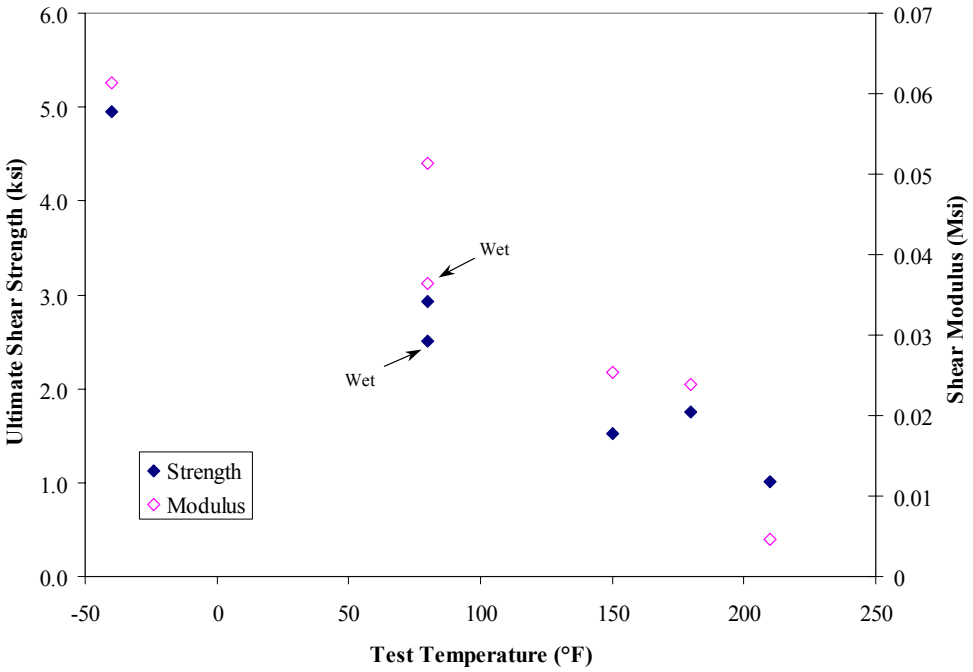

FIGURE A-5. ULTIMATE SHEAR STRENGTH AND INITIAL MODULUS OF LOCTITE ADHESIVE

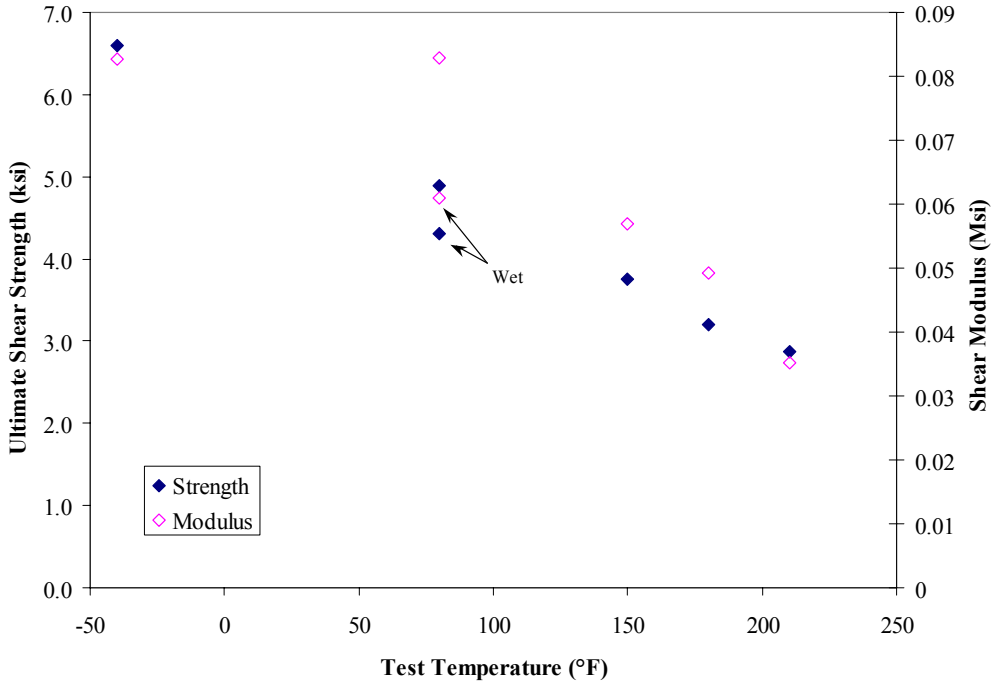

FIGURE A-6. ULTIMATE SHEAR STRENGTH AND INITIAL MODULUS OF EA9696 ADHESIVE

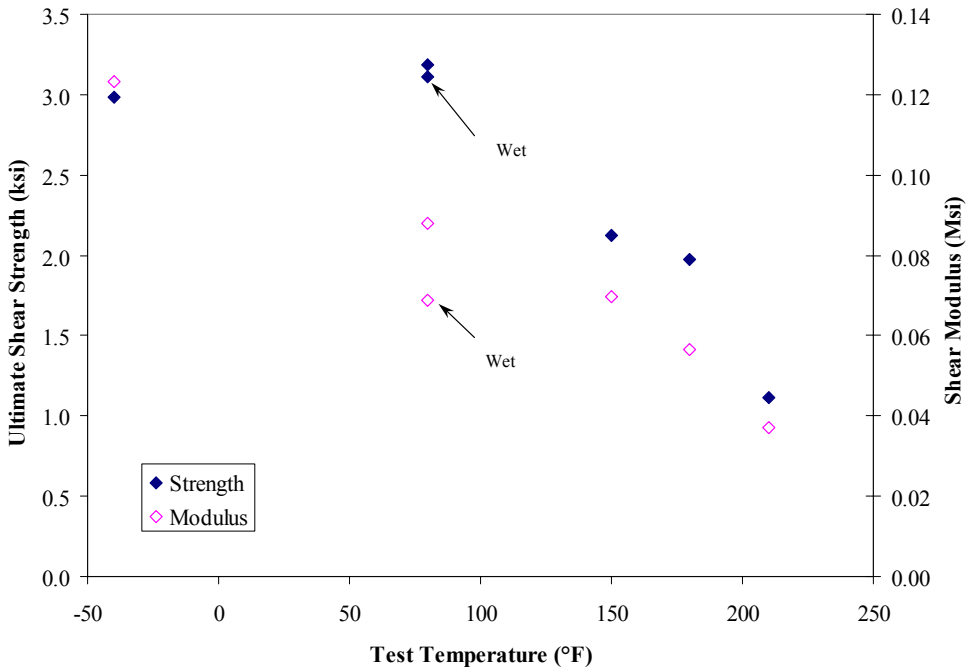

FIGURE A-7. ULTIMATE SHEAR STRENGTH AND INITIAL MODULUS OF ES6292 (0.06 inch) ADHESIVE

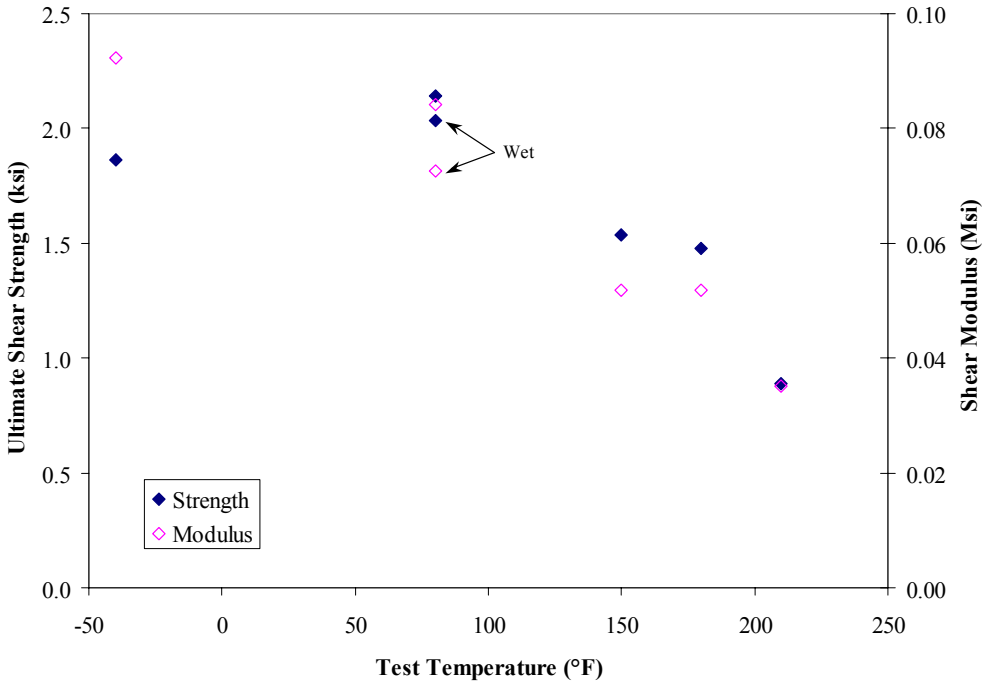

FIGURE A-8. ULTIMATE SHEAR STRENGTH AND INITIAL MODULUS OF ES6292 (0.16 inch) ADHESIVE

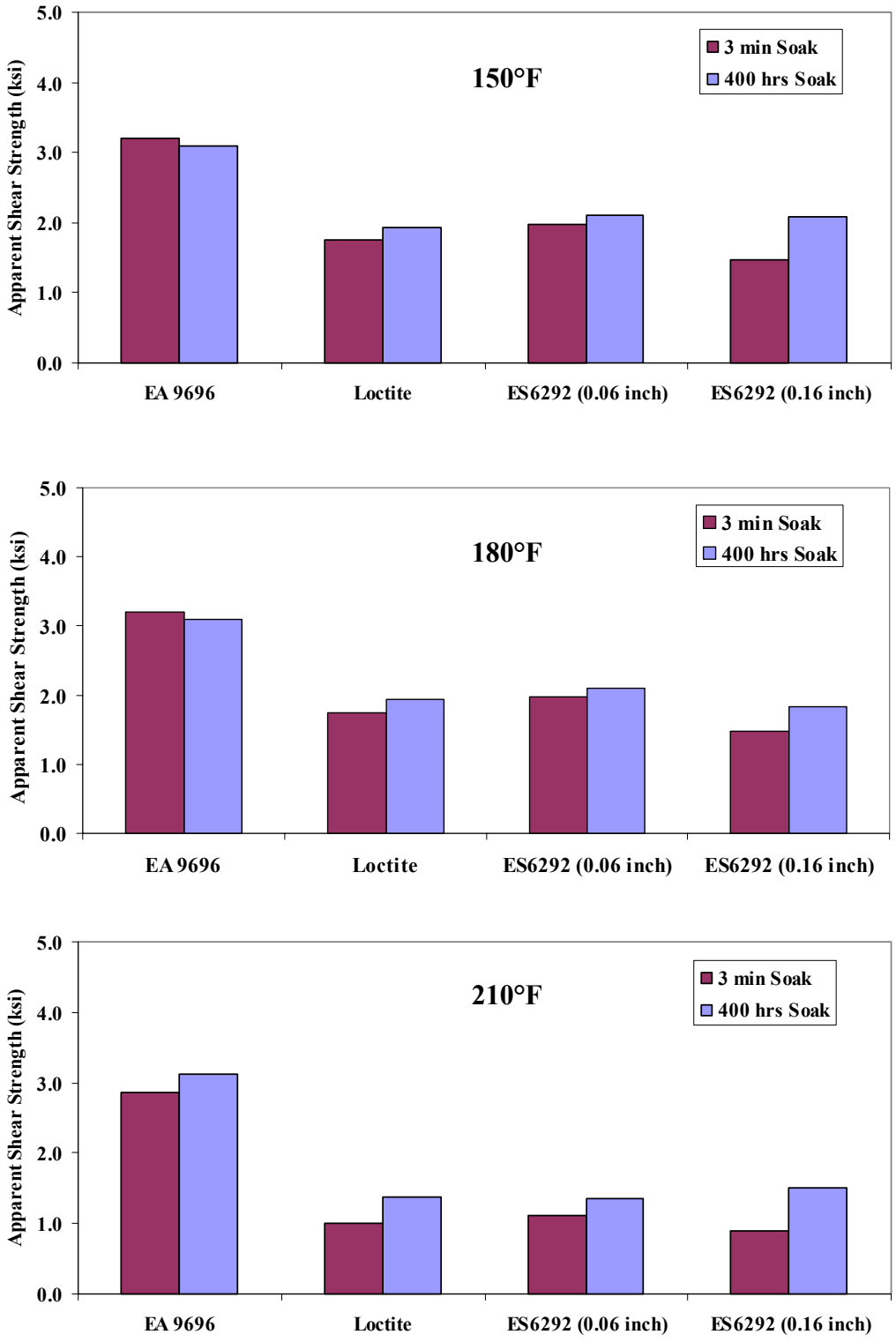

FIGURE A-9. COMPARISON OF APPARENT SHEAR STRENGTH OF TEMPERATURE-IMMERSED (SOAKED) SPECIMENS

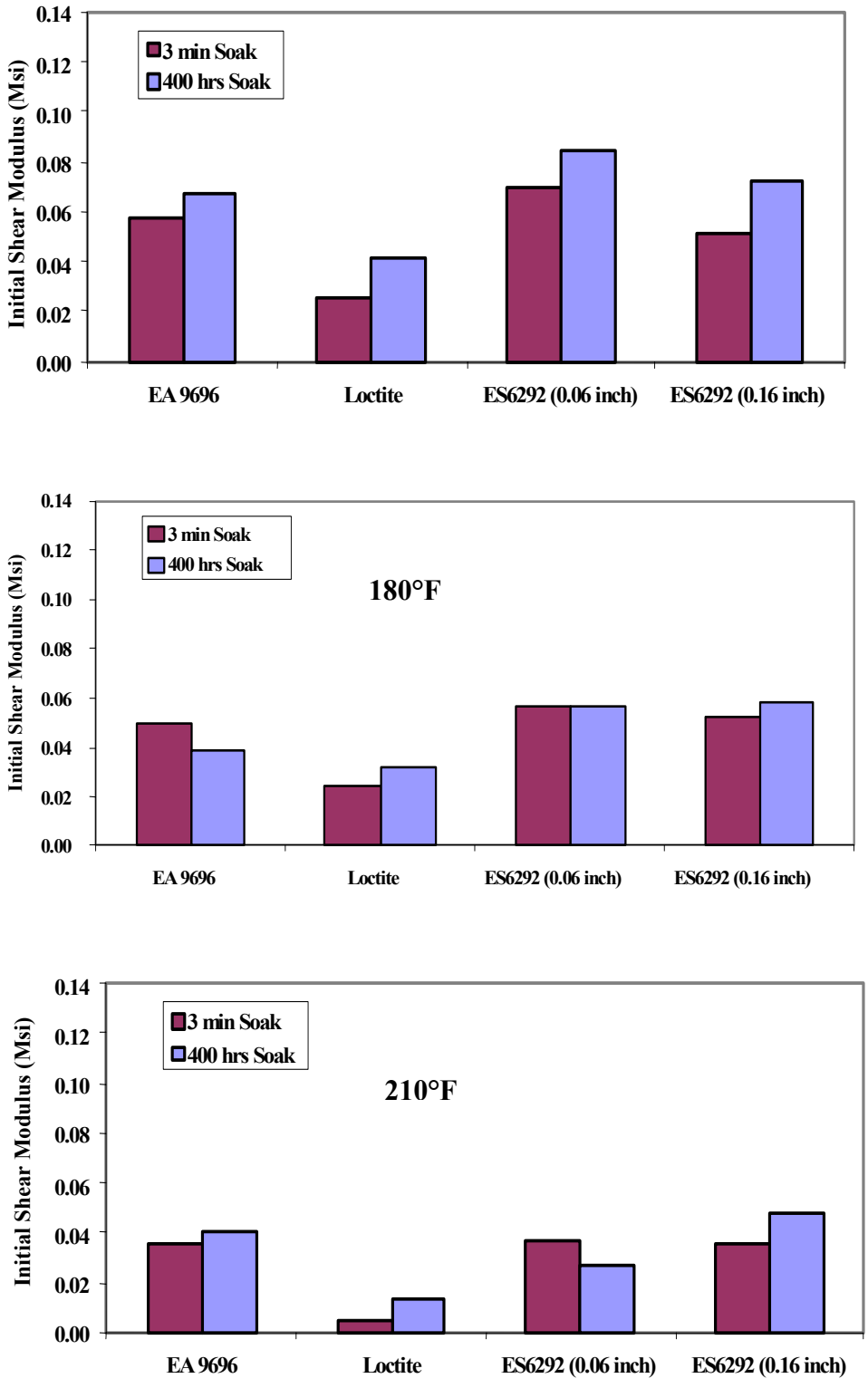

FIGURE A-10. COMPARISON OF SHEAR MODULUS OF TEMPERATURE-IMMERSED (SOAKED) SPECIMENS

APPENDIX B—FATIGUE STRESS LEVELS IN RELATION TO SHEAR STRESS-STRAIN PLOTS

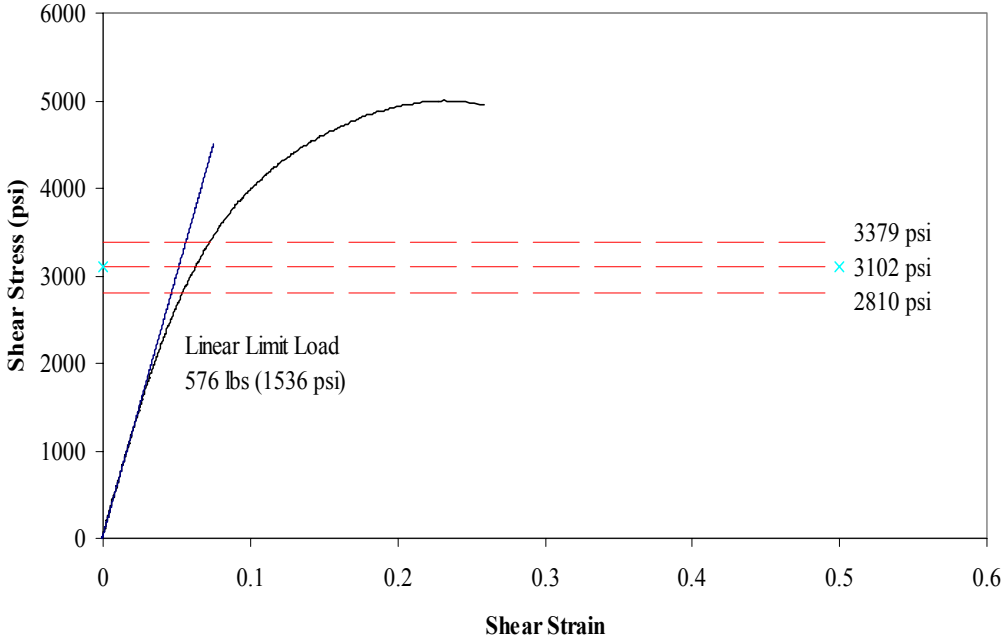

FIGURE B-1. LOCTITE CTD STRESS LEVELS

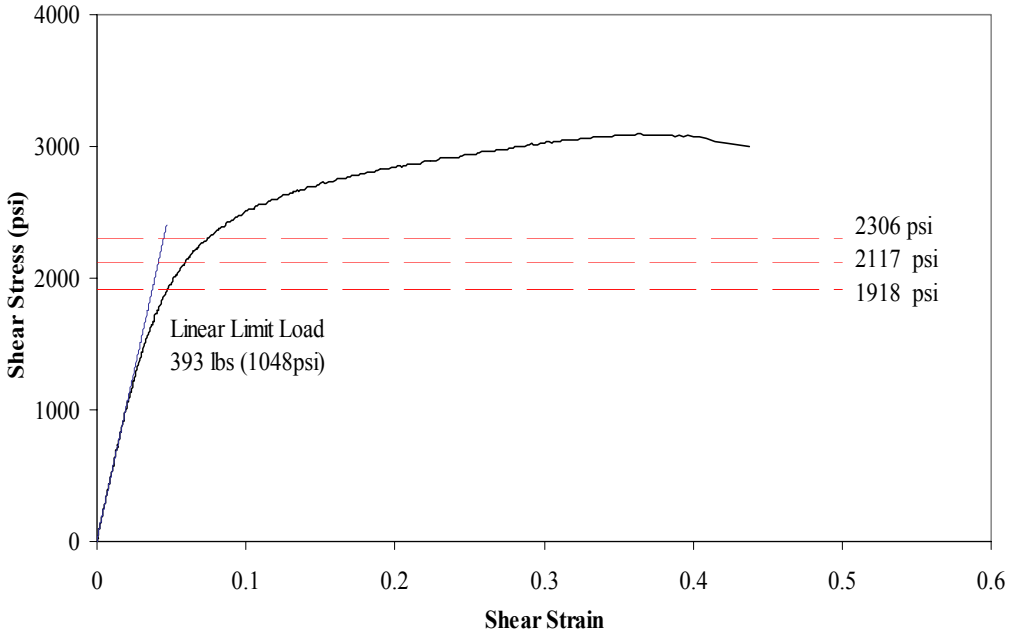

FIGURE B-2. LOCTITE RTD STRESS LEVELS

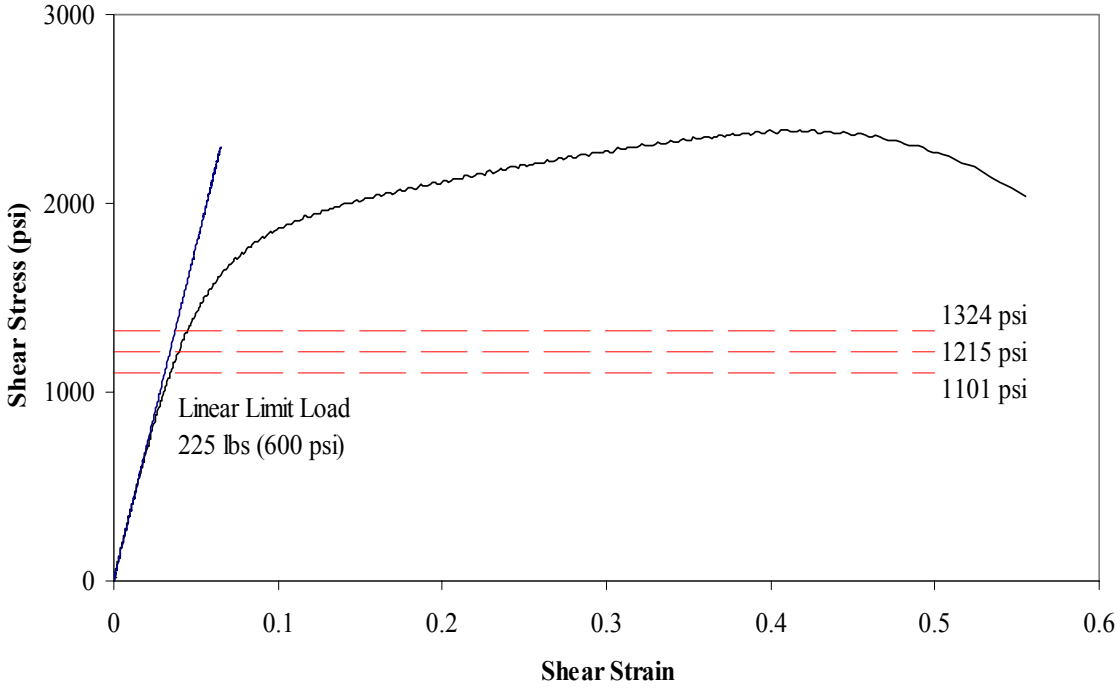

FIGURE B-3. LOCTITE RTW STRESS LEVELS

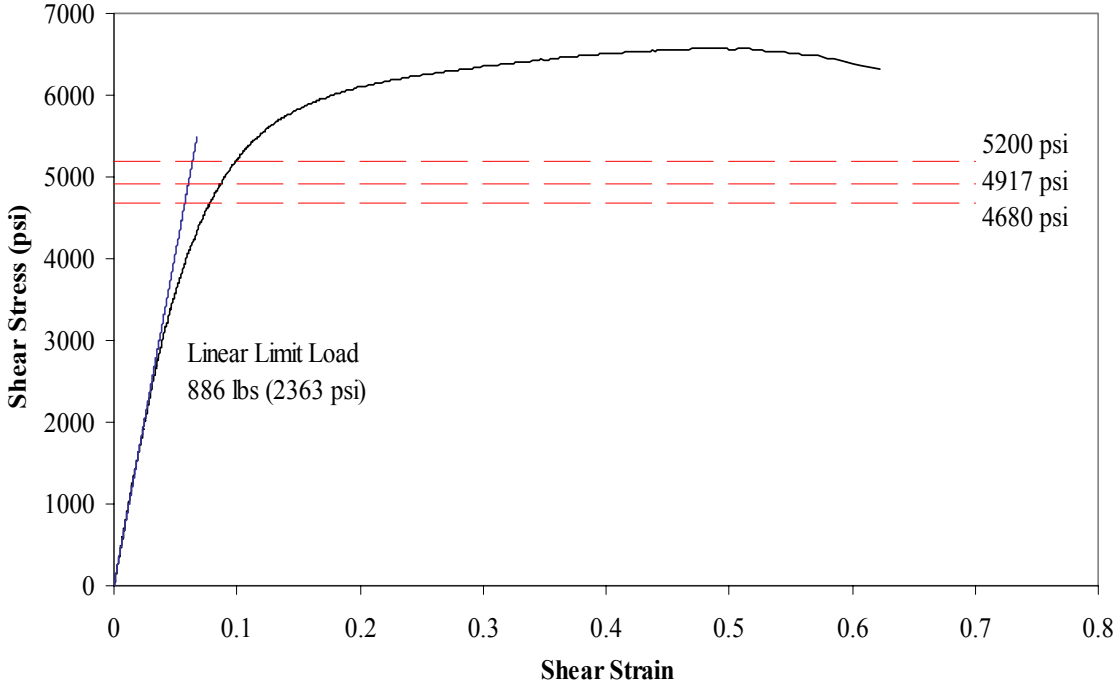

FIGURE B-4. EA9696 CTD STRESS LEVELS

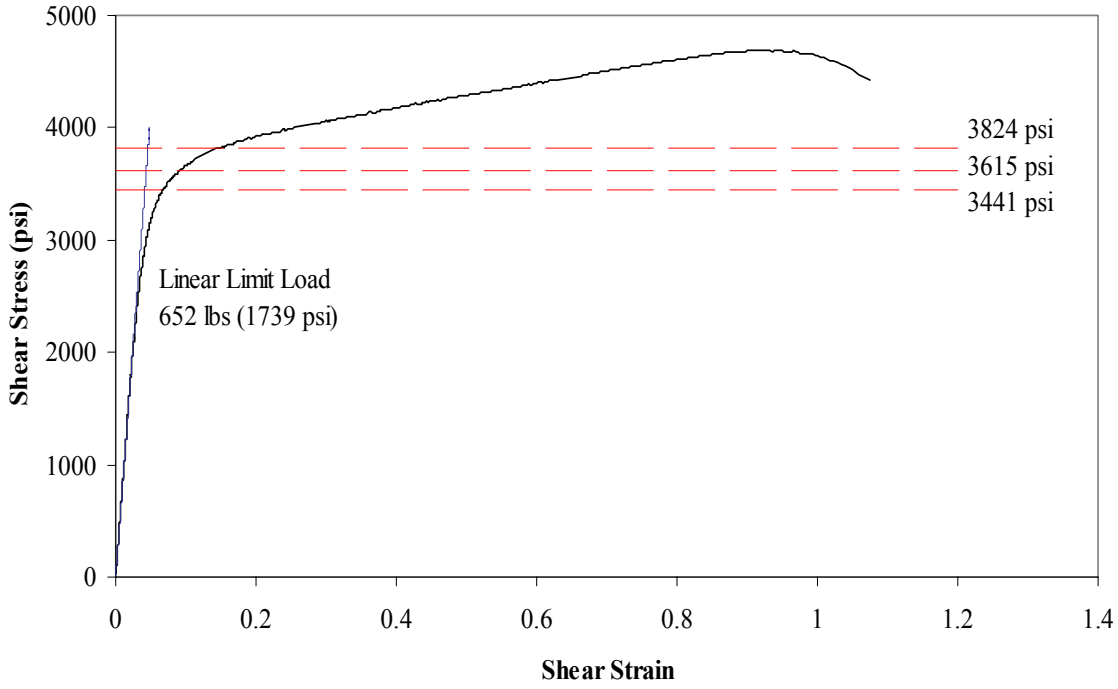

FIGURE B-5. EA9696 RTD STRESS LEVELS

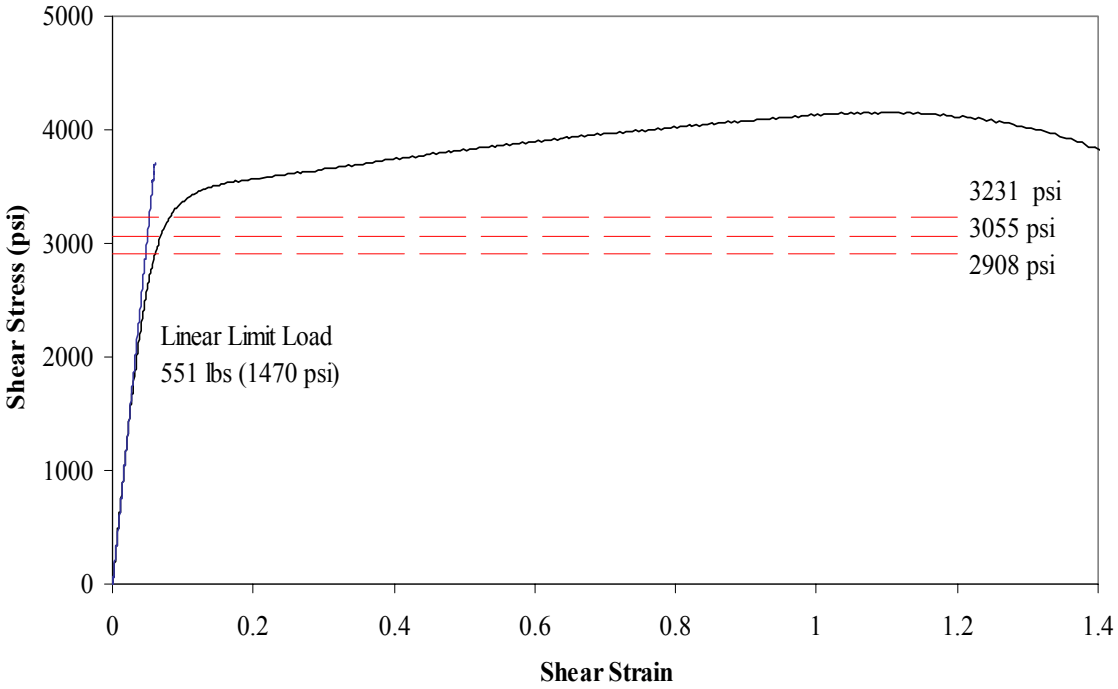

FIGURE B-6. EA9696 RTW STRESS LEVELS

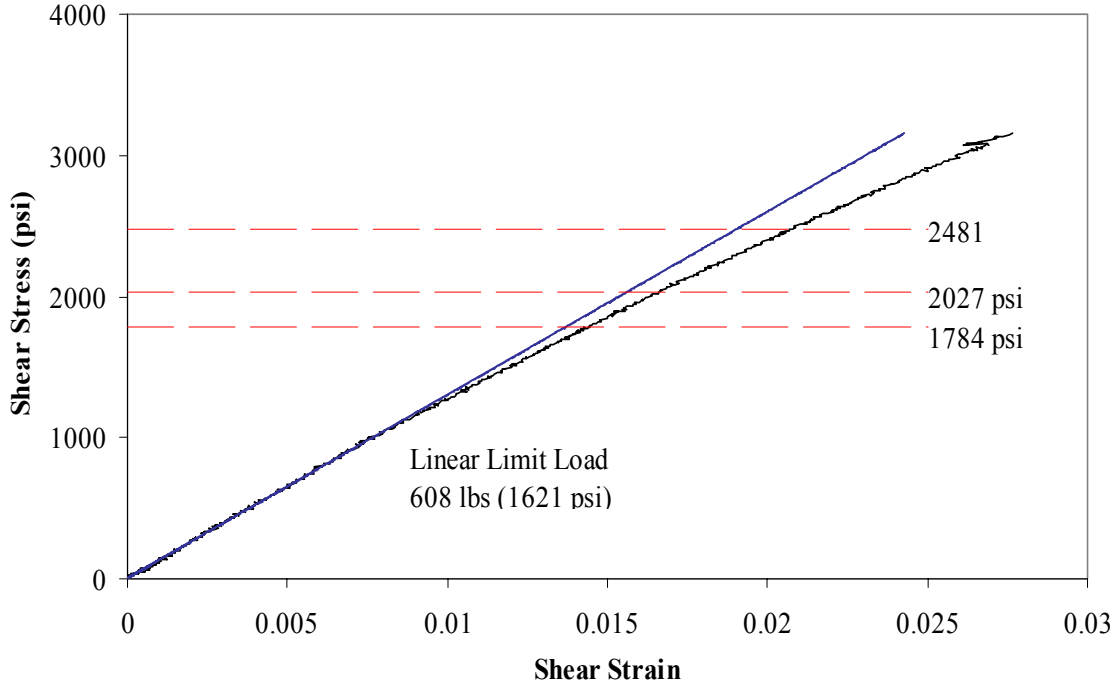

FIGURE B-7. ES6292 0.06-inch CTD STRESS LEVELS

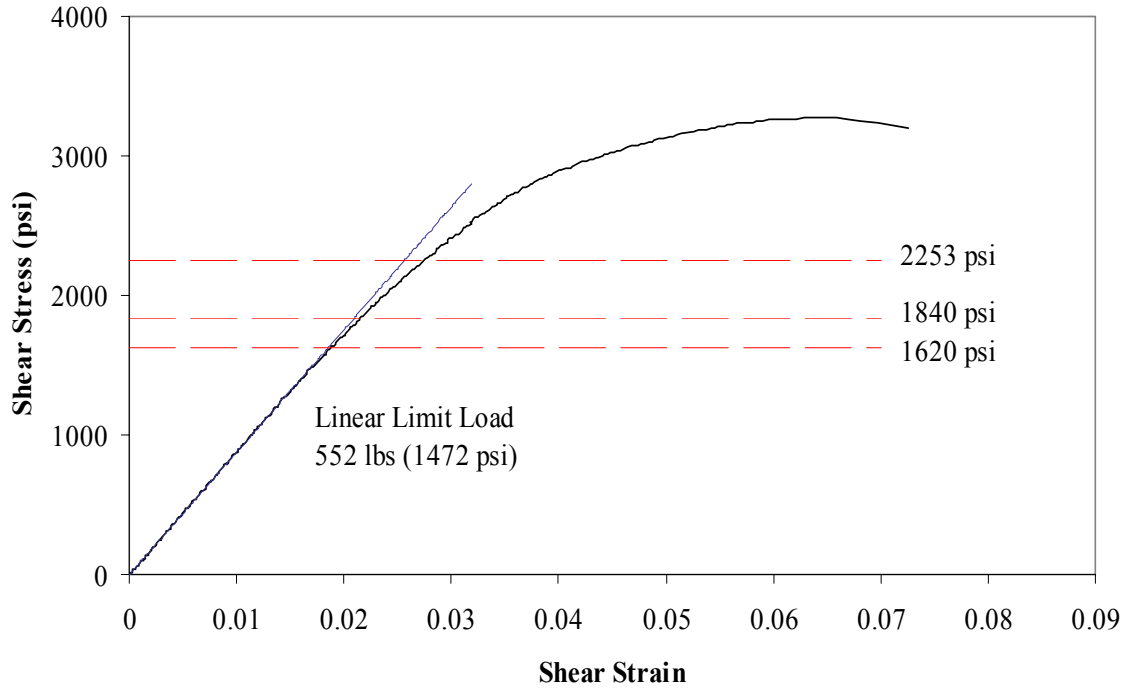

FIGURE B-8. ES6292 0.06-inch RTD STRESS LEVELS

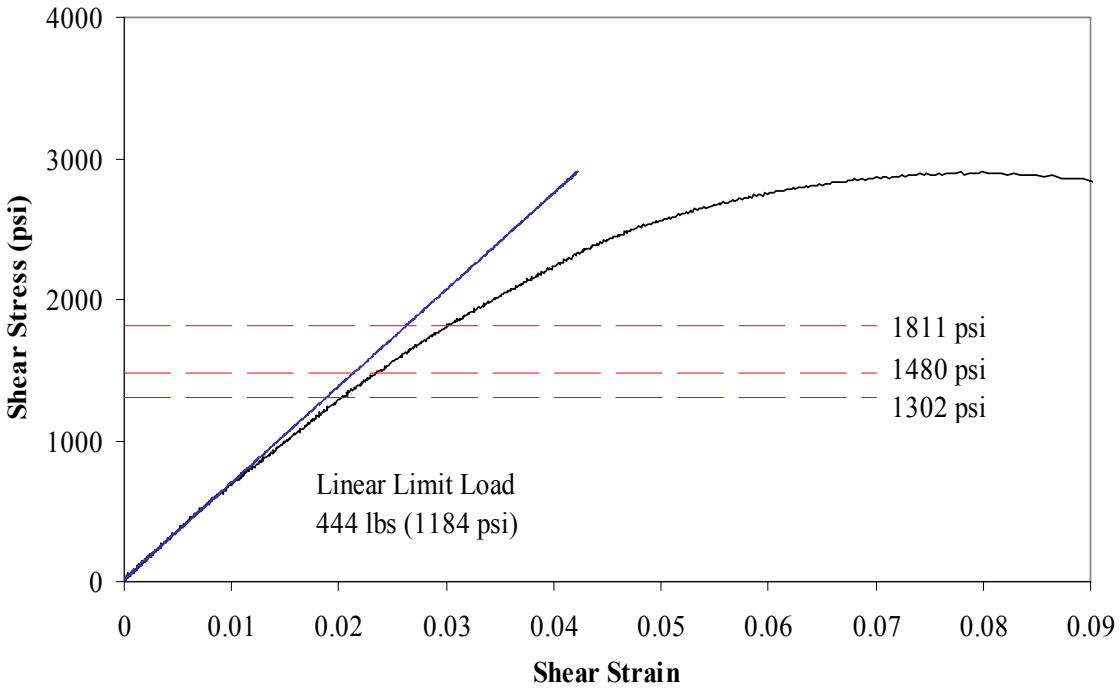

FIGURE B-9. ES6292 0.06-inch RTW STRESS LEVELS

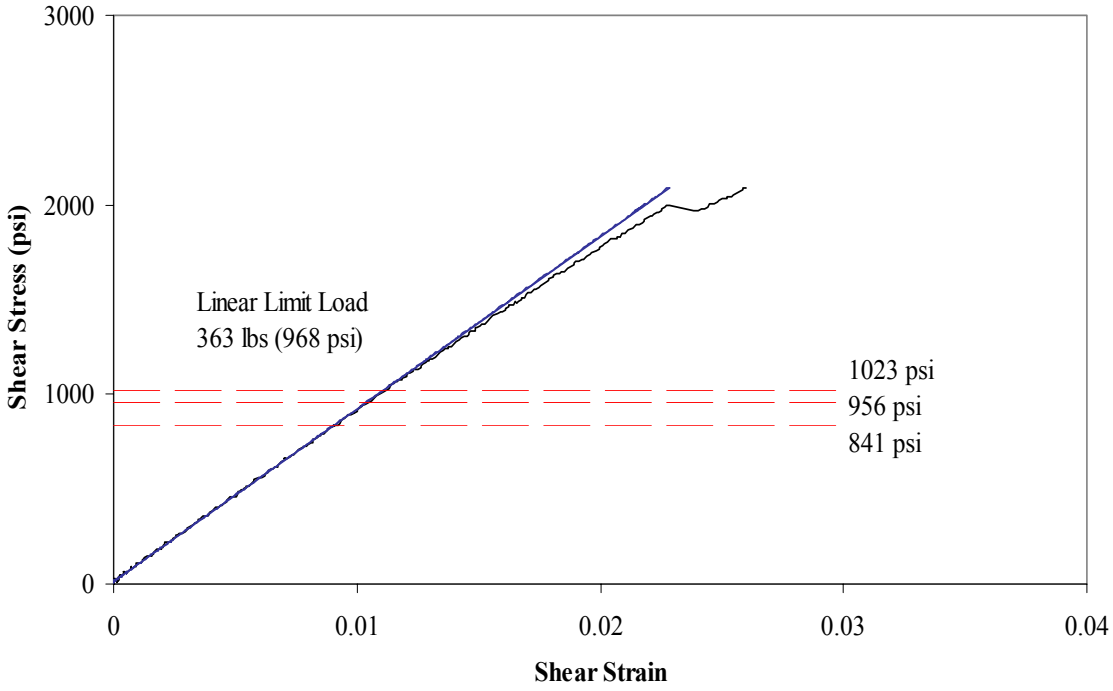

FIGURE B-10. ES6292 0.16-inch CTD STRESS LEVELS

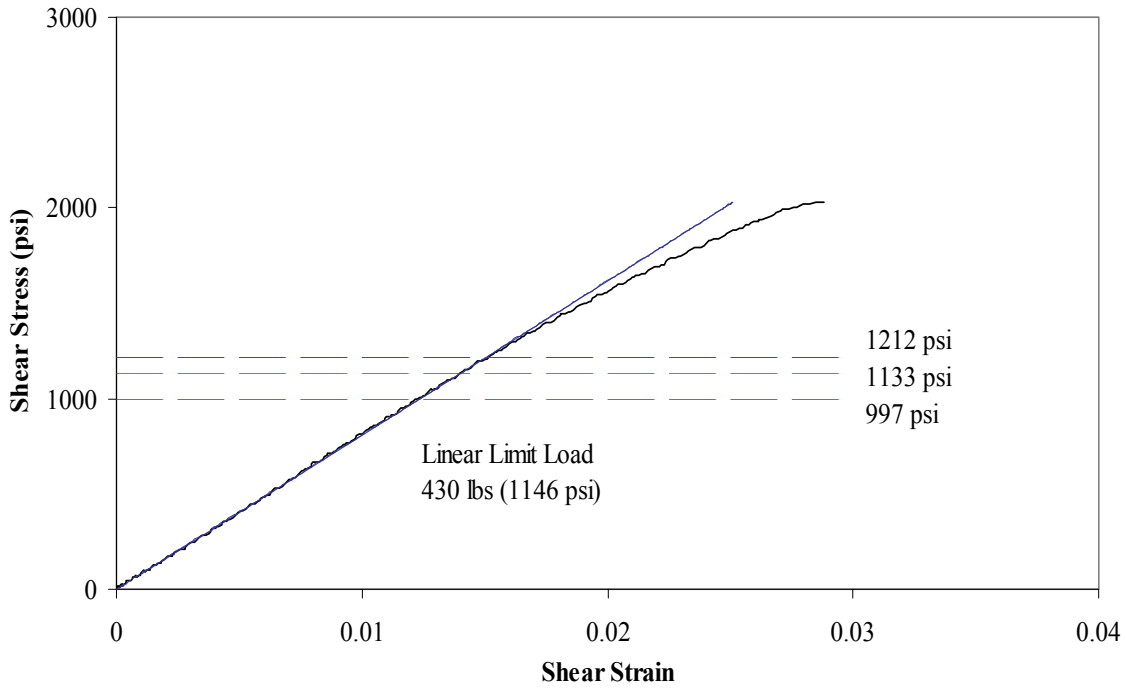

FIGURE B-11. ES6292 0.16-inch RTD STRESS LEVELS

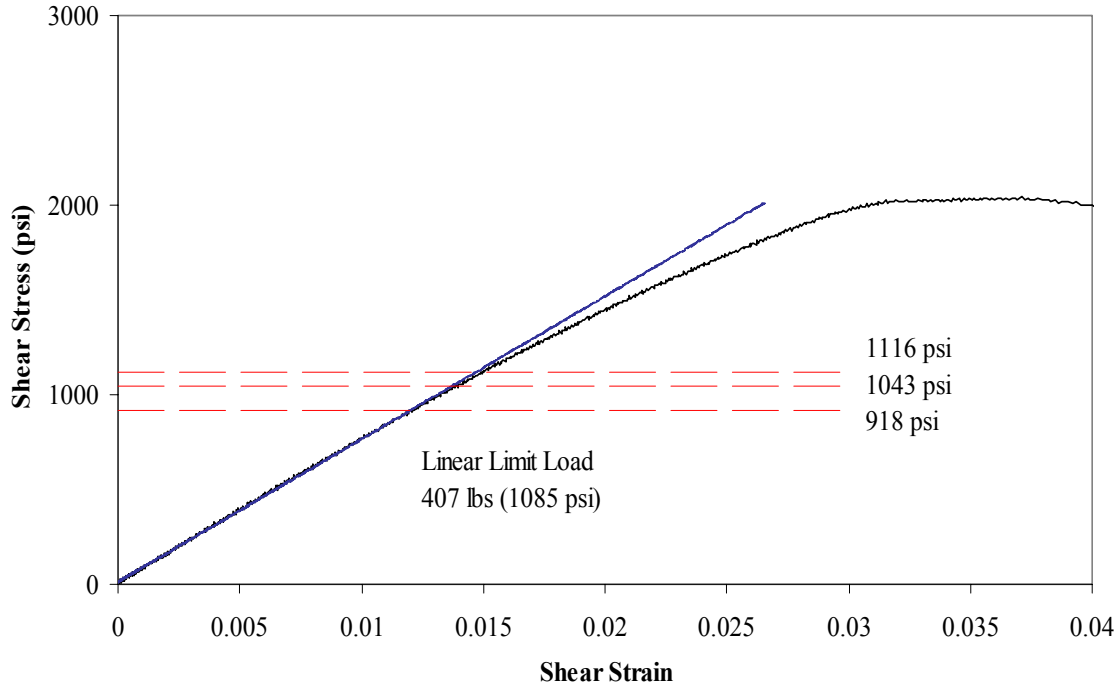

FIGURE B-12. ES6292 0.16-inch RTW STRESS LEVEL

APPENDIX C—STRESS RELAXATION TEST RESULTS

The results shown in this appendix were based on the stress relaxation data obtained at 150°, 180°, and 210°F using ALCOA stressing fixture (figures 4-25 through 4-36). These curves compare the decrease in shear stress as a function of time for each stress level. The amount decrease, $\Delta\sigma$, was calculated by subtracting the stress at a given time, $\sigma(t)$, from the initial applied stress, σ_0. These curves indicate the significance of stress relaxation as the stress level and temperature was increased.

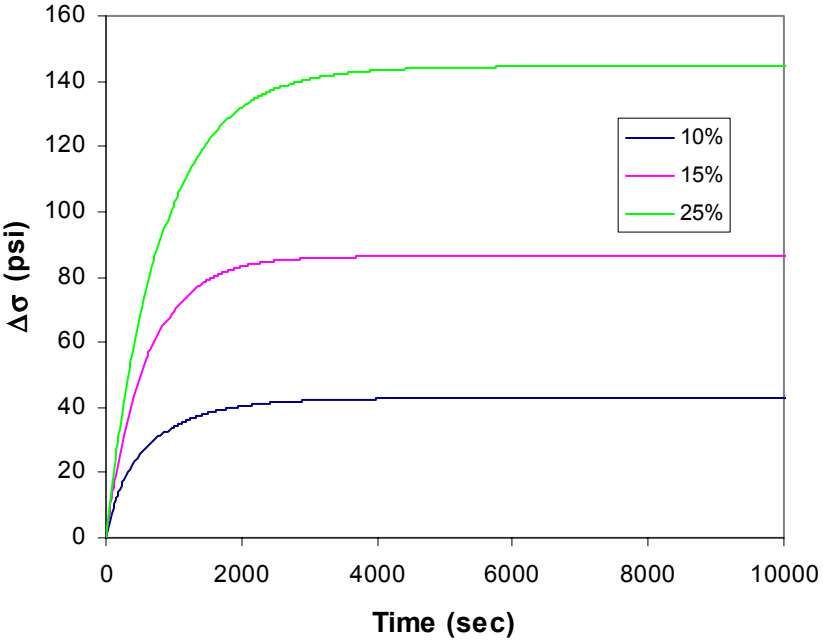

FIGURE C-1. STRESS RELAXATION (Δσ) FOR LOCTITE AT 150°F

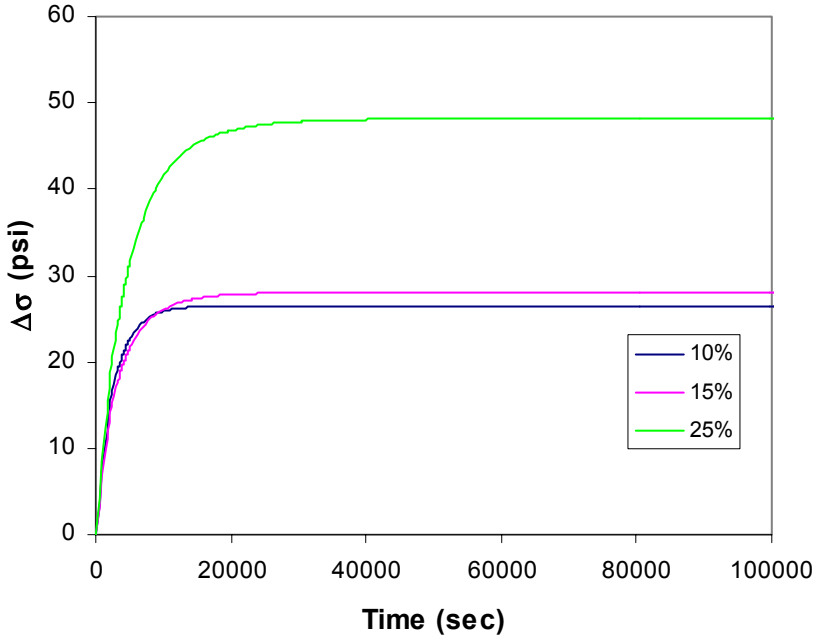

FIGURE C-2. STRESS RELAXATION (Δσ) FOR LOCTITE AT 180°F

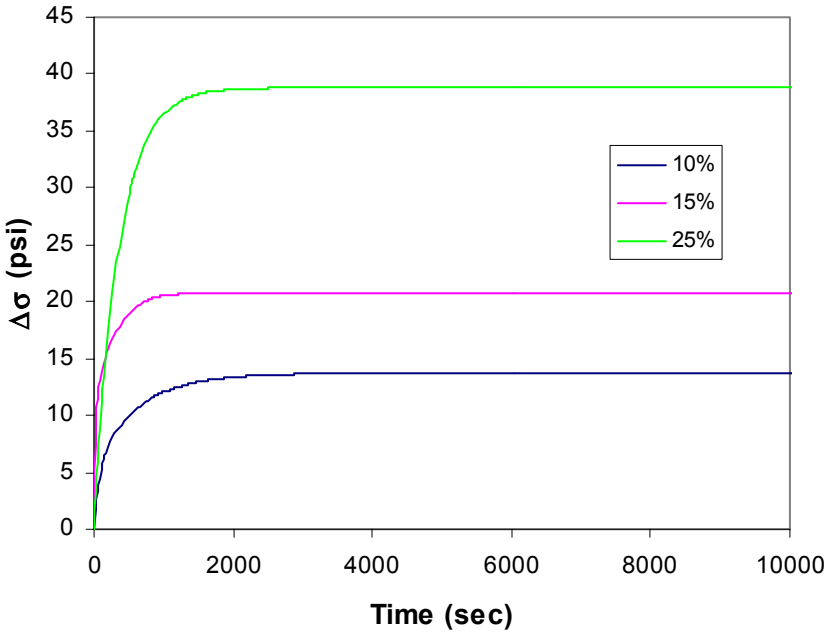

FIGURE C-3. STRESS RELAXATION (Δσ) FOR LOCTITE AT 210°F

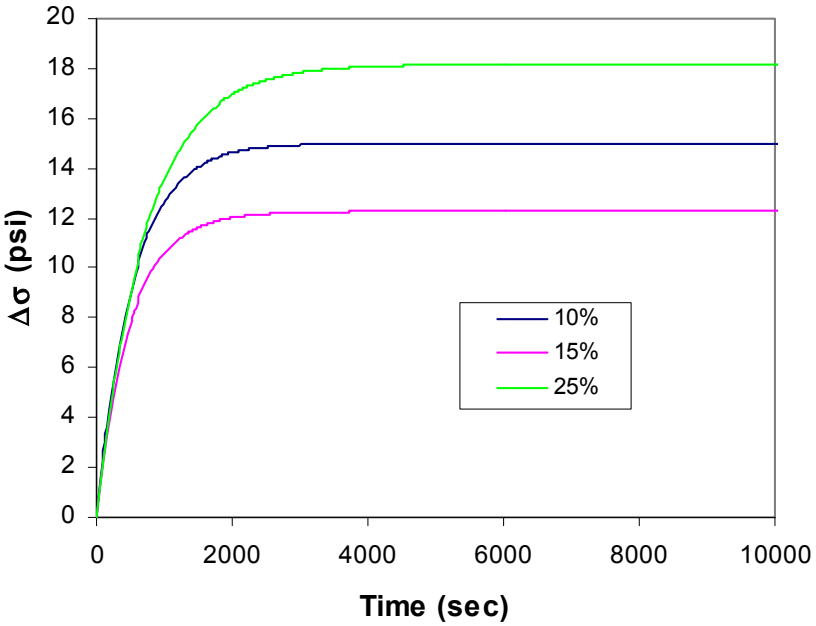

FIGURE C-4. STRESS RELAXATION (Δσ) FOR EA9696 AT 150°F

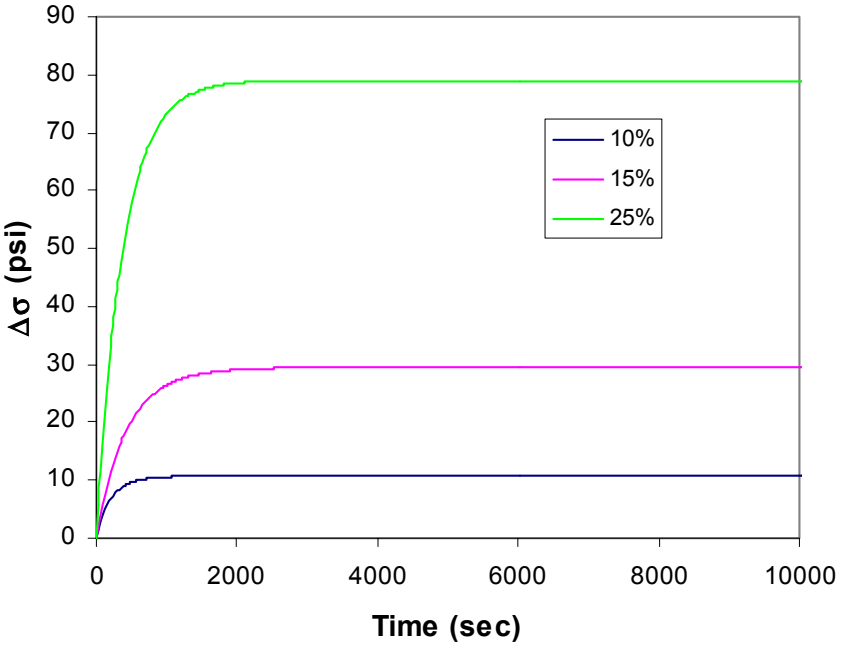

FIGURE C-5. STRESS RELAXATION (Δσ) FOR EA9696 AT 180°F

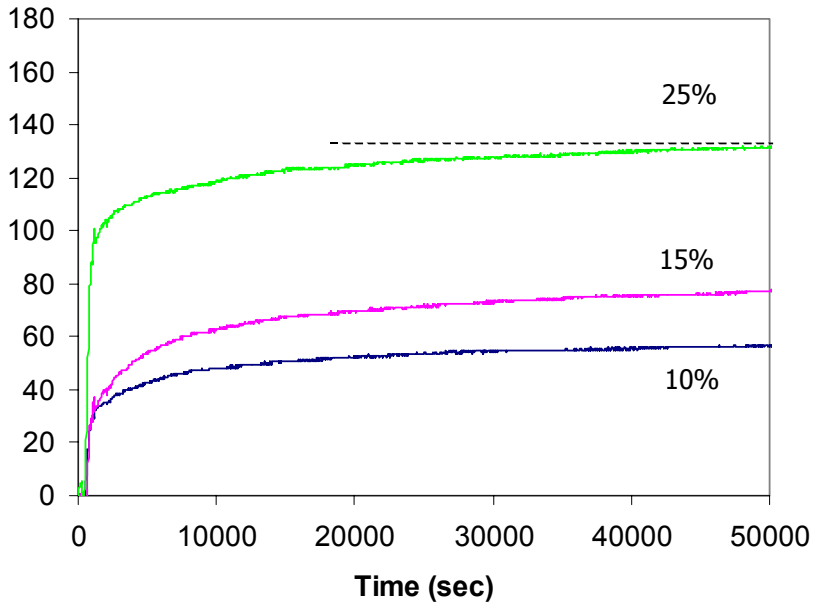

FIGURE C-6. STRESS RELAXATION (Δσ) FOR EA9696 AT 210°F (RAW DATA)

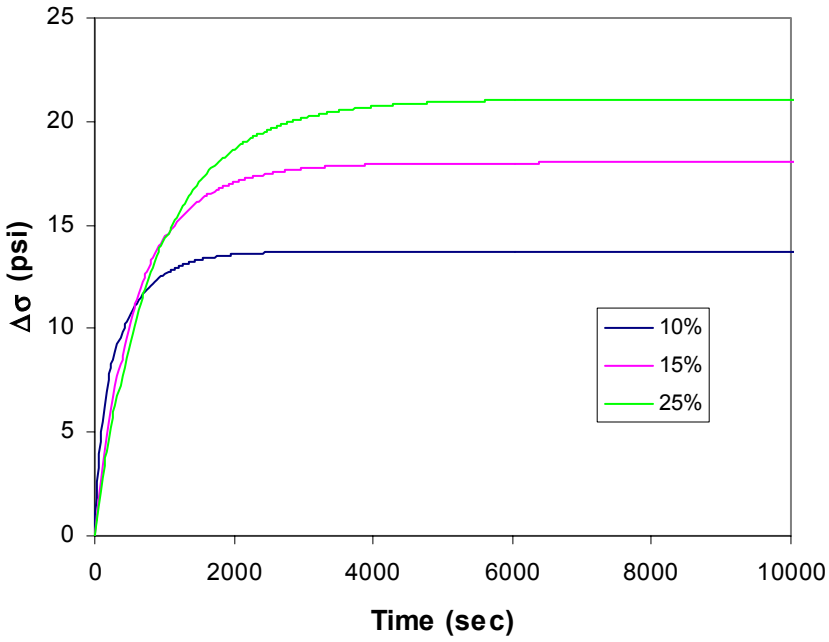

FIGURE C-7. STRESS RELAXATION (Δσ) FOR ES6292 (0.06 inch) AT 150°F

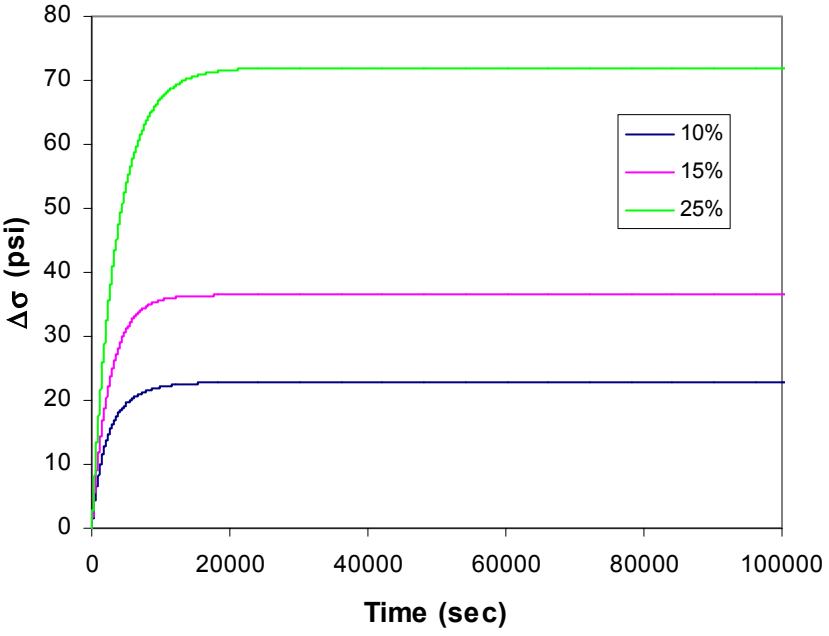

FIGURE C-8. STRESS RELAXATION (Δσ) FOR ES6292 (0.06 inch) AT 180°F

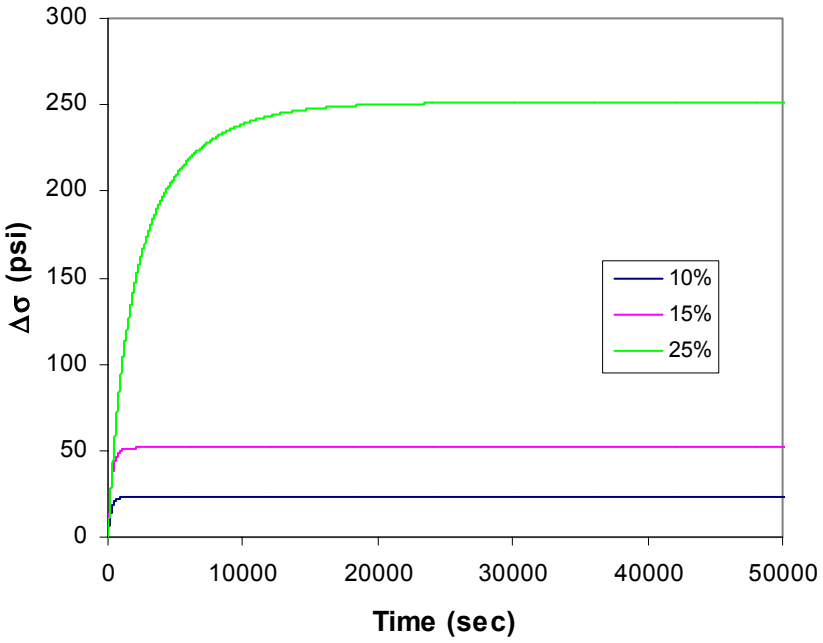

FIGURE C-9. STRESS RELAXATION (Δσ) FOR ES6292 (0.06 inch) AT 210°F

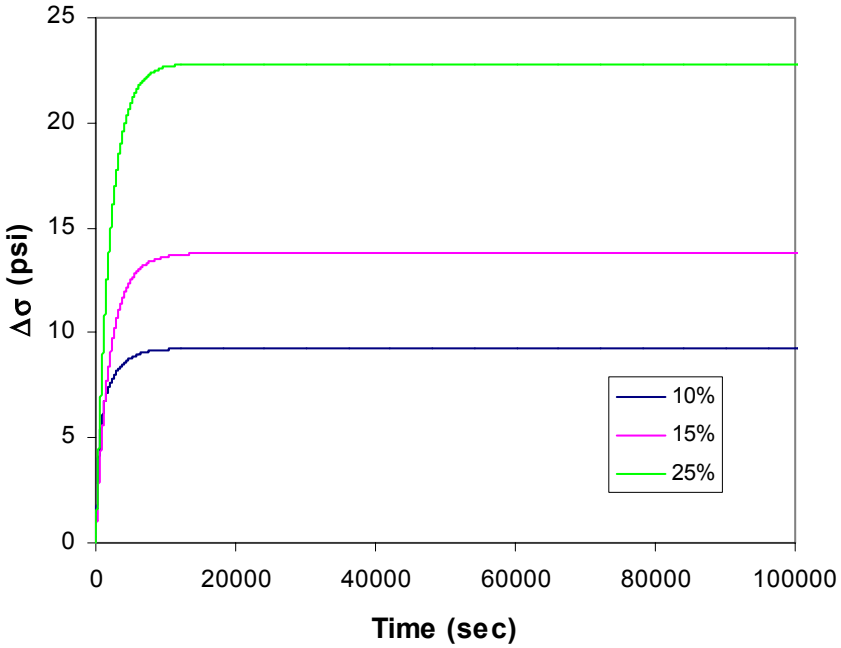

FIGURE C-10. STRESS RELAXATION (Δσ) FOR ES6292 (0.16 inch) AT 150°F

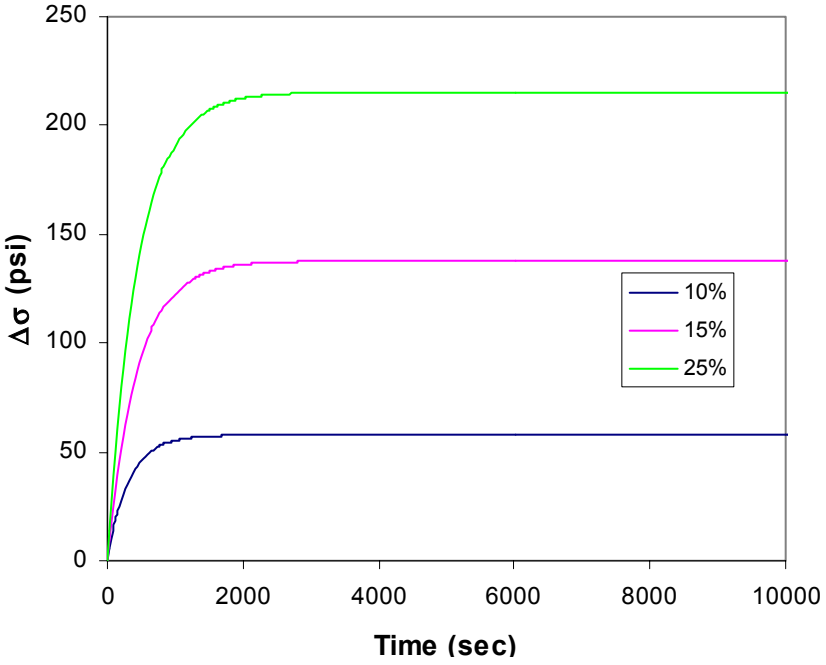

FIGURE C-11. STRESS RELAXATION (Δσ) FOR ES6292 (0.16 inch) AT 180°F

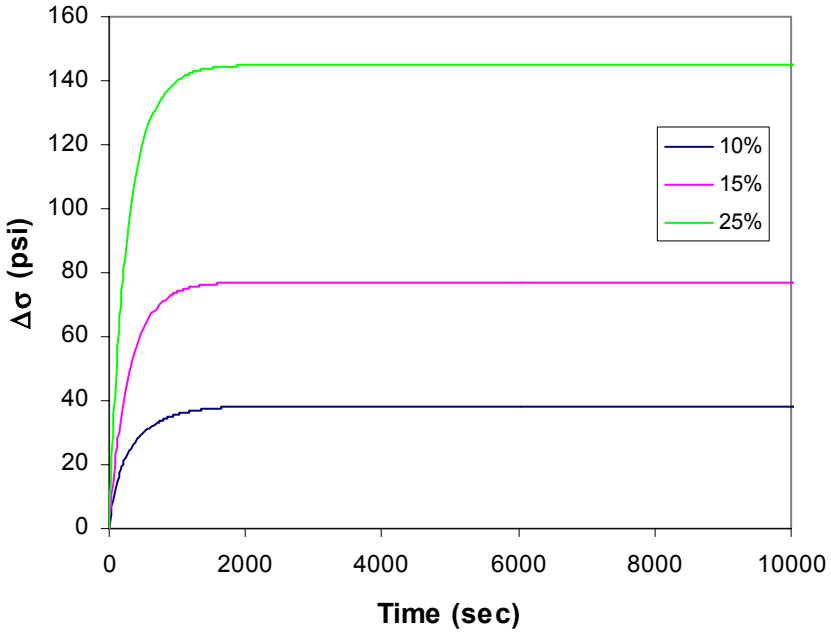

FIGURE C-12. STRESS RELAXATION (Δσ) FOR ES6292 (0.16 inch) AT 210°F